

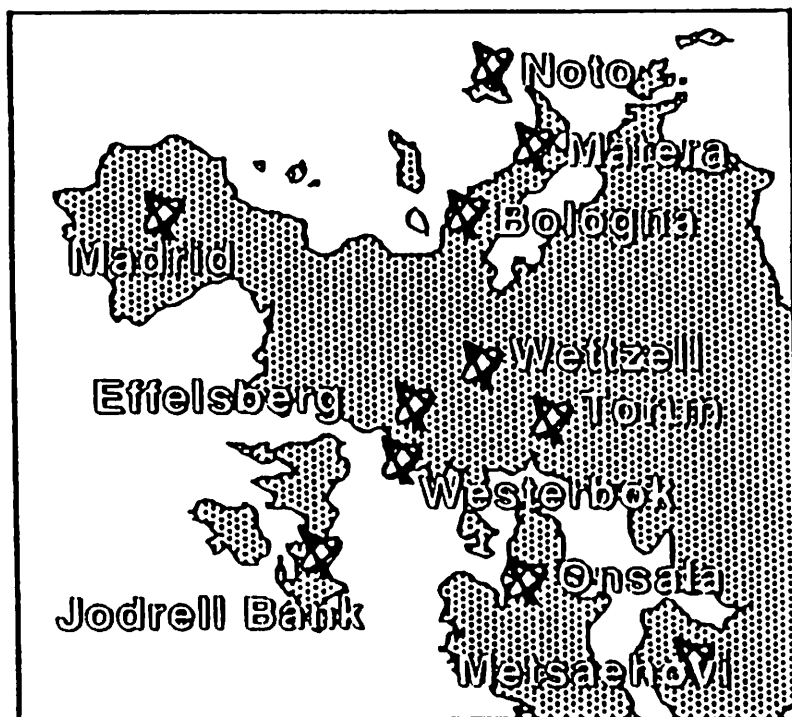
**INSTITUTO DE ASTRONOMIA Y GEODESIA**

**CONSEJO SUPERIOR DE  
INVESTIGACIONES CIENTIFICAS**

**UNIVERSIDAD COMPLUTENSE  
DE MADRID**

---

**PROCEEDINGS OF THE 7th WORKING  
MEETING ON EUROPEAN VLBI FOR  
GEODESY AND ASTROMETRY**



**MADRID - SPAIN**

**26 - 27 OCTOBER 1989**

**Edited by A. Rius**

## TABLE OF CONTENTS

Preface	iv
List of registered participants	v
Status Report on Global and European Geodetic VLBI J. Campbell	1
Organization of the European and Global VLBI for Astronomy R. W. Porcas	5
Status Report of Effelsberg Telescope - October 1989 R. W. Porcas	8
Status Report of the MPIfR, Bonn MK3(A) Correlator W. Alef	10
Status Report of the RT Wettzell R. Kilger	17
Status Report Netherlands Geodetic and Astrometric VLBI F. J. J. Brouwer, A. Jongeneelen, R. T. Schilizzi	21
Madrid DSCC Status Report A. Rius	23
Status Report from Noto P. Tomasi	25
The Medicina Station Status Report P. Tomasi, F. Mantovani	30
Agenzia Spaziale Italiana. Centro di Geodesia Spaziale VLBI Facility - Status Report B. Pernice	35
Status Report: Onsala Space Observatory B. O. Rönnäng, G. Elgered, J. Johnsson, B. Nilsson, K. Jaldehag	37
VLBI in Southern Europe P. Tomasi	39
VLBI Data Analysis of IRIS Campaign C. de Martino, G. Verrone, D. Picca	43
A Proposal: European Geodetic VLBI for the Determination of Land Subsidence and sea level rise F. J. J. Brouwer, R. E. Molendijk	49

The East-Atlantic Experiments: results for the European Stations J. Vierbuchen, N. Zarraoa	55
VLBI Surveying between DSS63 and DSS65 C. S. Jacobs, A. Rius	64
Accurate Space VLBI Station Position Determination S. Gorgolewski	68
On the Optimization of VLBI Observing Schedules H. Steufmehl	72
Determination of Correlation Coefficients between VLBI-Observables H. Schuh, A. Wilkin	79
OCCAM: A Compact and Transportable Tool for the Analysis of VLBI Experiments N. Zarraoa, A. Rius, E. Sardón, H. Schuh, J. Vierbuchen	92
Automatic Modelling of Clock Breaks in Geodetic VLBI Analysis E. Sardón, N. Zarraoa, A. Rius	103
Spectral Analysis of the "Wet" Delay: Preliminary Results G. Elgered	110
Galactic Masers as a Tool to Relate the Radio and Optical Celestial Reference Frames B. Rönnäng	113
Radioastronomical Analysis of IRIS Experiments: Status Report C. J. Schalinski, A. Witzel, W. Alef, J. Campbell, A. Alberdi	121
Testing the Computation of Source Structure Delay G. Zeppenfeld	126
Evidence for the Effect of Source Structure in Geodetic and Astrometric VLBI G. Petit, P. Charlot	133
Size and position of SgrA* J. M. Marcaide, A. Alberdi, P. Elósegui, M. J. Rioja, M. I. Ratner, I. I. Shapiro	140
Proper motion of the Quasar 1038+528 A P. Elósegui, J. M. Marcaide, I. I. Shapiro	147
VLBI Monitoring of the Milliarcsecond Structure of 4C39.25 at 2.8 and 3.6 cm A. Alberdi, J. M. Marcaide, P. Elósegui, C. J. Schalinski, A. Witzel	154
Phase-referencing using DEGRIAS A. A. W. Jongeneelen	160

## **Preface**

The "7th Working Meeting on European VLBI for Geodesy and Astrometry" was held in Madrid the days 26 and 27 October 1990. Participants from 7 countries presented 11 status reports of the different facilities located in Europe and 23 papers concerning different areas of current research on VLBI. (One status report and three papers have not arrived yet and therefore they will not be included in these Proceedings).

From the different contributions presented during the meeting, and partially collected in these proceedings, it seems that we could extract the following message: The reality, not any more a dream, of a consistent VLBI European Network for scientific applications requiring subcentimeter repeatability has appeared. That should be an extremely useful tool for many different fields.

The Meeting has been partially supported by the Instituto de Astronomía y Geodesia, Consejo Superior de Investigaciones Científicas, Madrid Deep Space Communications Complex, the Dirección General de Electrónica y Nuevas Tecnologías as well as the Spanish companies Inespal and Schwartz-Hautmont. E. Sardón and N. Zarraoa have provided efficient organizational support.

Antonio Rius



## **List of registered participants**

Antonio Alberdi, Inst. Astrofísica Andalucía, SPAIN  
Walter Alef, Max-Planck-Ins. Radioastron. , F. R. G.  
F. J. J. Brouwer, Meetk. Dienst RWS afd. TN-O, NETHERLANDS  
James Campbell, Univ. Bonn, F. R. G.  
Asunción Català, Universidad de Barcelona, SPAIN  
Agustín Chamarro, MDSCC-INTA, SPAIN  
Pedro Elósegui, Inst. Astrofísica Andalucía, SPAIN  
Robert Estalella, Universidad de Barcelona, SPAIN  
José Luis Gómez, Inst. Astrofísica Andalucía, SPAIN  
Jesús Gómez-González, Centro Astronómico de Yebes, SPAIN  
Stanislaw Gorgolewski, Radio Astronomy Observatory, POLAND  
José Carlos Guirado, Inst. Astrofísica Andalucía, SPAIN  
Manuel Hernandez, Universidad de Barcelona, SPAIN  
A. A. W. Jongeneelen, Sterrewacht Leiden, NETHERLANDS  
Richard Kilger, Wettzell Station, F. R. G.  
J. F. Lestrade, Bureau des Longitudes, FRANCE  
Josep M. Paredes, Universidad de Barcelona, SPAIN  
J. M. Marcaide, Inst. Astrofísica Andalucía, SPAIN  
Josep Martí Rivas, Universidad de Barcelona, SPAIN  
Axel Nothnagel, Univ. Bonn, F. R. G.  
Jorge Nuñez, Universidad de Barcelona, SPAIN  
Bartolomeo Pernice, A. S. I, ITALY  
Gerard Petit, Inst. Geographique National, FRANCE  
Angelo Poma, Stazione Astronomica, ITALY  
Richard Porcas, Max-Planck-Ins. Radioastron. , F. R. G.  
Denis Priou, Inst. Geographique National, FRANCE  
Antonio Rius, Inst. Astronomía y Geodesia, SPAIN  
B. O. Roennaeng, Onsala Space Observatory, SWEDEN  
Pilar Romero, Inst. Astronomía y Geodesia, SPAIN  
Esther Sardón, Inst. Astronomía y Geodesia, SPAIN  
Harald Schuh, DLRMD-TK/Esprit, F. R. G.  
Hermann Seeger, IfAG, F. R. G.  
Miguel J. Sevilla, Inst. Astronomía y Geodesia, SPAIN  
John South, MDSCC-NASA, SPAIN  
Heinz Steufmehl, Univ. Bonn, F. R. G.  
Paolo Tomasi, Inst. di Radioastronomia, ITALY  
José M. Urech, MDSCC-INTA, SPAIN  
Pablo de Vicente, Centro Astronómico de Yebes, SPAIN  
Ricardo Vieira, Inst. Astronomía y Geodesia, SPAIN  
Jost Vierbuchen, Univ. Bonn, F. R. G.  
Néstor Zarraoa, Inst. Astronomía y Geodesia, SPAIN  
Gunter Zeppenfeld, Univ. Bonn, F. R. G.

## **Status Report on Global and European Geodetic VLBI**

**J. Campbell**

**Geodetic Institute, University of Bonn  
Bonn, Fed. Rep. of Germany**

**ABSTRACT:** This paper gives a summary of the ongoing activities in the field of geodetic VLBI. On the global scale, the two main programs, the IRIS-Earth Rotation observation service and the Crustal Dynamics Project, are continuing to conduct regular VLBI experiments, and encouraging new stations around the world to participate in the campaigns. Europe is seeing a rapid expansion of its geodetic VLBI-net with the establishment of several new stations with full geodetic capability, especially in the Mediterranean, thus creating the world's most densely spaced VLBI-network of fixed stations for regional crustal motion research.

### **1. GLOBAL GEODETIC VLBI**

Since the introduction of the MkIII VLBI Data Acquisition System at the beginning of this decade, the two agencies involved, NOAA/NGS and NASA/GSFC, have been heavily committed to conduct observational programs of national and international scope. The global nature of the science behind this effort, i.e. the monitoring of the irregularities in the Earth's rotation and the detection and measurement of present-day plate motions, has caused the expansion of the initial projects into programs of truly international character.

The IRIS-program, which started in 1980 with a single-baseline interferometer, has grown to a set of three interleaved networks, the main element being formed by the original IRIS network, now called IRIS-A (Atlantic). This network has been operating with 5 stations since 1984 (Westford, Ft Davis (HRAS), and Richmond on the US-side, Wettzell and Onsala on the European side). From July 1989 IRIS observations have been shifted from Ft Davis to Mojave. An enlarged network including for the first time a station in the southern hemisphere (Hartebeesthoek near Johannesburg, South Africa) was started in 1986 (IRIS-S for South), with observations made every year in January and February (when a MkIII terminal could be brought to that station). The IRIS-S network will be able to operate all year round from December 1989, when a terminal will be installed at Hartebeesthoek permanently. Another network was created with the endeavour of the Japanese group of the Mizusawa Astrogeodynamics Observatory (formerly ILOM), combining stations around the Pacific, i.e. Kashima in Japan, Fairbanks (Gilcreek) in Alaska, and Mojave, California (IRIS-P for Pacific). Until the end of this year, when the new station near Hobart, Tasmania will become operational, the station of Richmond took part as the fourth station.

A new network of southern stations is in the making with two stations being built on the continent of Antarctica, and another possibly in South America (see Fig.1). The Antarctic antennas have both been primarily designed as download stations for Earth observation satellites, but later were modified to allow shared VLBI data acquisition. The Tahiti station is a project of the French Space Agency CNES, which is planning to build a 35m spacecraft tracking antenna, capable of being equipped with VLBI instrumentation.

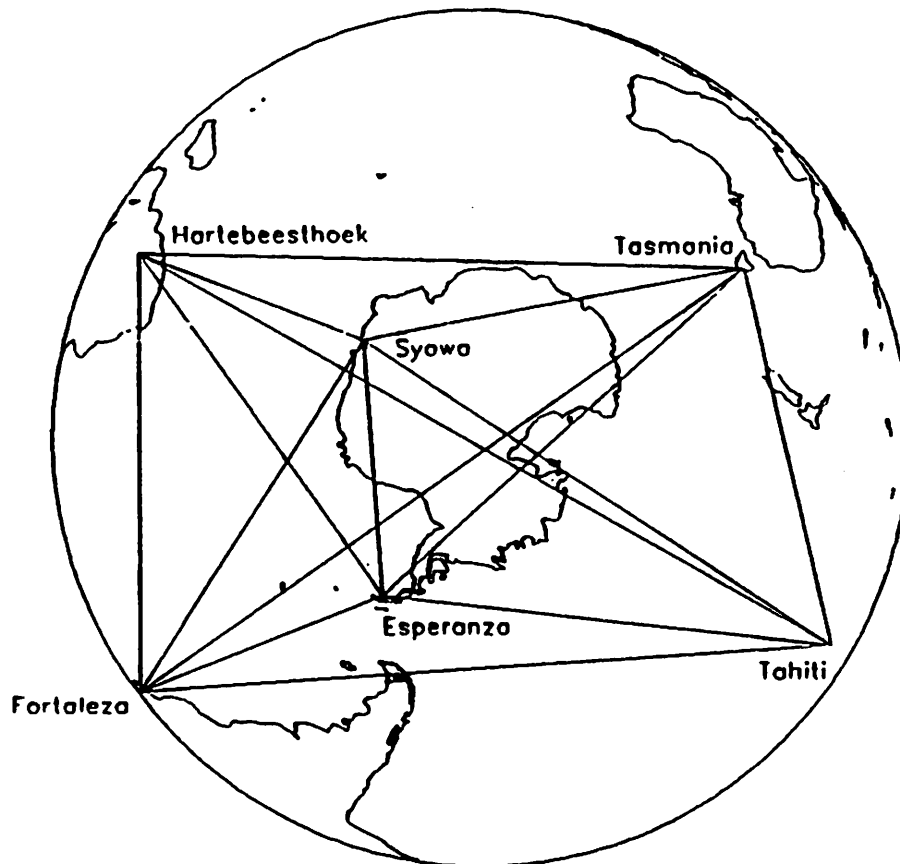


Fig. 1: Planned Southern VLBI-Network

The NGS has its own operations and data processing center and publishes the ERP regularly in its monthly bulletin. The Washington correlator, which has 5 stations, has been operating successfully since 1987. Thus, with Haystack there are at present two correlator centers available for the processing of geodetic VLBI data in the USA.

The NASA Crustal Dynamics Project, which has been created in 1982 is now nearing the end of its officially defined lifetime, but its activities will continue in the foreseeable future with the VLBI group at GSFC providing the leading support of the domestic and global VLBI campaigns. Up to now an average of 70 campaigns per year, 5 of which contain baselines to and in Europe has been scheduled, observed and processed by the Goddard VLBI group. The results are published yearly in the NASA Technical Memorandum series.

Baseline length rates have been derived for about half of the roughly 300 baselines around the globe. The agreement with the plate motion models is relatively good,

but most interesting are of course the cases of disagreement, where the measured rates have led to a revision of the assumed tectonic models. One such case is the motion of Kashima, which was thought to belong to the Eurasian plate, but actually suffers a compressional effect due to its proximity to the Pacific plate boundary.

On the R&D front the aims are to further increase the accuracy of the geodetic VLBI observations by looking at both instrumental and model improvements, the goal being to reach the millimeter level.

## 2. THE EUROPEAN GEODETIC VLBI NETWORK

The main factor which characterizes progress in geodetic VLBI in Europe has been the establishment of three additional stations capable of operating in the geodetic mode, i.e. observing simultaneously in the S- and X-band frequencies using the MKIII data acquisition terminals and the necessary ancillary equipment.

At the time of the 6th European VLBI Meeting in Bologna in April 1988, the NASA DSN Station near Madrid was still waiting to receive its MkIII terminal and at Matera and Noto in Italy the antenna constructions were nearing completion. From then onwards the growth of the geodetic VLBI network proceeded with increasing speed. The first and successful CPD-run with Madrid (E.ATL 3) took place on Aug. 31st 1988, followed by two more runs in the same year (Nov. 9 and Dec. 14). The station of Noto, which is a sister-antenna of Medicina operated also as a shared facility for both astronomy and geodesy, had its first and successful geodetic experiment on the 3rd of June 1989 (E.ATL-2) and four more in conjunction with the

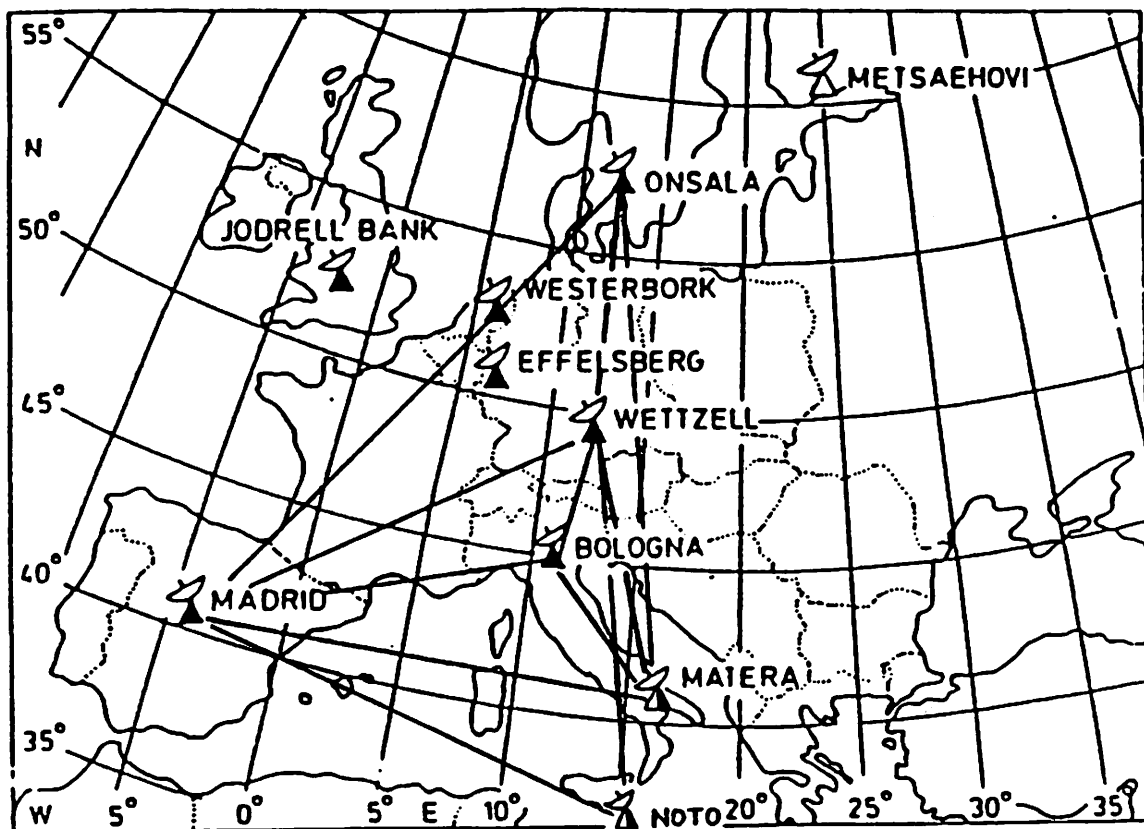


Fig. 2: The European Geodetic VLBI-Net in 1989

ongoing mobile VLBI campaign (EUREF). A problem for Noto was the availability of a MkIII-terminal, which could not be procured in time for the first experiments. Therefore the runs just mentioned were done with a travelling terminal, provided by NGS. The 20m Matera antenna, which is fully dedicated to geodetic VLBI, is now also coming close to having its first run.

In this meeting, reports about the status of the new stations and of the results of the first campaigns with more than two active stations in Europe are presented by the various groups involved. With its network of five active geodetic stations (see fig. 2), Europe is set to embark on a regional crustal motion campaign which is sure to produce significant results within three years from now.

### 3. DATA PROCESSING AND ANALYSIS CAPABILITIES

In Europe, at present there is just one MkIII correlation facility, operated by the Max-Planck-Institute for Radio Astronomy in Bonn, FRG. With the introduction of the high density head system, this correlator has been plagued with hardware and software problems, which still are not completely solved. With the installation of new electronics around the heads and newly updated software the problems should be tackled by the end of this year. Then five tape units (three high density and four regular, two tape drives offering both capabilities) will be available which in combination with two racks of correlator modules should allow the correlation of a five station mode C experiment in one pass. At present a 4 station, baselines capability is available, but with the two racks of new modules in flawless operation soon, the step to five stations should come a good deal closer.

The geodetic VLBI group includes one geodetic correlation supervisor and a contingent of student labor to carry out the correlation of geodetic experiments within the time allocated by the MPIfR to geodesy (25% of the total time). The CALC/SOLVE package to produce geodetic results is available both at the MPIfR and at the Geodetic Institute of the University of Bonn. The VLBI-Group at the Geodetic Institute is using this software for several ongoing projects, such as the analysis of IRIS- and CDP-campaigns, Intensive UT1- and Polar Motion observations, special experiments for relativity and tests on schedule optimization and source structure effects. In parallel, the Bonn VLBI software system (BVSS) is being developed into a full-grown multi-station analysis system with special features not available in standard CALC/SOLVE. This work is being performed in the frame of a cooperation between the VLBI groups in Bonn and Madrid (Acciones Integradas). More VLBI-analysis software is available also in the other European countries such as in Italy, France, the Netherlands and in Sweden, thus offering a wide spectrum of research aimed at the exploitation of the rich information content of VLBI-observations. Details about these developments are presented in special contributions in these proceedings.

## ORGANISATION OF EUROPEAN AND GLOBAL VLBI FOR ASTRONOMY

R.W.Porcas

MPIfR, Bonn, FRG

The VLBI technique is shared by many scientists across the world who operate in what is truly a "Global" observing community - the club of "VLBIers". Why, then, is it important to distinguish between astronomers, astrometrists and geodesists ? The answer lies in our different aims, which force different forms of data analysis, different observing strategies, and different choices of telescopes and observing frequencies. I will give some crude definitions, followed by one astronomer's caricature of their aims !

ASTRONOMER - interested in radio sources

ASTROMETRIST - interested in radio source positions

GEODESIST - interested in (instantaneous) locations on (rotating) Earth

### Astronomers:

-----

- want range of resolutions to study range of structural scales, e.g. Effelsberg-Westerbork (few 100 km)  
Owens Valley-Crimea ( 10,000 km)
- want telescopes at places that give good u,v coverage  
i.e. RELATIVE telescope locations are important
- want range of observing frequencies to measure spectral effects in radio sources, and hope to understand emission mechanisms  
e.g. 0.3 GHz ---> 90 GHz
- want to measure polarisation of radio source emission  
i.e. measure LHC and RHC
- want to observe both strong and weak sources  
e.g. 60 Jy ---> few mJy  
so, need BIG telescopes, long source tracks and integration times
- want to study a large number (N) of different sources (at least one per astronomer !!)

To achieve this, most astronomers throw away the valuable fringe-rate and delay residuals, don't attempt to calibrate phase, and only keep the amplitudes, and phase relationships, of the fringe visibilities. This results in radio source "hybrid maps".

### Astrometrists:

-----

- want all the above, but
- want also the radio source positions

They must keep the fringe-rates and delays and try to calibrate REAL phase (using phase-referencing, or dual-frequency S/X observing to measure the ionosphere). These are very close to geodesy requirements, and, since it involves a lot of work, not many people do this ! (most Europeans doing such work are here at the meeting)

## Geodesists:

-----

- would be happy with only 1 frequency (but use 2 for ionospheric correction)
- want telescopes at interesting geophysical locations
- are happy to just observe strong (point) sources (providing there are enough of them)
- are content with small antennas
- always observe the same sources
- use short integrations (and then rush away to another point in the sky a long way away)

To achieve their dubious aims, geodesists recklessly throw away the precious amplitude information (which they never calibrate anyway) and keep only fringe-rates, delays (and phases) !

A large fraction of astronomical VLBI is organised by the two observing networks - the U.S.Network, set up in the mid-1970's, and the European VLBI Network (EVN), established in 1980. I will describe some elements of the latter.

## Who is the EVN ?

-----

Various autonomous European astronomical institutes make available the following array of antennas for VLBI observations. Full EVN participation is indicated by "F" ; associate status "A" indicates that the antenna has a rather restricted availability. A feature of the list is the extreme diversity of antenna size, surface accuracy and steerability !

F	Effelsberg, F.R.G	100 m diameter
F	Westerbork array, Netherlands	25 m x 14 elements
F	Jodrell Bank, U.K.	76 m / 25 m
F	Onsala, Sweden	25 m / 20 m
F	Medicina, Italy	32 m
F	Noto, Sicily	32 m
F	Cambridge, U.K. (from 1990)	32 m
A	Torun, Poland	15 m
A	Simeiz, Crimea, U.S.S.R.	22 m
A	Puschino, U.S.S.R.	22 m
A	Wettzell, F.R.G.	20 m
A	Nancay, France	8000 sq.m

## What is the EVN ?

-----

There are 5 key elements which make up the EVN :

- 1) An agreement between observatory directors to give 45 days a year of observing time for EVN observing. In 1989 this was allocated in 4 observing "sessions" :
 

March/April	wavelengths 1.3, 2.8, 6.0 cm
June	wavelengths 90, 18.0 cm
September/October	wavelengths 1.3, 2.8, 6.0 cm
November	wavelengths 18, 21, 3.6/13 cm

Note, not all antennas can observe at all wavelengths.
- 2) A program committee, which meets 3 times a year to rate observing proposals (91 received in 1989). This has a Chairman (at present RWP) who traditionally acts also as VLBI scheduler, a Secretary,

and includes representatives from the 5 main European VLBI institutes and 4 "at large" representatives from the European astronomical community.

- 3) The EVN Consortium Board of Directors, which had its first formal meeting in 1985. It has no funds, but attempts to coordinate and foster the evolution of VLBI in Europe, and is engaged in a major fund-raising attempt (plans large 20-station Data Processing Facility using 16 million ECU requested from EC)
- 4) The Technical Working Group (TWG) consists of technical representatives from the EVN observatories. It meets ca. twice a year, discusses and coordinates relevant technical matters. Some major themes are implementation of High Density Recording (Mk3A) in Europe and VLBA compatibility.
- 5) The Telescope Friends at each observatory, who perform "absentee observing" on behalf of astronomical investigators. They receive and execute observing schedules sent for the various astronomical projects by the investigators.

#### Global observations

-----  
Astronomers are no respectors of national boundaries and VLBIers are certainly no respectors of continental ones. At least 75 % of EVN proposals require U.S. telescopes in addition, to give long, high-resolution baselines, i.e. most proposals are "global". This requires close coordination of EVN and U.S. Network activities, as shown in the following list :

- same proposal deadlines (3 per year)
- joint (but separate) refereeing of global proposals (using different systems !)
- joint observing sessions
- common recording standards (Mk2, Mk3, Mk3A,...)
- common frequency and polarisation schemes
- collaboration between European and U.S. Schedulers to construct a session observing plan consistent with all technical and observatory constraints (a nightmare !)

The organisation of the present astronomical VLBI networks involves a fine balance between collaboration, competition, and autonomy for the EVN and U.S. Network, their constituent observatories and the astronomical community.

In the U.S. the National Radio Astronomy Observatory is building an array of 10 antennas, each 25 m, and a 20-station correlator, dedicated to full-time VLBI - the VLBA. This will replace the present U.S. Network, and hopefully remove some of the problems associated with the present manner of operation. We expect the EVN will be an important part of many VLBA observations, not least because of the larger collecting area of European antennas !



# STATUS REPORT OF EFFELSBERG TELESCOPE - OCTOBER 1989

R.W.Porcus MPIfR, Bonn, FRG

The Max-Planck-Institut fuer Radioastronomie operates a 100m diameter radio telescope at Effelsberg, in the Eifel Mountains. This is still the world's largest fully-steerable single-dish radio telescope, although the new, 100m-class antenna planned by the U.S. National Radio Astronomy Observatory for its Green Bank, W.Virginia site will rival it in the coming years. Despite many demands for a variety of radio-astronomical studies, VLBI accounts for up to 90 days a year of observing time in Effelsberg. A large fraction of this time is used for observations organised by the European and U.S. VLBI Networks ; the remainder is used for special projects, most notably mm-wavelength VLBI observations. Observing proposals for the 45 days committed to the EVN are assessed by the EVN Program Committee. All other proposals are refereed by the PKE (Programmkomitee Effelsberg), sometimes received via the U.S.VLBI Network, in which Effelsberg is also an associate member. Nearly all the VLBI observations are astronomically motivated, although Effelsberg did take part in a few geodetic observations with a borrowed S/X receiver some years ago, and more recently took part in the 6 cm GINFEST campaign, scheduled by the EVN.

The list of receivers at present available for VLBI use in Effelsberg is given below ( P = prime focus, S = secondary focus).

P	0.6	1.4	1.6		22.0	43.0	GHz
S				5.0	8.4	10.7	GHz

Geodesists will no doubt be pleased to hear that we plan to add an uncooled S-band system, using an offset paraboloid mounted on the X-band horn (cf Onsala 20m system) to give a simultaneous S/X -band capability. No date is yet fixed for this.

Other improvements planned are :

- combining the 1.4 and 1.6 GHz systems in a single box for easier operation
- converting the present single-channel maser receiver at 22 GHz to left-hand-circular polarisation
- adding a new dual-polarisation 22 GHz receiver to the secondary focus to give better frequency "agility"
- adding a dual-polarisation 15 GHz receiver to the secondary focus, for observations with VLA and VLBA
- adding a 90 GHz receiver (prime focus) - there is still a very significant gain over the inner 60m of the antenna !

We hope that in a few years time our VLBI receiver list will look like this :

P	0.6	1.4/1.6			22.0	43.0	90.0	GHz
S			5.0	2.3/8.4	10.7	15.0	22.0	GHz

A summary of equipment available for VLBI observing in Effelsberg is given below:

100m antenna - drive rates 20 deg/m (azimuth), 20 deg/m (Elevation)

H-maser (Smithsonian) frequency standard ( + Rubidium standard)

Loran C receiver

GPS time receiver

Mark 2 Formatter(s) and VME recorder(s)

Switching box (Smithsonian) - for, e.g. 1 s switching line VLBI

Mark 3 Recorder and terminal (Haystack, 1980); upgraded to high density recording (Mk3A) from 1990.

Mk3 Field System written for PC (Greybe, Schulze, Graham..) instead of the normal HP system. This also interacts with the Microvax telescope drive system. Upgraded for high density recording 1990.

Phase calibration injection - this is normally put in the I.F., so delay between receiver and terminal is not calibrated !

VLBA record terminal - we PLAN to get one in the coming years !

# **Status Report of the MPIfR, Bonn Mk3(A) Correlator**

**W. Alef**  
*Max-Planck-Institut für Radioastronomie*  
*Bonn, Federal Republic of Germany*

**ABSTRACT.** A schematic overview of the Mk3 VLBI system is given. The present correlator configuration at the MPIfR in Bonn is shown, including hardware, software, and manpower. The short and medium term planning are presented. The present MPI correlation policy and a summary of the statistics on correlator time usage of the last three years are given at the end.

## **1. Introduction**

The broad-band Mk3/Mk3A VLBI system (Rogers et al., 1983) is well established in the astronomical and geodetic community for estimating geodetic parameters with significantly improved precision and for a variety of astronomical observations, which were not possible with the less sensitive Mk2 VLBI system. At present data recorded with the Mk3 system, the narrow track Mk3A system, and the VLBA system in Mk3 compatible mode can be correlated at four Mk3/Mk3A correlators, three of which are regularly used for experiments of the astronomical and geodetic networks: Haystack Observatory (Mk3 – 6 mode B baselines, Mk3A – 10 mode B baselines), Naval Research Lab Washington (Mk3A – 10 mode B baselines), Max-Planck Institut Bonn (Mk3 – 6 mode B baselines, Mk3A – 6 mode B baselines). While the correlator in Washington is exclusively used for correlating Geodetic VLBI observations, the other two correlators are used both for Geodesy and Astronomy. The Caltech Block II system has Mk3 capability, but is mostly used for Mk2 analysis.

## **2. Short Overview of the Mk3 VLBI System**

### **2.1 DATA ACQUISITION**

The antenna signals from either two polarizations or two frequencies — as in S/X observations — are mixed down from the radio frequency to the intermediate frequency (IF) range (see figure 1). The IF signals are input to two IF distributors which have a normal (NOR) and an alternate (ALT) input and distribute the signals to the odd and even video converters. Each video converter houses an independent local oscillator phase-locked to the frequency standard. Each video converter mixes a different part of the IF frequency down to the video frequency range of 0 to 2 MHz. Both upper and lower sidebands are generated. The formatter digitizes the signals from the resulting 28 channels. The digitized data is then recorded on 28 tracks of a Honeywell 96 recorder.

As each video converter has an independent local oscillator, a test signal (phase calibration signal) is used to later determine and remove the unknown phase offsets between the converters and thus allow a coherent integration over the observed frequency band.

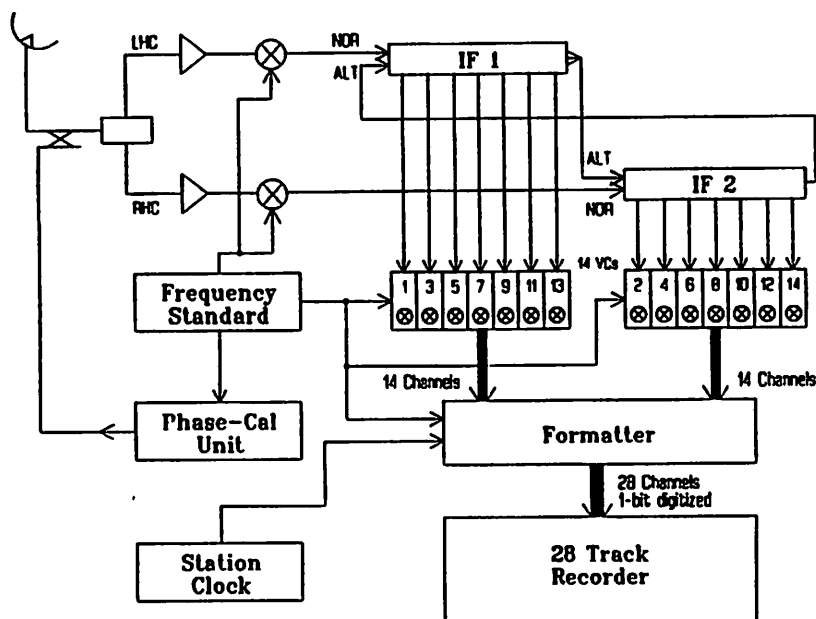


Figure 1: *Mk3 data acquisition*. The major components of a Mk3 data acquisition system are: 2 IF distributors, 14 video converters, a formatter which digitizes the incoming 28 data channels, a 28 track recorder, and a phase-cal unit.

The phase-cal unit generates sharp pulses at a rate of 1,000,000 per second (locked to the frequency standard) which are injected in the signal path. They cause sine-waves in the spectrum which extend up to a few 10 GHz with a spacing of 1 MHz.

## 2.2 MK3 CORRELATOR

### 2.2.1 Correlator Hardware

A Mk3 correlator consists of three major components: the instrumentation recorders, the correlator, and the control computer (see figure 2). The initial fringe fitting, archiving, and other postprocessing is performed with an additional computer which is connected to the control computer, i.e. via a shared disc.

The recorded tapes are played back at the correlator. The correlated data and the time information from the tapes is sent to the control computer. The computer synchronizes the playback tape drives and supplies the correlator with the necessary a priori data for the correlation.

In the correlator the data coming from the 28 tracks of the recorders are correlated pairwise in so-called correlator modules. Each of these modules is a complete VLBI correlator with decoders, delay compensation, fringe rotation, complex cross-correlation, and integration. 14 such modules are organized in so-called CAMAC crates, with 6 crates in one rack. One crate is thus capable of correlating data recorded in modes 'B' or 'C' of one baseline<sup>1</sup>.

<sup>1</sup>See also chapter 'Present Correlator Configuration'

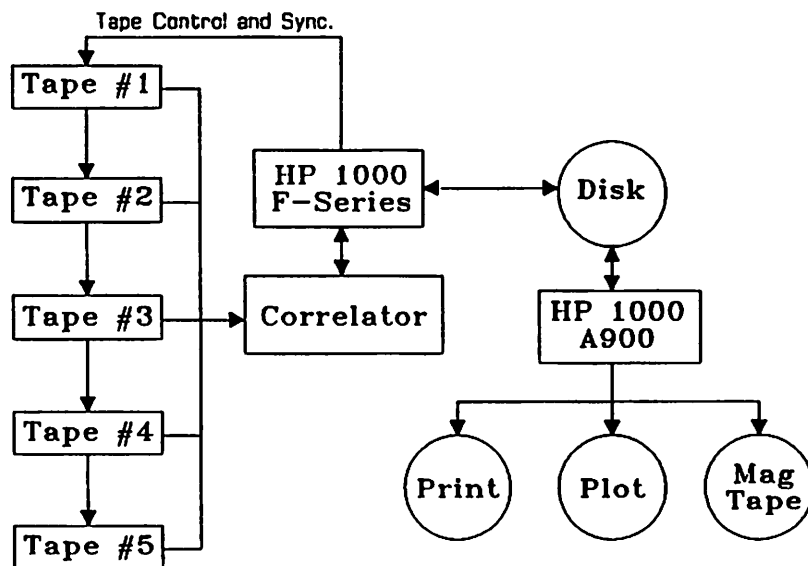


Figure 2: Block diagram of Mk3A correlator. The playback units and the correlator are controlled by an HP 1000 computer. The recorded data with the embedded time information is sent to the correlator; the correlated data and the time information are received by the HP 1000 F computer and are written to a disk. Another computer integrates the raw data and does the fringe interpolation (*fringe fitting*) before the data is archived on magnetic tape.

### 2.2.2 Correlator Software

The Mk3 software (see figure 3) comprises programs to generate schedules ('SKED') and machine readable schedules ('DRUDG'), which are executed at the observatories by the 'field system'.

At the correlator the observing logs and the schedule file are used as input to the correlation. The correlation supervisory program 'COREL' controls several programs which are used during various stages of the correlation process. The correlated data is temporarily stored on disks. The fringe search and interpolation is done by the program 'FRNGE'. Finally the data is archived on magnetic tapes.

A rudimentary data base system allows efficient retrieval of data for fringe fitting (re-fringing), global fringe fitting, or data export.

## 3. Present Correlator Configuration at Bonn

### 3.1 CORRELATOR HARDWARE

The Bonn Mk3 correlator was built in 1982. At the beginning it consisted of three tape drives, six correlator crates, and an HP 1000 F computer for running the correlator and for doing the post-processing.

In autumn 1989 four Honeywell 96 recorders were available for playing back Mk3 formatted data. Two of these playback units were already equipped with narrow track heads (Mk3A upgrade). A fifth recorder only fitted out with a Mk3A head had just become operational (see figure 4). In addition to the original six crates of Mk3 correlator modules six crates of the newer design Mk3A modules had been installed as part of a project to double the correlator capacity.

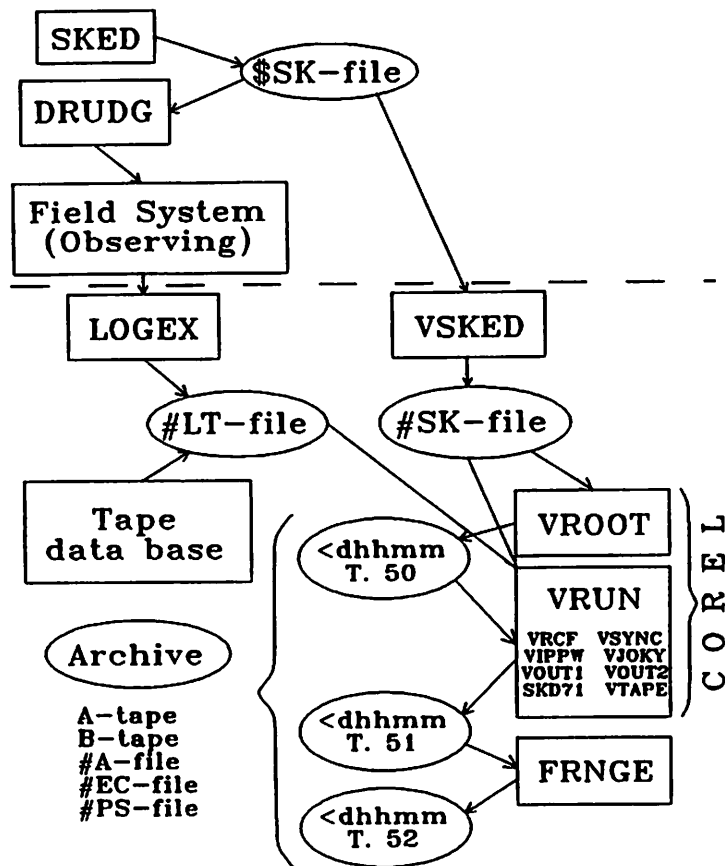


Figure 3: *Diagram of Mk3 correlator software.* Program names are in rectangular boxes; file names are shown surrounded by ellipses. Above the dashed line the programs and files are displayed which deal with the schedule preparation and observing; the bottom half of the figure shows programs and files which are needed in the correlation process.

The postprocessing is now done with an HP1000 A900 which is nearly three times faster than the older F-series computer. The disc space for storing correlated data has been enlarged to about 400 Mbytes. This disc is shared between the correlator computer and the computer for the post-processing. Post-processing has been enhanced by increasing the disc space on the A900 to 600 Mbytes.

### 3.2 MANPOWER

The VLBI correlator group is led by an engineer. Two operators are responsible for running the correlator, for the tape handling, and for maintenance of the hardware. Two technicians are responsible for repairing and upgrading the correlator and the tape drives. Two scientists devote half of their time to supervise the correlation, and maintain the correlator and system software. About three students operate the correlator during weekends and nights.

The Bonn geodesists have helped to finance the correlator and thus get reserved time on the Mk3 correlator. They correlate independently of the astronomers. The geodesists have one supervisor and about ten students who work as operators and handle the Mk3 tapes.

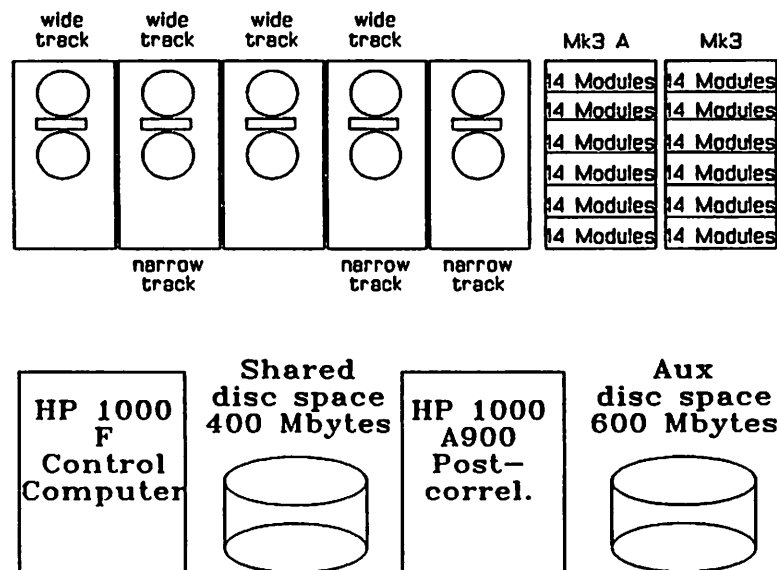


Figure 4: *Status of the Mk3 correlator.* The Mk3 processor comprises five tape drives of which three are equipped with narrow track heads and four with wide track heads, two correlator racks with six crates each, and two computers with 1 Gbyte of disc space.

### 3.3 SOFTWARE

Software for schedule preparation (SKED/DRUDG) is installed on the HP1000 A900. In addition we now have the PC-SKED program written by Alan Rogers (Haystack) available on a "386" personal computer. The correlation software from Haystack is installed on the HP1000 F. It is regularly updated together with the software for fringe fitting and archiving which resides on the A900. The Alef&Porcas method of antenna-based fringe fitting is fully implemented on the A900 as well as the geodetic CALC/SOLVE software (Clark et al., 1985).

## 4. Future Mk3A Correlator Configuration

### 4.1 SHORT TERM PLANS

In the course of 1990 we plan to have five playback units ready all equipped with narrow track MK3A heads. Four of these recorders will still have the old wide track heads in addition. The correlator expansion to 12 crates with Mk3A modules will probably be finished in 1990 as well. This would give a correlator capacity of 10 baselines in mode B and C, and 6 baselines in mode A. We hope to get an additional operator/technician.

### 4.2 LONG TERM PLANS

The correlator control computer is fairly old by now and will become the biggest bottleneck in the correlation process. We plan to replace it with a new HP1000 model announced by HP (A1200?) which should increase the computer power for controlling the correlation by about a factor of five. It should then be possible to correlate simultaneously with the 12

crates of Mk3A modules and the 6 crates of the old Mk3 correlator provided that we have enough playback units. Approximately one man year is needed for adapting the software.

The correlator could be enlarged to 15 crates of Mk3A modules which would allow correlating six stations in mode B or C simultaneously. Some major parts for such an extension exist already, but no plans have been made and thus no money is available.

Two more tape drives will be installed at the correlator in the context of the EVN proposal for a large European correlator. One Honeywell 96 will be bought. It will be equipped with VLBA-style control electronics as well as one of the existing tape drives. The hope is that playback of narrow track recordings will be better by a factor of 10 to 100, and that control of the tape drives during the correlation will be much more reliable. It should thus be possible to correlate at double speed. Another tape drive will be delivered by the British company Penny & Giles who also produce instrumentation recorders. They plan to produce a VLBA-compatible tape unit. In the context of this project the VLBI group will be enlarged by one engineer and hopefully one technician.

## 5. MPIfR Correlation policy

As the Bonn geodesists have helped to finance the correlator they get a fixed amount of correlator time. They operate the correlator quasi independent of the MPI staff. The geodesists produce "B-tapes"<sup>2</sup> which are input to CALC/SOLVE or other geodetic software.

In absentia correlation is done by the MPI staff for astronomical observations. This includes correlation, recorelation of obviously bad data, determination of manual phase-cals, if they stay constant during an observation, the initial fringe fitting, and archiving. The principal investigator has to verify that the correlation was done properly. He has to do the re-fringing, possibly antenna based fringe fitting (Alef and Porcas, 1986), and exporting of his/her data. In the future when archiving on DAT based cassette systems becomes available MPI could save a whole experiment on one such cassette. The principal investigator could then do the fringe fitting at his/her home institute.

## 6. Statistics of Correlator Usage

The load on the correlator shows a gradual increase from 1987 to 1988. The time used by the geodesists increased from about 500 hours to 900 hours; the time used by the astronomers grew from 900 to 1000 hours. In 1989 the correlator was much less used: the geodesist only needed about 350 hours and the astronomers 400 hours till autumn 1989. This is mostly due to the initial installation of two narrow track heads. This technique is still marginal and a lot of time was needed to reduce the unacceptably high error rates of Mk3A recordings. In addition we had a long period of problems with the Mk3 tape drives which are still not quite under control.

1. Alef, W. and Porcas, R.W., 1986: *Astron. Astrophys* **168**, 365
2. Clark, T.A., Corey, B.E., Davis, J.L., Elgered, G., Herring, T.A., Hinteregger, H.F., Knight, C.A., Levine, J.I., Lundqvist, G., Ma, C., Nesman, E.F., Phillips, R.B., Rogers, A.E.E., Ronnang, B.O., Ryan, J.W., Shupler, B.R., Shaffer, D.B., Shapiro, I.I., Vandenberg, N.R., Webber, J.C., Whitney, A.R., 1985: *IEEE Transactions of Geoscience and Remote Sensing*, **GE-23**, No. 4, 438

---

<sup>2</sup>These are archive tapes which do not contain the raw correlator data any more.



3. Rogers, A.E.E., Capallo, R.J., Hinteregger, H.F., Levine, J.I., Nesman, E.F., Weber, J.C., Whitney, A.R., Clark, T.A., Ma, C., Ryan, J., Corey, B.E., Counselman, C.C., Herring, T.A., Shapiro, I.I., Knight, C.A., Shaffer, D.B., Vandenberg, N.R., Lacasse, R., Mauzy, R., Rayhrer, B., Shupler, B.R., Pigg, J.C., 1983: *Science*, **219**, 51

## STATUS REPORT OF THE RT-WETTZELL

R. Kilger  
TU - München  
Wettzell, Germany

The purpose of my short review is to report of the activities at the radiotelescope in Wettzell since our last meeting in Bologna in spring 1988. The first part of my paper will deal of our participations in international observing programs, the second part of our efforts in improving hard-and software implementation at our measuring system.

The antenna at Wettzell is dedicated to geodesy, therefore the main emphasis is put on following geodetic observing programs:

- IRIS-A : The participation in IRIS-A is our basic effort in geodetic observing campaigns. The standard configuration of the net until June 16/17, 1989, or IRIS-550, was: Westford, Fort Davis, Richmond and Wettzell; beginning at June 21/22, 1989 or IRIS-551 Mojave Base Station overtook the part of Fort Davis. Fort Davis now has a new VLBA-antenna and is part of the VLBA-network. The old "IRIS"-antenna has been closed, as far as I know. This is an opportunity to remember, that the old Fort Davis antenna started IRIS in September and October 1980 during an intensive campaign together with 4 antennas in Europe and USA to monitor polar motion. After this intensive campaign Fort Davis continued the measurement together with Haystack antenna in a single baseline interferometer. Until the beginning of 1984 the network normally consisted of only 2 antennas, namely Fort Davis and Westford, which replaced Haystack later on. At the beginning of 1984 Richmond and Wettzell joined the net forming a 4 station configuration with normally 6 baselines. From that date the name of the observing program was changed from POLARIS to IRIS and later IRIS-A. IRIS-A is observing on a regular 5 day period and determining:
  - $x + y$  of the coordinates of the rotational pole of the earth,
  - UT1-UTC, as well as changes in the length of the day,
  - lengths of the baselines between the participating observatories, as well as their changes with time,
  - nutation and precession,
  - coordinates of the observed radio sources,
  - performance of the hydrogen masers,
  - atmospheric zenith height parameters, etc.The results of the observing program are published in the monthly issued IRIS, Earth Orientation Bulletin, A+B by NGS. [1]
- IRIS-S : During February and March 1989 IRIS-S has been performed, as in the last years. The net consisted of Hartbeesthook in South Africa, Westford and Richmond in USA, and Onsala, Medicina or Wettzell in Europe. The advantages of the net are long North South baselines, which are sensitive regarding the coordinates  $X + Y$  of the rotational pole, and the possibility of determining the coordinates of radio sources in the southern hemisphere, which normally are known with less precision, than in the northern hemisphere.

- **INTENSIVE** : Based on the values of  $X + Y$  of the pole and the coordinates of the radio sources, determined by IRIS-A, it is possible to determine with a single (East-Est) baseline interferometer:
  - UT1-UTC and length of the day,
  - performance of the hydrogen masers at the observatories,
  - atmospheric zenith height parameters.

The net consists of the radiotelescopes of Westford and Wettzell, forming an East-West-interferometer with a 6000 km baseline. 4 radio sources are recorded twice. The measurement is performed daily at the same sidereal time, except every fifth day, when a 24-h IRIS-A session takes place. The results together with additional details are published in the IRIS, Earth Orientation Bulletin, A+B. [1]
- **Shanghai** : In July 88 the radiotelescopes at Shanghai, Kashima and Wettzell performed a session based on a proposal of the Geodetic Institute in Bonn. Main purpose of this session was to verify the performance of the new MK-III observatory at Shanghai.
- **SHAWNE** : Initially it was intended to include Shanghai, Hartbeesthoek and Wettzell into the session thus allowing the determination of  $X+Y$  and UT1-UTC. Finally Shanghai and Wettzell observed in an East-West single baseline interferometer at 12 days in May 1989. The session has been correlated at MPIfR in Bonn. When the data are analyzed the results could be compared with the referring results of the interferometer Westford - Wettzell.
- **EUROPEAN MOBILE CAMPAIGN** : In 1989 a VLBI campaign was performed in Europe including the mobile radiotelescope MV-3, which normally operates in North America. Worldwide there are only 3 mobile telescopes available and only 2 of them are really mobile. MV-1 is practically fixed at Vandenberg in California. Basing on an idea and under the overall control of Prof. Dr. Seeger, IfAG, MV-3 observed at the places:
 

- Hohenbunsdorf (FRG)	together with	Noto and Wettzell,
- Metsehoivi (Finland)	" " "	Onsala " " ,
- Tromsø (Norway)	" " "	" " " ,
- Carnoustie (Scotld.)	" " "	" " " ,
- Brest (France)	" " "	Noto " " ,
- Grasse ( " )	" " "	" " " ,

At every occupation there were performed about 4 days of observation. The main purpose of the session was to determine exact positions at those places, thus providing the GPS community with fiducial points for further densification with GPS. The campaign has been performed quite successfully despite of the fact that a swarm of reindeers caused a severe accident in northern Finland. The container turned over in to the ditch of the road; the damage was so heavy, that one truck has been lost.

Another difficulty was the lacking permission of Algeria to measure at Tiaret. Therefore this occupation had to be cancelled.

The whole session started at June 20th and ended at September 20th, 1989. The correlation of the test tapes prior to each session has been done at Bonn (Arno Müskens), the sessions itself have been correlated at USNO at the Washington correlator facility.

- CDP : Due to budget cuts at the CDP-program the amount of serving sessions has been reduced.  
Following CDP-sessions have been performed:  

	1988	1989 performed	1989 planned totally
- POLAR	2	-	1
- E.ATL	5	2	3
- W.ATL	3	-	-
- ASTROMETRY: In the past period since our meeting in Bologna Wettzell participated in Astrometry measurements together with Harvard University, Prof. Dr. Shapiro and Dr. N. Bartel. They apply the phase reference mapping technique to investigate the radio structure of quasars in the submilliarc scale. One measurement was performed in May 88, 3 in February and March 89. An additional measurement is planned in November 89.  
In December 88 Wettzell participated in a VLBI-MK-III measurement to determine the deflection of radiowaves passing the gravity field of Jupiter. The measuring campaign was originated by Prof. Dr. Schneider and Dr. Schuh.  
  
End of August 89 a Wettzell built MK-II Formatter became operational. After a successful test run Wettzell participated in 3 MK-II sessions in October 88 based on proposals of MPIfR, Dr. Kus, Dr. Porcas and Dr. Alef. In June 89 3 subsequent MK-II sessions were performed, suggested by Dr. Schalinski, MPIfR.

Since April 88 following activities were carried out regarding hardware:

- Formatter MK-II : In August 88 a MK-II Formatter got operational, built in Wettzell in cooperation with MPIfR (H. Bösl). It was tested successfully with the radiotelescope in Effelsberg and used in some astronomy sessions.
- Receiver : The performance of our Helium S/X-receiver has been improved slightly by applying new cables between the front end of the receiver in the dewar and the following components.  
Wettzell had phase stability problems caused by the Local Oscillator. The problem has been detected by carefully performed analysis of CDP-sessions. Some other stations had similar problems. A modification within the Local Oscillator removed these instabilities being a function of the elevation angle. The modification was suggested by A.E.E. Rogers and Brian Corey of Haystack Observatory.
- Computer : Wettzell replaced the old HP-1000-F computer by a new HP-1000-A900 in June 1989. Wettzell is running presently the version 7.1 of Field System Software.

**High Density :** The High Density recorder at Wettzell still makes problems as  
**Tp Recorder** at all other observatories (MV-3). Wettzell replaced the first HD-heads after 10 months of operation in November 88. Haystack said, they were simply worn out. The second unit worked quite reliably with less technical breakdowns than the previous unit, but presently, after 11 months of operation, we can no longer read the first 4 tracks in X-Band. Therefore we have no control of the write performance of these tracks.

**Tapes :** Since April 1989 Wettzell is recording the Intensive runs on shorter and therefore lighter tapes in high density. This saves transportation costs. The tapes are sent with Express Mail Service, a postal service, guaranteeing a shipping time between Wettzell and the correlator in Washington of 2 days including customs. This procedure allows results of UT1-UTC within 1 week.

**Maser :** Wettzell has 2 masers operational, EFOS-1 and EFOS-3. The ion pump of EFOS-1 has been replaced in February 88 and of EFOS-3 in May 88. In October 89 EFOS-3 stopped operation due to a worn out vacuum pump. The ion pumps of both masers meanwhile have been replaced and both masers are operational again.

1	SUBCOMMISSION INTERNATIONAL RADIO INTERFEROMETRIC SURVEYING (IRIS)	IRIS-EARTH ORIENTATION BULLETIN, Bulletin a and IRIS-OBSERVATORIES PERFORMANCE REPORT, Bulletin B
---	--	---

## **STATUS REPORT NETHERLANDS GEODETIC AND ASTROMETRIC VLBI**

Paper presented at the 7th Working Meeting on European VLBI for Geodesy and Astrometry,  
Madrid, Spain, 26-27 October, 1989,

by

**Frits J.J. Brouwer,**  
Survey Department of Rijkswaterstaat, Delft  
**Anton A.W. Jongeneelen,**  
Astronomical Observatory of the University, Leiden  
**Richard T. Schilizzi,**  
Neth. Foundation for Research in Astronomy, Dwingeloo

### **1. Introduction**

This status report briefly summarizes the developments in the field of geodetic and astrometric VLBI in the Netherlands since the last meeting of the Working Group in Bologna, Italy in April 1988.

The items addressed are: the status of the Westerbork Synthesis Radio Telescope (WSRT), VLBI observations at the WSRT, scientific research topics and the status of the European correlator in Dwingeloo.

### **2. Status of the WSRT**

With its MARK-II and MARK-III systems and H-maser, the WSRT is fully equipped for astronomical and astrometric VLBI observations at 6, 18, 21, 49 & 92 cm. Participation in geodetic campaigns is however restricted due to the lack of S/X-band (3/13 cm) receivers.

Fortunately, the development of a Multi Frequency Front End system (MFFE) will remedy this situation. This front end should combine 8 observing bands in one box, in the range 3.6 to 92 centimetres. Some of these wavelengths (such as S/X) can be observed simultaneously. Change of wavelength can then be achieved in a matter of minutes, as opposed to the days of work (the WSRT has 14 dishes!) which it takes now. The MFFE system should be fully operational in 2-3 years time.

Finally, the NFRA is coordinating the construction of the 6 cm receiver for the Russian RADIOASTRON space VLBI satellite, in cooperation with the MPIfR in Bonn.

### 3. VLBI-observations

Due to the lack of an S/X-receiver, the WSRT could not participate in any geodetic observation campaign. On the other hand, a few astrometric VLBI observing sessions were held at the WSRT via the EVN-programme; we mention:

- in June 1988: the global VLBI network with 10 stations for a phase-referenced VLBI experiment on M81 and two reference sources; observations were made with MARK-III for 19 hours; proposal by: Jongeneelen, De Bruyn, Schilizzi, & Brouwer.
- and other proposals by a.o. Lestrade, Quirrenbach, and Alef.

### 4. Scientific research

In the field of geodetic applications of VLBI, work at the Faculty of Geodesy of the Delft University of Technology was mainly directed towards the further development of the Delft multi-station VLBI network analysis software suite and towards simulation studies for the optimal design of VLBI campaigns.

This research has led to two M.Sc. theses, the first by Boer on the estimability of gravitational deflection by the Sun; the second by Molendijk on the estimability of plate tectonic motion.

Recently, the main responsibilities for geodetic VLBI research in The Netherlands have been taken over by the Survey Department of Rijkswaterstaat.

In the field of astrometric VLBI, research at Leiden University is directed towards determination of the proper motion of M81 using several epochs of observations by phase referenced VLBI. The idea is to determine position changes at the 20 micro arcsecond level for intervals of two years.

The same approach may also be applicable to galactic Mira's.

### 5. European correlator in Dwingeloo

The EVN-application for a 20 stations European VLBI correlator to the European Community passed through the scientific advisory committees of the EC with flying colours, but the total amount of money required was not available. Consequently, only a tape recorder study was financed (440.000 ECU). Under this contract, two projects are now in progress; one to build a MARK-III/VLBA compatible playback terminal for the Bonn correlator (by Penny and Giles Data Systems Ltd, UK); the other by MPIfR to reshape a Honeywell recorder to VLBA compatibility.

The decision on the full proposal awaits further developments in the EC Framework Programme. There is some likelihood that the revised Framework Programme will include the possibility for funding the infrastructure of large scientific institutes.

## Madrid DSCC Status Report

A. Rius  
Instituto de Astronomía y Geodesia (C.S.I.C.-U.C.M.)

### 1. Introduction

This report summarizes the present instrumentation available at the NASA Madrid Deep Space Communications Complex (MDSCC) for Geodetic and Astrometric VLBI.

### 2. Availability

The Radio Astronomy program in the DSN is composed of the following segments:

- A) Applied Radio Astronomy in direct support of the DSN
- B) Support of the NASA Office of Space Sciences and Applications (OSSA)
- C) Host Country Observations
- D) Radio Astronomical observations which require the unique capabilities of the DSN. Proposals submitted to the JPL Radio Astronomy Experiments Selection Panel.

### 3. Instrumentation

#### Front End Areas

Telescopes	DSS63				DSS65	
Diameter	70 m				34 m	
Bands	L	S	X	22 GHz	S	X
Efficiency	.6	.7	.7	.4	.6	.7
System T (K)	35	20	20	60	55	21/40
Surface RMS (mm)		6-7				5

#### Time and Frequency

2 Redundant Hydrogen MASERS

#### Recording terminals

- 1 Mark III DAT (with two recorders)
- 2 Mark II BWS

#### Other equipment

SNR-8 ROGUE GPS Receiver

Pressure, humidity and temperature sensors integrated in the system.



### **Conventional Geodesy**

A geodetic survey of a local control network around the antennas has been performed at the site by the Geodesy Division of the IGN-E

### **Geodetic VLBI Experiments**

During the reported period the DSS65 has participated in the EATL3-88, WATL3-88, EATL4-88, EATL5-88, EATL1-89, EATL2-89. Results of these experiments could be found in these proceedings.

## REPORT FROM NOTO STATION

Paolo Tomasi

Istituto di Radioastronomia - C.N.R.  
Bologna - Italy

**ABSTRACT.** Here is presented the activity of the new V.L.B.I. antenna built by the Istituto di Radioastronomia - C.N.R. in the southern part of Sicily, near Noto. Preliminary results in astronomy and geodesy are presented together with plans for the future activity.

### 1. INTRODUCTION

The southernmost VLBI facility in Europe was built by Istituto di Radioastronomia of C.N.R. during 1988 and finished by the end of the year. Its approximate position is latitude 36.87 deg. and longitude 14.99 West, that means in the south-eastern part of Sicily, near the town of Noto. The antenna is a twin of the one in operation at the Medicina station (near Bologna) since five year, also used in VLBI for astronomy and geodesy.

The antenna is a parabolic 32 meters dish, driven by HP 1000 E series computer (with Field System 5.4 running on it). Hydrogen maser, as frequency standard was installed on March 21. It is Ephos 5 produced by Oscilloquartz.

The site was selected to provide a better UV coverage for European (and global) VLBI network, from the astronomical point of view. From geodesy point of view, the idea was to provide a fixed VLBI facility on African plate (or near the boundary of African and Eurasian plates).

### 2. ACTIVITY IN RADIOASTRONOMY

The very first radio source detected by the Noto antenna was Cas A, on January 13, with the 10.7 GHz (2.8 cm.) cooled receiver (total system temperature about 70 K). The antenna efficiency at different elevation, using the source 3C84, is shown in fig. 1. At 45 degrees of elevation it is 55 %, that means the theoretic efficiency for this kind of antenna.

The quality of the antenna surface was tested using the 21.7 GHz (1.3 cm) cooled receiver of the Medicina antenna. The surface quality is good enough to have an efficiency grater than 30 % at every declination, with a peak of 35 % around 45 degrees of declination.

The first VLBI test was performed at the beginning of March with the 10.7 GHz receiver. With the Noto antenna, the Effelsberg and Medicina antennas were involved, in a MarkII VLBI experiment with good results: fringes were detected at all baselines, even if the presence of Rubidium as frequencies standard at the Noto station, provided only few seconds of

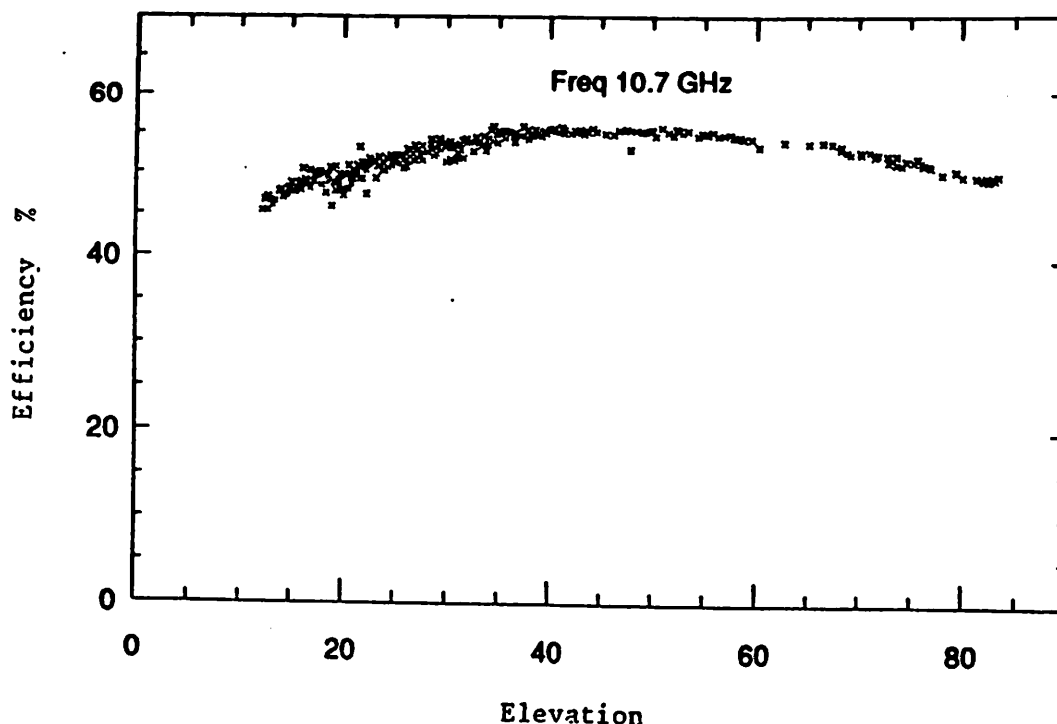


FIGURE 1. Noto antenna efficiency curve at 10.7 GHz

coherence at this frequency. After the installation of Hydrogen maser, the antenna took part, from April 4 to 9, at the VLBI run at 10.7 GHz.

At the end of May, with the S/X receiver (on long term loan from NASA) the Noto antenna, with that of Medicina and Madrid participate to an astrometric VLBI campaign for selecting new astrometric reference sources.

New VLBI observations with Medicina and Wettzell antennas was performed on CygnusX-3 source in June. As expected, due to dimension of the emitting regions, nothing was detected on the baselines with Noto, but on the baseline Medicina - Wettzell, a very preliminary results, suggest the presence of some features, giving an upper and a lower limit to the dimension of the active region.

A number of total power observations (single dish) was done both at 10.7 and 21.7 GHz, for measuring the variation of the total flux density of the source.

At the end of July a week of observation at 22 GHz was used in order to test the performances of a new autocorrelator of the Arcetri Observatory (Florence).

More VLBI observations, at 10.7 GHz and 21.7 GHz was done in September.

## 2. ACTIVITY IN GEODESY

During this year there was a very intense activity in geodesy, at the station. That was possible because the NGS sent on loan, to the Noto station, one MarkIII Dat and recorder for EUREF experiment. In the same time NASA, as mentioned before, sent an uncooled S/X receiver (Kwajalein receiver). That receiver was mounted at the primary focus of the antenna, and the efficiency was found to be 35 % and 40 %, at X and S bands respectively.

The first VLBI geodynamic experiment was EATL-2 on June 3. The experiment was a great success. The Noto antenna had data quality results, similar to the others stations, and even more important the intra-Europe baselines have formal error of 1.9 to 2.9 mm. The geocentric station position for Noto, from this experiment, is:

$$x = + 4934564.885 \pm 0.008 \text{ m.}$$

$$y = + 1321200.266 \pm 0.004 \text{ m.}$$

$$z = + 3806484.777 \pm 0.009 \text{ m.}$$

The rest of the geodynamic VLBI activity was connected with EUREF experiment. This experiment, involving three fixed VLBI station (Onsala, Wettzell and Noto), and one mobile, was defined for establish a number of well defined reference position along Europe, to be used as master station for GPS receiver involved in setting the new European geodetic network.

Noto antenna participated at the first European occupation, Hohenbuenstorf (Germany). Six days of observations and 170 MarkIII tapes recorded, from June 21 to 27.

In July the Noto antenna took part also, to two 24 hours Navnet experiments (NAVNET28 and NAVNET29).

For the Noto antenna the EUREF experiment was supposed to restart with the Brest occupation (August 24). Unfortunately, due to an accident during the move of the mobile antenna, the recorder was damaged and one occupation had to be repeated, causing a general delay on following occupations. That produce a conflict at Noto station between geodynamic and astronomical schedules. We took part at the Brest occupation (August 30, September 5), but only 24 hours of Grasse occupation was observed.

In table 1 it is possible to have a quick look of the whole activity of the station during this year.

One more Navnet experiment (NAVNET31) was observed on September 10. The last occupation of EUREF experiment, Tiaret (Algeria), was cancelled and Noto observed IRIS570 and IRIS571; then the MarkIII DAT was shipped back to South Africa.

Two GPS campaign were performed on the site, one in June as part of EUREF experiment, the second one in August as part of the Calabrian arc experiment. A link between the VLBI antenna and GPS observing point was produced by Prof. Bilardi, of Rome University and the results are presented in fig. 2.

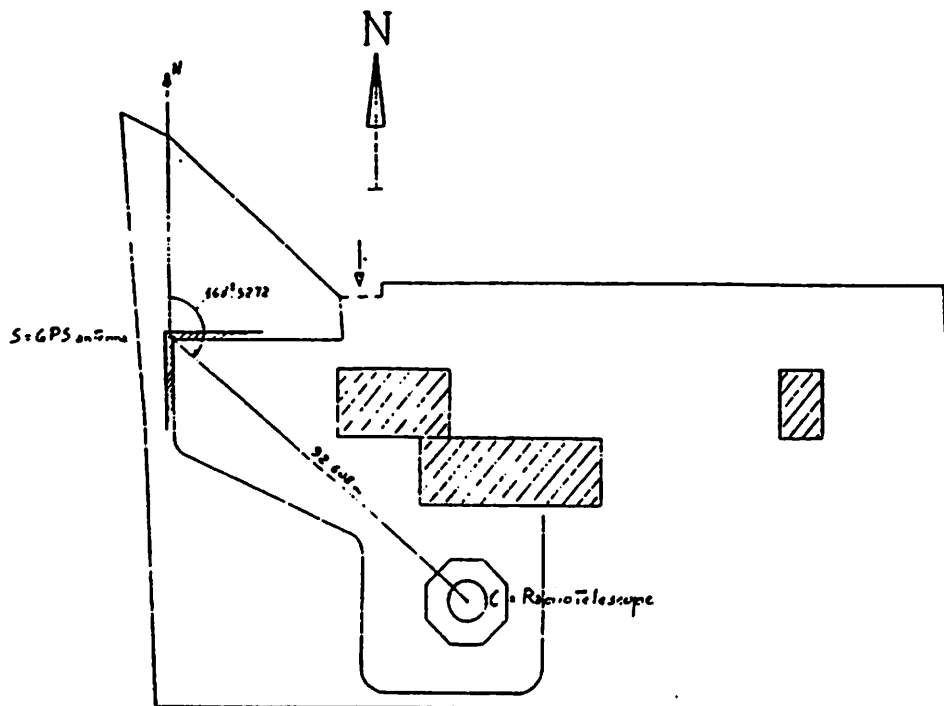


FIGURE 2. Map of the Noto site. S = GPS antenna; C = radiotelescope

$\overline{SC} = 92.608 \text{ m.}; [\angle SC] = 168.5272 \text{ deg.}; \Delta H = H_C - H_S = 18.843 \text{ m.}$

### 3. THE FUTURE

During next year it will be a large improvement in the receivers situation. That is very important from astronomical point of view. In fact, the station at present have only one cooled receiver (10.7 GHz). A new 6 cm. cooled VLBI receiver is under construction and should be ready for March 1990.

But also for geodynamic a large improvement is on the way. A new S/X plus 1.3 cm. receiver for primary focus, is under construction at the Medicina station. When it will be finished the S/X cooled receiver and the 1.3 cm receiver actually at the Medicina station will be transferred permanently to Noto, probably in June 1990.

The station, like the one of Medicina, will be involved primarily in astronomical VLBI, but a lot of time will be devoted to geodesy, if the NASA will provide a MarkIII DAT, for 1990. A MarkIII Dat from NASA should be in Noto on early 1990 (January and February) and on the end of the year (in particular for EUROPE experiments), but others experiments can be planned.

In any case we are preparing a number of MarkII geodetic experiments with Matera, Medicina and Noto. We intend to extend this experiments also to Madrid and possible to Wettzell in order

to measure the regional deformations in the south-western Europe, also with MarkII VLBI. Data coming from these MarkII experiments will not be of the same quality, of the ones coming from standard MarkIII experiments. But in this way Noto can participate also when MarkIII Dat is not present, we can use normal video cassette and it is possible to correlate the data very quik at the Medicina correlator (the old Blok 0 correlator from J.P.L.).

A new VLBA data aquisition terminal, is already funded, and will be ordered early next year for the Noto station. It will be a fully compatible one, to allow also geodetic VLBI observations.

During the 1990 a laser ranging platform, for colocation, will be built at the antenna site.

TABLE 1

NOTO STATION ACTIVITY			
	TECHNICAL	ASTRONOMY	GEODESY
OCTOBER 28	DEDICATION DAY		
JANUARY	POINTING	POINTING	
FEBRUARY	POINTING	EFFICIENCY AT 10.7 GHz	
MARCH	MASER	FIRST VLBI TEST	
APRIL		FIRST VLBI RUN AT 10.7 GHz EFFICIENCY AT 21.7 GHz	
MAY	S/X AND MARKIII INSTALLATION		25 FIRST S/X TEST
JUNE		ASTROMETRY AND CYGX-3	EATL-2 EUREF
JULY		22 GHz LINE	NAVNET 28 - 29
AUGUST	MASER RESTARTED		EUREF
SEPTEMBER	DRUDG INSTALLED	VLBI RUN	EUREF NAVNET IRIS 570 -571

## THE MEDICINA STATION STATUS REPORT

Paolo Tomasi and Franco Mantovani

Istituto di Radioastronomia - C.N.R.  
Bologna - Italy

**ABSTRACT.** The activity of the Medicina V.L.B.I. station operated by the Istituto di Radioastronomia - C.N.R., Bologna, is presented. Results from VLBI in geodesy and anomalous misclosures obtained by the East-Atlantic (EATL-1, 1989), are discussed.

### 1. INTRODUCTION

Since the previous working meeting the station was very active in the geodesy field, not restricted to the VLBI observations only. In fact, the antenna was involved in several geodynamic experiments and in particular: few IRIS experiments, five EATL, experiments designed to measure the motion between North America and Europe, and the JUPITER experiment, planned to test the general relativity theory on a source passing nearby Jupiter.

At the end of 1989 the antenna took part to four GNUT experiments. These experiments were organized by USNO for testing the idea of setting up a different VLBI network for UT1 determinations.

The Medicina antenna was stopped during 1989 summer, for resurfacing (July - September 1989), nevertheless in the first part of 1989 the antenna took part to a number of VLBI experiment for geodesy. The first one was the EATL-1 in January (with Madrid, Onsala, Wettzell and Westford). In February the antenna participated to few IRIS south experiments, with Fort Davis, Richmond and Westford, in U.S., Wettzell in Europe and HarRAO in South Africa. The experiments ended when NGS and CDP decided to move the MarkIII DAT to Noto for the Euref campaign (Tomasi, 1989).

In the mean time the site was actively involved in collocation experiments, with mobile Laser Ranging (April, May 1988) and GPS (April 1988 and April 1989). During the mobile Laser ranging experiment the weather conditions were very bad and only few passes were recorded, consequently the scientific results of the experiments are very poor.

### 2. RESULTS

The most important result from the set of experiments during 1988, was the determination of the precise position of the VLBI antenna. At the JPL CDP meeting of April 1989 J. Ryan classified Medicina within the 32 VLBI sites having positional formal error less than 1 centimetre. In fact the actual position of the station is:

$$x = + 4461371.758 \pm 0.004 \text{ m.}$$

$$y = + 919595.806 \pm 0.003 \text{ m.}$$

$$z = + 4449559.510 \pm 0.006 \text{ m.}$$

During 1989 the Eatl experiment, originally designed for measuring the Atlantic enlargement, become really an European experiment. In fact, from the original participation of two European station we moved on including now Wettzell, Onsala, Madrid and Medicina. And for Eatl-2 (June 3, 1989) the Noto antenna substituted the Medicina one. The Eatl data are still under studies (Vierbuchen and Zarraoa, 1989) and we will analyze the same data running SOLVE into the Medicina HP-1000 computer.

The Eatl-1 experiment (January 1989), was particularly good. It was correlated at the Washington correlator and the formal errors of the European baselines was within five millimetres.

The good quality of data allowed a discovery of group delay closure error of -20.7 ps on the triangle Wettzell, Onsala and Medicina (J.Ray - CDP email 1989). A similar misclosure was found on the same triad for Eatl-5 of 1989 (J. Ray - CDP email 1989). In previous experiments a similar result was never found, but we have to consider that no previous experiments had data good enough to allow the discovery of misclosure of that amount. Who is responsible: station, correlator or something else? After the Eatl-2 with Noto replacing Medicina, good data quality, and no misclosures obtained, the fault was supposed to be at the Medicina station.

In any case we want to pin point that the Eatl-2 was correlated at the Haystack correlator, while Eatl-1 was correlated in Washington. This suggest that more test should be also planned at the Washington correlator.

A good check for the Washington correlator will be to recorrelate a good experiment already correlated at Haystack, or to correlate an experiment with Noto and Medicina twice (with tapes from different stations on different recorders). Europe 1 on January 26 1990 will be the first experiment including Medicina and Noto and it should be used for that.

At the end of 1988 the Medicina antenna participated to a few Gnut experiments (three were 8 hours and one 16 hours). From Gnuts, including Medicina, we got an UT1 determination with a formal error of 0.020 milliseconds.

### 3. LOCAL SURVEY

A complete local geodetic survey was carried on by Telespazio in May 1989. From the report (Cenci et al., 1989) we present here the map of the site and reference monuments on figure 1.

The geocentric coordinates for the marker "O" (monument 7546) of figure 1 (the reference point on the mobile Laser Ranging platform), is :

$$x = + 4461425.003 \pm 1 \text{ m.}$$



$$y = + 919459.240 \pm 1 \text{ m.}$$

$$z = + 4449509.395 \pm 1 \text{ m.}$$

Table 1 presents the vectors of the monuments in the local reference system.

TABLE 1  
VECTORS IN LOCAL REFERENCE SYSTEM (METERS)

MARKER	UP	EAST	NORTH	DISTANCE
O	0.0	0.0	0.0	
A	2.1320	-7.9123	24.9403	26.2521
B	2.0586	-12.3328	67.4279	68.5774
C	2.1452	1.8831	42.5173	42.6131
D	1.9421	25.3524	50.6353	56.6609
E	1.9449	35.3005	40.7440	53.9443
F	-0.0023	-63.9632	74.7444	98.3769
G	-0.3766	35.1365	421.2287	422.6919

In the same local reference frame the invariant point of the VLBI antenna is:

$$\text{North} = 50.668 \pm .004; \text{East} = 35.250 \pm .003; \text{Up} = 17.724 \pm .006.$$

The monuments "A", "B", "C", "F" were measured with GPS and traditional technique by Italian I.G.M. and linked to the national geographic network. Also the position of the antenna rotation axis was linked to the national geographic network.

From these measures we have the WGS 84 position of marker "A":

$$x = + 4461344.629 \pm 0.016 \text{ m.}$$

$$y = + 919561.838 \pm 0.016 \text{ m.}$$

$$z = + 4449553.824 \pm 0.016 \text{ m.}$$

The geographic coordinates of the same marker "A" are:

$$\text{LAT} = 44^{\circ} 31' 10''.5756 \quad \text{LON} = 11^{\circ} 38' 47''.861$$

and the coordinates of the rotation axis of the radio-telescope are:

$$\text{LAT} = 44^{\circ} 31' 11''.4092 \quad \text{LON} = 11^{\circ} 38' 49''.817$$

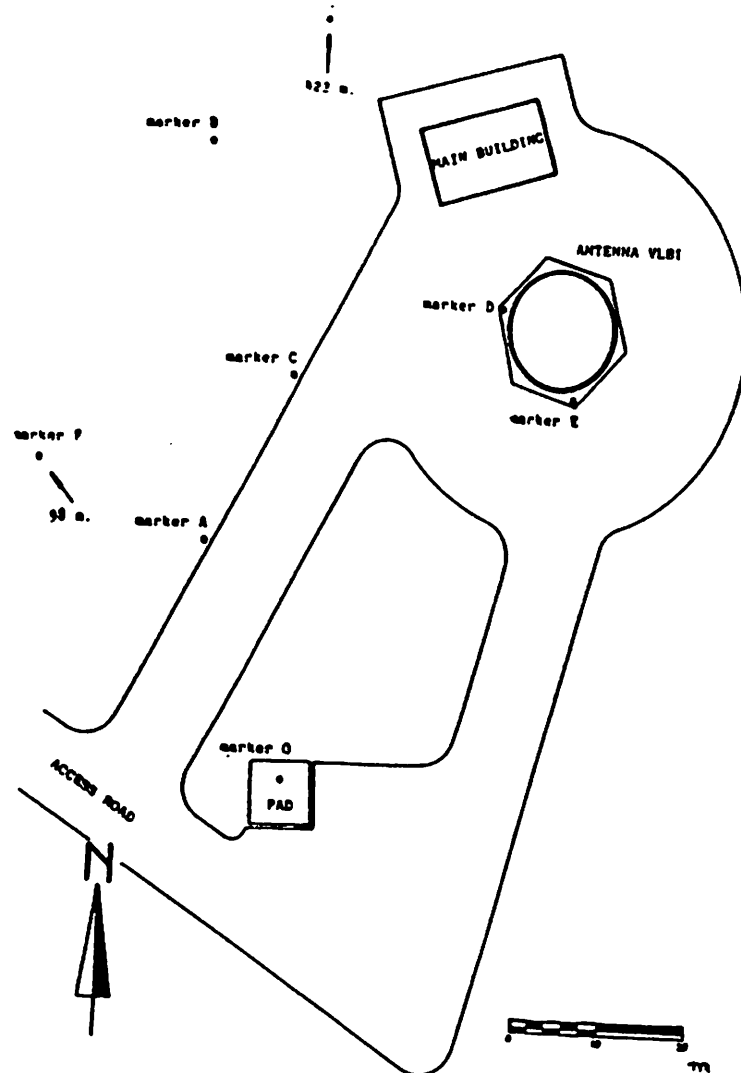


FIGURE 1 Plan of Medicina Site

### 3. THE FUTURE

The Institute policy continues to assign priority to VLBI observations for the use of the antenna. Astronomical VLBI, both European and U.S. networks comes first, then geodesy.

For technical reason, time for geodesy will be preferably allocated on a fortnight basis, three or four time along the year, in cooperation with NGS, CDP and others Institutions.

It is planned to allocate more time to measure regional deformations and in particular for measuring the Medicina Noto baseline.

A new cooled S/X receiver, for primary focus of the dish, is under construction in the Institute microwave laboratory.

The system temperature of the new receiver is expected to be about 50 K, and it should be ready for June 1990.

A new HP Unix work station is funded and will be installed in Bologna and mainly used for geodetic VLBI data reduction.

## 5. REFERENCE

Cenci a., Vicomanni G., Bianco G., Caporali A.  
Telespazio report December 1988

P. Tomasi

Proceedings of the VII working meeting for geodesy and  
astrometry. 1989, in press.

Vierbuchen J. and Zarraoa N.

Proceedings of the VII working meeting for geodesy and  
astrometry. 1989, in press.

AGENZIA SPAZIALE ITALIANA

Centro di Geodesia Spaziale

VLBI Facility - Status Report

B. Pernice

The VLBI antenna at Matera Center for Space Geodesy is colocated with the long time operating SAO/SLR station and, for the end of 1990, a fixed ROGUE GPS receiver and a PRARE station are foreseen at the site. This will candidate the site as a geodetic fundamental station in the Mediterranean region.

The antenna is not operating yet but in May 1990 there will be the check out job done in cooperation with NASA/CDP at the site, intended to ready the station for geodetic VLBI campaigns.

The 20 m dish antenna has been designed and built to be mainly dedicated to geodetic VLBI (S/X band receiver system) but it has the capability to operate up to 25 GHz for radio astronomy observations. The main technical features are shown in Tab.1.

At the site is now installed the MARKIII DAT (from Signatrom Inc.) with a standard density tape recorder that will be shifted to high density as soon as possible.

The H-Maser EFOS VIII (from Oscilloquartz S.A.), housed in its thermal and magnetic passive controlled "bunker" at the site, will be integrated in a complete timing and syncro-system, monitored and controlled by an HP 9000/310M computer, by June 1990.

The computing facilities of the station, aside from the HP 1000/A400 VLBI field system, feature an HP PC VECTRA ES/12 and an HP 9000/835S with UNIX OS, with CALC/SOLVE package already installed for VLBI data analysis, both linked to the VAX cluster on DECnet.

Tab.1

PARAMETERS	UNITS	S BAND	X BAND
RF IF receiver sys:			
- Working RF Band	GHz	2.2 to 2.4	8.2 to 8.6
- 2dB Instant Band	MHz	140	400
- Working IF Band	MHz	190 to 330	100 to 500
- RF IF Gain	dB	70	70
- Gain Stability	dB/24h	+/- 2	+/- 2
	dB/1h	+/- 0.1	+/- 0.1
- Image Rejec. Specs.	dB	30	30
- Image Rejec. Meas.	dB	64	47
- 2 MHz Group Delay	nsec	-1	-1
- Input Level	dBm	-97	-90
- Output Level	dBm	-27	-20
Operation Specs.:			
- External Temp.	°C	-10 to 40	-10 to 40
- Wind Speed	Km/h	36 to 50	36 to 50
- Struts. Therm. Diff.	°C	<5	<5
- VLBI Sys. Sens.	JY	1	1
- Circ. Polarization		Right	Right
Spec. Sys. Noise Temp.	°K	140	140
Meas. Sys. Noise Temp.	°K	97	90

## **STATUS REPORT: Onsala Space Observatory**

**B.O. Rönnäng  
G. Elgered  
J. Johansson  
B. Nilsson  
K. Jaldehag**

### **Observations**

The geo-VLBI program is running smoothly with one to two 24-hour long experiments once per month in subprojects of the IRIS and CDP programmes.

Onsala also participated in the European mobile VLBI campaign, which is part of the EUREF project, during the period when the MV-3 VLBI system visited Mätsehoivi in Finland, Tromsø in Norway, and Brest in France. The obtained positions of these sites and several others will be used, among other things, to establish the European first order GPS reference frame.

A long term programme with S/X -band differential VLBI observations of 3C345/NRAO512 and 3C273B/4C39.25 started in 1987. The principal investigator is Tang Guiquang.

### **Water Vapour Radiometry**

A comparison with the Kalman filter method developed by Tom Herring shows that the WVR and Kalman filter methods give a weighted RMS scatter in the Onsala-Haystack/Westford baseline of 13 and 14 mm, respectively using 126 measurements from the period 1980-1988. However, using only the last 37 experiments the corresponding scatter becomes 10 mm for the WVR and 12 mm for the Kalman filter method. (Elgered et al. 1989 ).

In a joint project with NASA-GSFC a J03-radiometer were placed at Onsala for comparison measurements (G. Elgered et al. 1988, England et al. 1988 ). The two radiometers gave estimates of the wet delay that were in good agreement. Preliminary results for a two week long subset of the data gave an rms difference in wet delay of 5 mm including a bias of 1 mm.

### **GPS**

A local GPS network around the observatory has been established using WM-102 GPS-receivers (Johansson et al. 1988 ). The baselines of the network varies from 10 km to 100 km. The post-processing is performed using the Bernese software 3.1 running on a MacIntosh SE/30.

A CIGNET tracking station is in operation since December 1987.

Money has been allocated to invest in a new GPS tracking receiver.

## **New projects**

The geo-VLBI activity will be extended to include the Swedish-ESO submillimetre telescope (SEST) in Chili, with the first observations in April and June 1990. The Mark III equipment will be supplied by NASA-GSFC but the long term goal is to equip SEST with a complete VLBI system for geo- as well as astro-VLBI. The problem of regional crustal deformations will be handled by simultaneous GPS observations in cooperation with other groups, if possible.

## **Technical Development**

The observatory now owns two H-maser. However one of them still suffers from decreasing output power and is presently (Nov. 1989-Jan. 1990) in Switzerland to be repaired.

Development is under way to improve the X-band sensitivity by means of a new dual frequency feed and to increase the bandwidth as planned at Haystack Observatory and NASA/GSFC.

The upgrade of the water vapour radiometer will start in January 1990. It has been operating for 10 years in nearly all geodetic VLBI experiments. New back-end electronics, a PC-based data acquisition system, and improved temperature stability of the reference load will be installed.

The Mark III Field System is now running on a Hp A400 computer.

## **References**

Elgered, G., J.M. Johansson, B.O. Rönnäng, T.A. Clark, M.N. England, M.W. Hayes, and C.E. Kuehn, "REX-88: An Experiment Involving Water-Vapor Radiometry and Other Methods to Estimate the Wet Delay", *EOS*, 69, p. 1149, AGU Fall Meeting, 1988.

Elgered G., J.L. Davis, T.A. Herring, and I.I. Shapiro, "Geodesy by Radio Interferometry: Water Vapor Radiometry for Estimation of the Wet Delay", accepted for publication in *J. of Geophys. Res.*, 1989.

England, M.N., C.E. Kuehn, M.W. Hayes, T.A. Clark, G. Elgered, J.M. Johansson, B.O. Rönnäng, "REX-88: Water Vapor Radiometer Intercomparison -- Instrumental Performance and Data Quality", *EOS*, 69, p. 1149, AGU Fall Meeting, 1988.

Johansson, J.M., G. Elgered, and B.O. Rönnäng, "A Local GPS Network Around the Onsala Space Observatory", *EOS*, 69, p. 1150, AGU Fall Meeting, 1988.

## V.L.B.I. in Southern Europe

Paolo Tomasi

Istituto di Radioastronomia - C.N.R.  
Bologna - Italy

**ABSTRACT.** A project of V.L.B.I. observations for measuring regional deformation in southern part of Europe is presented. The actual hardware situation, new antennas in southern part of Europe already active, provide a potential European regional network for geodynamics and geodesy. The focus is pin pointed to the interactive zone between African and Eurasian plates and in particular to Italy.

### 1. INTRODUCTION

Without doubts the Mediterranean area is a very interesting one from geodesy and geodynamics. It is the area where African and Eurasian plates are colliding, and it is a very unstable area as is proved by its high seismicity.

For that the area was and is intensively monitored and studied with classic and space technique. Really only the South-eastern area was intensively studied, on large scale, by spatial method, as it is mobile Satellite Laser Ranging (S.L.R.). With this technique, in many cases linked together with GPS, many positions in eastern Mediterranean was surveyed in recent past and still are surveying.

For the western part of Mediterranean area the activity with mobile S.L.R. was less intense even if a number of places are routinely occupied by mobile laser equipment and the fixed station of Matera is working since 1983.

In any case a new powerful space technique is becoming more and more important in Europe: V.L.B.I. In fact, since 1987, at the Wegener/Medlas conference, J. Campbell (1988), pin pointed the potentiality of this technique in Europe, a large improvement in the hardware, and also in man power, come into the field.

In mid 1987 there was only three active stations, Onsala, Wettzell and Medicina fully equipped for geodynamical VLBI observations, and only one fully dedicated. Moreover, from the geodynamical point of view, the three antennas were almost aligned in North South direction and on stable European plate, with the exception of Medicina.

Now in Europe we have two more VLBI stations on intermediate area, Madrid (Spain) and Matera (Italy), and one more on African plate, or at the border of colliding zone, near Noto (Sicily). Noto and Madrid are already active in geodynamical VLBI, and Matera is expected to be operative at the beginning of 1990. For the Noto antenna (Tomasi, 1989) the starting experiment was East Atlantic 2 on June 89. In reality this experiment was no more an East Atlantic experiment, designed to measure the Atlantic enlargement, but the first European one. And with particularly good results! Every European baselines were computed with few



millimetres errors.

We can then consider that an European VLBI network is already active and more can be done in the future.

## 2. EXPECTED CRUSTAL MOTION

The motion of African plate and Eurasian plates is very difficult to assess for the possible presence of a number of microplates that can strongly modify the relative motion in the colliding area. In any case a reasonable scenario for the Mediterranean area is presented by Drewes and Geiss (1986). In this scenario it is considered only the horizontal motion, and we know that in many European areas also vertical motion is present, and in Italy there are historical records of large vertical motion.

In any case, from Drewes and Geiss (1986), at least for the horizontal motion, Onsala and Wettzell stations are on stable Eurasian plate, and can provide a stable baseline as a reference. From VLBI observations we have enough observations to confirm that (Campbell, 1988). Medicina, Madrid, Matera and Noto are on active areas, with expected horizontal velocity of 1 to 2 cm./year.

If we are going in the details of the expected motion in the southern part of Italy (Geiss and Drewes, 1988), in relation to different tectonic models, with or without a Ionian micro-plate, we can expect a different orientations in the velocity field but the same amount of 1 to 2 cm./year.

The expected velocity is totally within the capability of the actual VLBI technique. In fact, the Atlantic enlargement, about 15 mm/year, was measured in about five year with an error of 0.7 mm/year (Haystack Onsala baseline). That baseline was intensively observed during the last five years, and that is the main reason of the good results. However, the data quality of VLBI observations had a large improvement in the last year and, from the results of East Atlantic 1 and 2 (1989), we can easily conclude that European VLBI geodynamical data can be far better than transatlantic data.

That depends also from the diameters of the new operating antennas: Madrid, 34 meters dish, Noto 32 meters dish, the last one also with uncooled receiver, can provide data of good quality, as proved by 1989 S/X observations (E-Atl2, Euref and Navnet).

## 3. THE FUTURE OBSERVATIONS

Before starting plans for observations it is better to describe the situation on the VLBI stations. From 1987 (Campbell, 1988) major modifications happens at:

- Medicina, where an S/X cooled receiver is now present;
- Madrid, where a MarkIII Dat is now available;
- Matera, where construction is finished and MarkIII Dat will be available from January 1990;
- Noto, where an S/X uncooled receiver (from NASA) is available,

Field system is running on HP 1000 E, and a MarkIII Dat will be available (on loan from NASA) in January, February and also in October, November and December 1990. A VLBA terminal (fully compatible for geodetic VLBI will be available only from 1991).

In order to evaluate the possibility of a number of new observations, we have also to consider the hours of observations at each station. We know that Onsala, Wettzell, Madrid and Medicina antennas are havily scheduled, then not much time will be available for new observations. Matera will probably have more time available, at least at the beginning of the operations. Noto will have more time available than Medicina, at least for few years, because the antenna will have only few receiver available for astronomical VLBI, in the near future. A strong limit will arise for the lack of MarkIII Dat, but at least for 1990 (as was for 1989) the antenna will have the terminal from NASA.

From this situation it is reasonable to propose a regular number of 24 hours MarkIII observations, for all the European stations, three to five every year for about 4 years. That probably will provide a good geodetic informations without a large occupation of overscheduled antennas.

The schedule should be the same of East Atlantic experiment 1989.

A natural extension of the project could be the use of mobile VLBI antenna to establish a VLBI link with the North Africa (Algeria, Tunisia and Marroc). In fact, the Euref experiment have planned one occupation in Tiaret, Algeria. But the occupation was cancelled for political reason.

On particular baselines, the observations could be densified in time, using MarkII terminal, used in the past, and still used at present at the Robledo station near Madrid.

For intermediate distances, like the Italian baselines, and perhaps also for longer baselines, time multiplexing is a still valid technique. The observations are simpler, less quantity of tapes, just to remember one aspect, and can be easily correlated at the Medicina correlator (the old Block 0 on long term loan from JPL).

A connections with others technique will be very useful. In particular GPS observations, on a small network, will strongly help to understand the dynamic on particular regions. VLBI observations with the station of Noto, Matera and Medicina, could be connected with the Calabrian arc project seems.

#### 4. CONCLUSION

The conditions to establish a European VLBI network for geodynamics and geodesy are already on the field. The VLBI facilities covered a large part of Europe from North to South and are fully equipped with standard MarkIII Dat.

The study of regional deformations in Europe can be performed with VLBI technique with a small number of experiments per years. MarkII time multiplexing can be also used, on shorter baseline, for time densifications of baselines measurements. Some experiments with mobile VLBI on North Africa, will largely

improve the scientific results of the VLBI measures.

A connection with other spatial technique, in particular GPS seems very useful.

## 5. REFERENCE

J. Campbell

Proceeding of the III conference on the Wegener/Medlas Project.  
Baldi and Zerbini editors. 1988, pag. 361.

H. Drewes and E. Geiss

COSPAR XXVI Plenary Meeting, Symposium 2. "Application of Space  
Techniques for Geodesy and Geodynamics", 1986

E. Geiss and h. Drewes

Proceeding of the III conference on the Wegener/Medlas Project.  
Baldi and Zerbini editors. 1988, pag. 153.

P. Tomasi

Proceeding of The VII working meeting for geodesy and astrometry.  
1989, in press.

# VLBI DATA ANALYSIS OF IRIS CAMPAIGN

C. de Martino  
G. Verrone, D. Picca

Space Geodesy Center, Matera  
Dep. of Physics, Bari

Geodetic VLBI data have been analyzed. Baseline lengths and their time rates, have been estimated from a subset of data, spanning five years, of the IRIS project and using VLBI3 software. A standard least squares estimation has been carried out, the "a priori" standard deviations of the data had to be modified to account for systematic biases due to mismodelling of the clocks and atmosphere. VLBI3 has given results in good agreement with the ones obtained using the same campaign data and performed elsewhere, mostly in U.S.A.

## INTRODUCTION

A weighted least squares estimation can be performed via VLBI3 trying to minimize and randomize the differences between computed and observed delays (residuals). Theoretical uncertainties, computed from the SNR of observations do not realistically represent statistical standard deviations. So, to account for systematic errors, mainly due to random variations in the frequency standards, or insufficient modelling of the clocks and atmosphere behaviour, a new standard deviation had to be considered, so that the observation noise could be assumed to be a zero mean random process [1], [2]. That is to say the weights (reciprocal of variances) of the data had to be modified. A constant standard deviation, *bias*, is computed for each observing session, baseline by baseline, by an external routine to the VLBI3 software, so that the  $\chi^2$  per degree of freedom of the postfit residuals is near unity. The new standard deviation of the observation is computed adding in a root sum squared way to the "a priori" uncertainty, the *bias*.

## DATA ANALYSIS

The data we have analyzed, spanning five years, 1984-88, are a subset of 74 observing sessions of the IRIS data, including the stations of Westford, Wettzell and Ft. Davis. The criterion used to perform our analysis was to span a time interval, with one or two observing session per month, useful to meaningfully estimate the time rate of changes of the baselines.

Onsala station has been included only in the first step of our analysis, spanning two years, 1985-1986, with a subset of 14 observing sessions, owing to the criterion we used to select the observing sessions to be included in our analysis.

The first step was intended to assess the reliability of the "reweighting" technique: we analyzed a data set extended over three years, 84-86.

In the second step we extended the analysis to the 87-88 years.

We have not considered in this analysis the baselines including the Richmond station, owing to problems related to the special mounting of this antenna.

Using software VLBI3, developed at MIT (Massachusetts Institute of Technology) years ago and our routine BIAS, we have estimated the stations coordinates, except the reference one, usually Westford, the coordinates of all radio sources, except the right ascension of 3C273, which defines the origin of right ascension circle, and baseline lengths. The clock behaviours, at each station, can be modeled via polynomials (one or more for observing session). The atmospheric delay is very poorly determined because we can estimate only a correction to average zenith delay.

## RESULTS AND DISCUSSION

In Tab.1 are summarized the results obtained in the first step of the analysis, for two baselines including Onsala station, compared with the CDP values published in NASA-Technical Memorandum 100682.

The weighted mean of the estimated baseline lengths are listed with their WRMS, their slopes and the biases.

The compared values show differences in a range from a few millimeters to a few centimeters.

**Table 1**

	vbl3 85-86	cdp
<b>westford - onsala</b>		
length (cm)	560074147.5 +/- 0.4	560074150.0 +/- 0.3
WRMS (cm)	6.2	2.3
slope (cm/year)	0.7 +/- 0.2	1.2 +/- 0.2
N. of observations	2363	global solutions
bias (cm)	6.9	
<b>onsala - wettzell</b>		
length (cm)	91966101.1 +/- 0.2	91966100.3 +/- 0.2
WRMS (cm)	1.1	0.6
slope (cm/year)	0.5 +/- 0.1	0.0 +/- 0.1
N. of observations	850	global solutions
bias (cm)	3.0	

The added standard deviations range from 0.13 to 0.25 nanoseconds, that is to say the models used systematically need a correction of about 3-7 cm. This is mainly due to the atmosphere because the correction needed increases with increasing baseline lengths [5]. The influence of atmosphere on the baseline lengths is clearly seen if we consider the Onsala-Wettzell baseline, Fig.1. This european baseline is the shortest one considered in our analysis and its WRMS scatter about the mean is only 1.1 cm. whereas for longer baselines, Westford-Wettzell and Wettzell-Ft.Davis it is as high as 7.5 cm. and 10.9 cm., Fig.2-3.

That is to say the reweighting technique we apply once per observing session is able to account for a first order correction to the mismodelling of the clock and atmosphere, so that the residuals are not fully randomized and a more refined analysis is needed.

On this five years time span we estimated the best-fit slope of the baseline lengths. The slopes obtained in this analysis differ from the CDP ones, as in the case of Westford-Ft.Davis where we have a positive value, but on the contrary the Wettzell-Ft.Davis slope has the same value. On the other side CDP values are based on a wider time span, on a much more dense data set and on a network widely distributed, including mobile stations.

Of corse, we do not claim these slopes represent actual rates of changes of the baseline lenghts; our sparse time series cover a time too short, compared to geological times, to draw conclusive statements on baseline changes.

## CONCLUSIONS

The analysis we have performed was primarily intended to assess the reliability of the "reweighting" procedure to account for systematic biases. The strategy adopted with all the limiting factors, time

**Table 2**

	vib13 84-88	cdp
<b>westford - wettzell</b>		
lenght (cm)	599832530.3 +/- 0.2	599832534.3 +/- 0.1
WRMS (cm)	7.5	1.9
slope (cm/year)	0.53 +/- 0.03	1.34 +/- 0.08
N. of observations	4963	global solutions
blas (cm)	4.5	
<b>westford - ft.davis</b>		
lenght (cm)	313492797.6 +/- 0.1	313492798.9 +/- 0.1
WRMS (cm)	4.1	1.7
slope (cm/year)	1.22 +/- 0.01	-0.56 +/- 0.04
N. of observations	5093	global solutions
blas (cm)	4.2	
<b>wettzell - ft.davis</b>		
lenght (cm)	841756148.3 +/- 0.3	841756144.0 +/- 1.8
WRMS (cm)	10.9	3.3
slope (cm/year)	0.09 +/- 0.10	0.09 +/- 0.20
N. of observations	2568	global solutions
blas (cm)	3.9	

span, data density and so on, gives results which are of considerable quality when compared with the CDP results, which are based on a more sofisticated models for clocks and atmosphere, on a much higher time span, on a very high quantity of data and on a different strategy adopted in the data

analysis (Global Solution) performed with the CALC-SOLVE software. Moreover care must be taken in comparing these results owing to the fact that also the CDP results are subject to refinements due to different models and strategy adopted. This implies that much better results will be established with a wider time span and more dense data.

### ACKNOWLEDGEMENT

We wish to thank Prof. J.Campbell of the Geodetic Institute of the University of Bonn, and Doct. H.Schuh, FRG, for supplying data and helpful discussion.

**This work is supported by Agenzia Spaziale Italiana.**

### REFERENCES

- [1] T.A.Herring, I.I.Shapiro, T.A.Clark, C.Ma, J.W.Ryan, B.R.Schupler, C.A.Knight, G.Lundqvist, D.B.Shaffer, N.R.Vandenberg, B.E.Corey, H.F.Hinteregger, A.E.E.Rogers, J.C.Webber, A.R.Whitney, G.Elgered, B.O.Ronnang, J.L.Davis Geodesy by Radio Interferometry: Evidence for Contemporary Plate Motions J.G.Res. vol.91, N.B8, p.8341-8347, 1986
- [2] T.A.Clark, B.E.Corey, J.L.Davis, T.A.Herring, H.F.Hinteregger, C.A.Knight, J.L.Levine, G.Lundqvist, C.Ma, E.F.Nesman, R.B.Phillips, A.E.E.Rogers, B.O.Ronnang, J.W.Ryan, B.R.Schupler, D.B.Shaffer, I.I.Shapiro, N.R.Vandenberg, J.C.Webber, A.R.Whitney Precision geodesy using the MARKIII very long baseline interferometer system IEEE Trans. Geosci. Remote Sensing, GE-23, p.438-449, 1985
- [3] T.A.Herring  
Very Long Baseline Interferometry and its contribution to Geodynamics in Space Geodesy and Geodynamics. A.J.Anderson and A.Cazenave eds. Academy Press, 1986
- [4] J.W.Ryan, C.Ma CDP Data Analysis - 1987 NASA Technical Memorandum 100682, 1987
- [5] T.A.Herring  
Precision of Vertical Position estimates from VLBI J.G.R., vol.91, N.B9, p.9177-9182, 1986

# FIGURES

Figure 1

ONSALA - WETTZELL

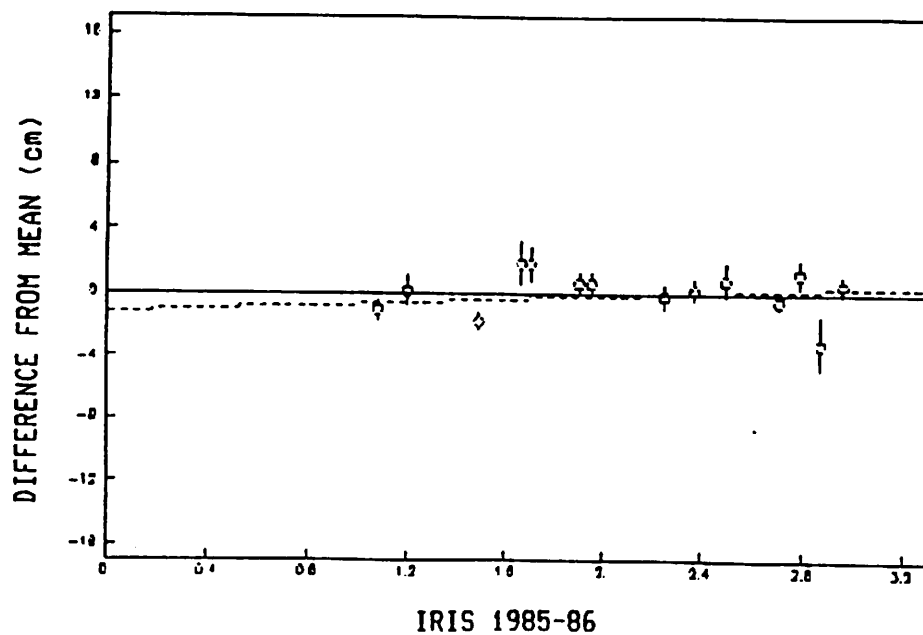
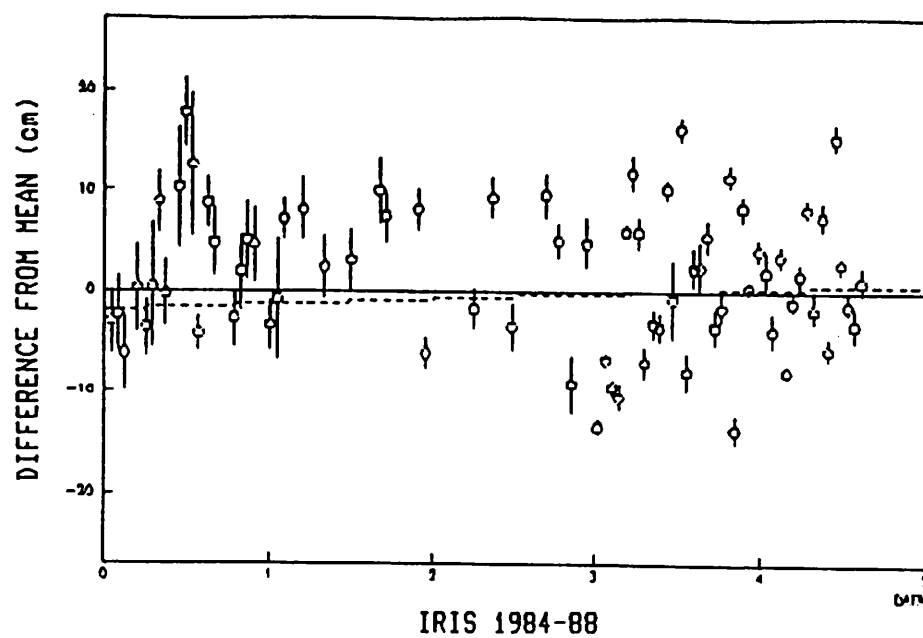


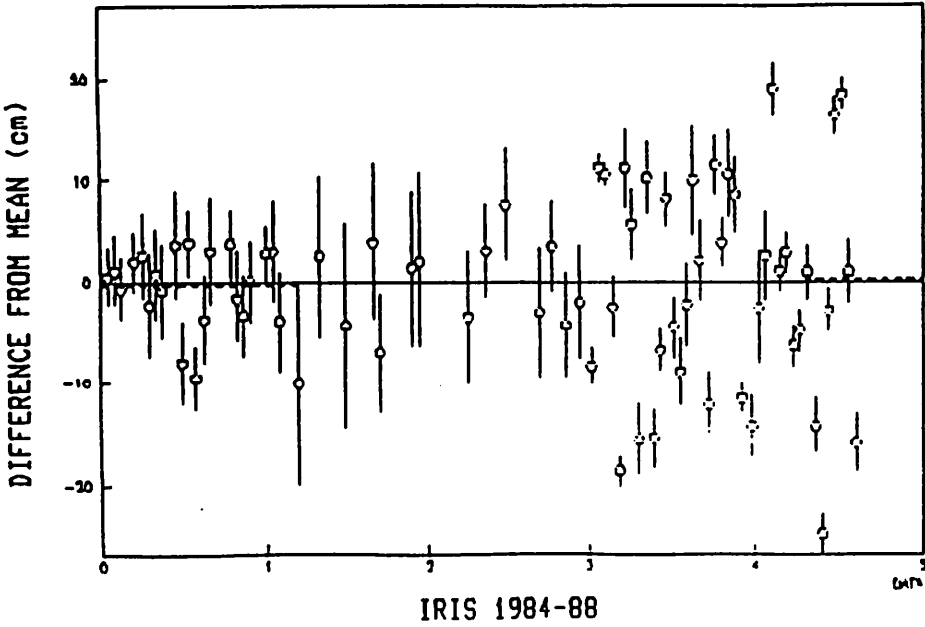
Figure 2

WESTFORD - WETTZELL





**Figure 3**  
FORTDAVIS - WETTZELL



# **A Proposal: European Geodetic VLBI for the determination of land subsidence and sea level rise**

Paper presented at the 7th Working Meeting on European VLBI for Geodesy and Astrometry,  
Madrid, Spain, 26-27 October 1989

by

**Frits J.J. Brouwer and Ronald E. Molendijk**  
Survey Department of Rijkswaterstaat, Delft.

## **1. Introduction.**

This paper is a proposal for the organization of a series of geodetic VLBI observing sessions by the European VLBI Network (EVN) for the determination of land subsidence and sea level rise on a continental scale.

The background for this proposal is our opinion that under the Crustal Dynamics Project (CDP), attention is too much focussed on horizontal deformations and hardly at vertical ones. Furthermore, we believe that there is a need for a typical European effort in the field of the application of geodetic space techniques to crustal deformations and this area of land subsidence and sea level rise is a prominent candidate.

That this proposal originates from The Netherlands, one of what is called the Lower Countries, is obvious, as we in The Netherlands - also in view of Fig. 1 - are much more afraid of vertical deformations, i.e. sea level rise, than of horizontal ones, i.e. earthquakes.

## **2. Land Subsidence and Sea Level Rise in The Netherlands.**

In The Netherlands we have some 10 tide gauges checking the Mean Sea Level (MSL) along the North Sea coast (Fig. 1). The observed sea level rise at these gauges varies between 10 and 22 cm/century. (N.B. all data records are at least a century long). This presents a rather big variation over such a small area, part of which certainly can be explained by local effects (currents, coastal erosion, etc.). Nevertheless, the major question remains: what part of these numbers is (eustatic) sea level rise and what part is land subsidence? Obviously, it should not happen that land subsidence is mistakenly considered as sea level rise due to climatic change and global warming! (N.B. The sea level rise expected from the latter is approximately 70 cm/cy).

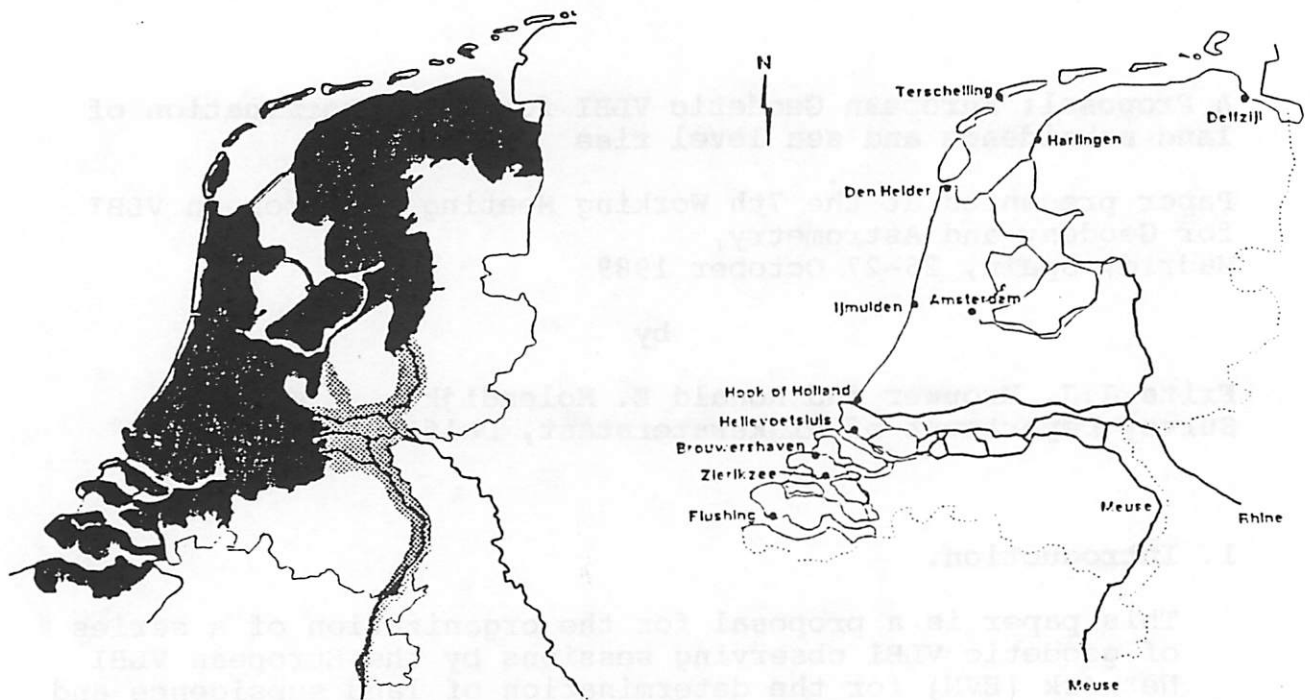


Figure 1. The Netherlands without water defence with inundation due to the sea (black) and inundation due to the major rivers (grey) - left figure - and the 10 main Dutch tide gauges - right figure.

In The Netherlands much effort has been put into research for the determination of land subsidence on the basis of over 60 years of levelling. Since the 1920's in total 3 primary levellings have been surveyed and after that also a set of secondary levellings with national coverage. On the basis of these data we have identified two areas along the coast with significant land subsidence, reaching a magnitude of over 7 cm/cy: North of Amsterdam, around Alkmaar and around Rotterdam (Fig. 2). On the other hand, the area around Zandvoort seems to be completely stable. The final valuation of the significance of these data is at present still in progress.

### 3. The European case.

The analogous approach could also be applicable to the European case of measuring land subsidence in the perspective of sea level rise. However, the Unified European Levelling Network (UELN, Fig. 3) is not useful for this, since it has not been resurveyed at different epochs and its connections to the tide gauges are doubtful.



**Figure 2.** Land subsidence in the Netherlands estimated on the basis of 60 years of levelling; 3 cm/cy (grey) and 6 cm/cy (black).

Consequently, an approach based on the application of the Global Positioning System (GPS) and VLBI according to Fig. 4 seems more realistically. In this scheme, VLBI provides the "backbone" of the reference system, so that repeatedly - combined with some levelling - the relative heights of the zero points of a large number of tide gauges can be determined in a quick and accurate way. Over the years, the vertical motions of the tide gauges can thus be monitored, by handling the data as a "deformation problem". As a result the recorded sea level rise can be freed of the vertical crustal movement part.

#### **4. Considerations for a VLBI height campaign.**

As a major contribution to the above scheme, we would like to propose a series of VLBI campaigns, directed at the determination of the relative heights of the VLBI antenna's.

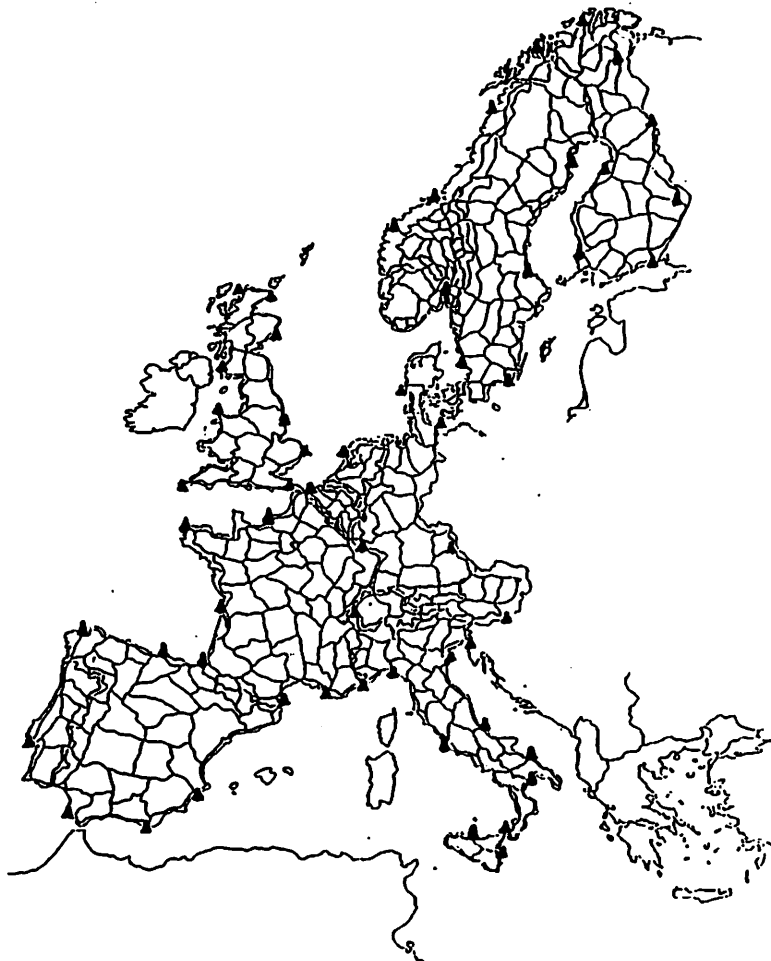


Figure 3. The Unified European Levelling Network (▲ = main tide gauges).

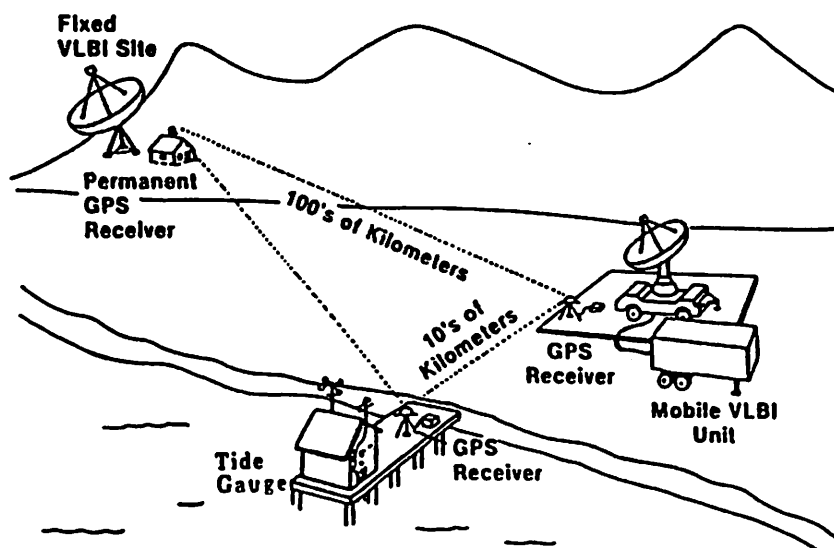


Figure 4. Simultaneous surveying with GPS and VLBI.

We summarize the reasons why VLBI is essential:

- it provides the "backbone" to GPS;
- it provides centimetre accuracy over thousands of kilometres;
- in Europe a number of VLBI stations are near the coast and others are "safely" in the central part;
- the matter is just well suited for a typical European effort.

The observations should of course be S/X, so that in the not too far future (say mid 1990) some 8 European VLBI stations should be able to participate (Fig. 5), i.e.

- Wettzell (D)
- Effelsberg (D)
- Onsala (S)
- Madrid (E)
- Bologna (I)
- Matera (I)
- Noto (I)
- Westerbork (NL)

We would like to have some 2-3 experiments per year, not more due to logistics, for the next 2-3 years, as a start, just to prove the feasibility.

From the organisational side, matters as the commitments of the participants, the set-up of a coordinating centre, the availability of MARK-III tapes etc., should be discussed at some stage.

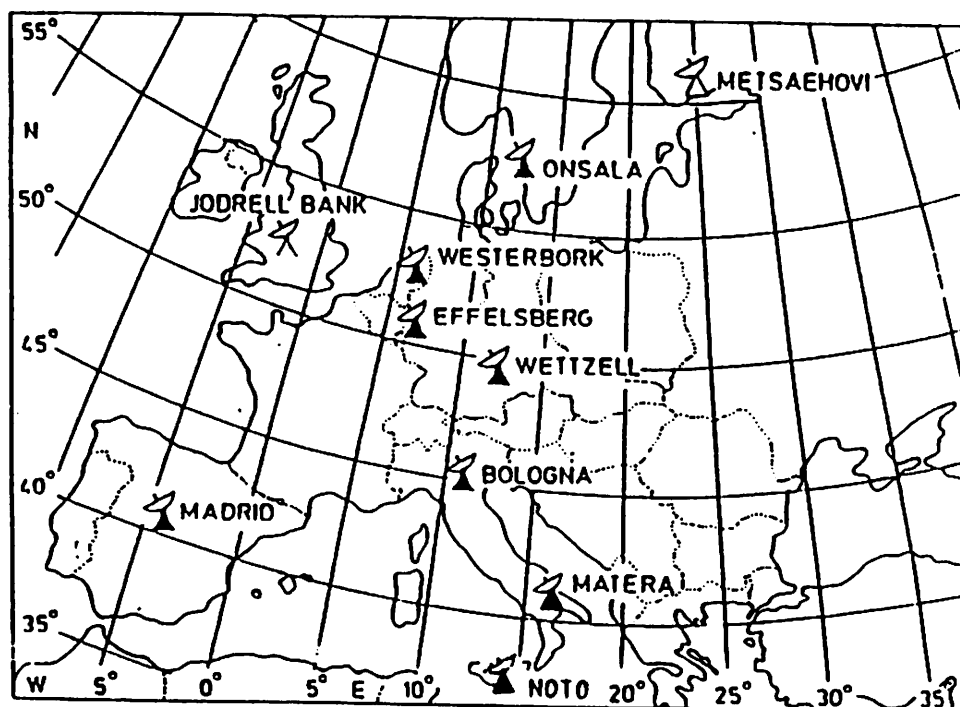


Figure 5. The eight possible participants in a European VLBI Height Campaign.

From the scientific side however, we identify two major items that should be addressed, as one realizes that it is very difficult to reach centimetre accuracy in height over continental distances, namely:

- the matter of an optimized observing schedule, as most of the time the "standard" IRIS or CDP schedules are taken. It is obvious that a campaign aiming at precise height differences requires a different schedule from one directed at plate motion determination. So, some work has to be done in this field.
- the need for re-assessment of correction models: it is common knowledge that the accuracy of geodetic space techniques (both VLBI, GPS and SLR) in vertical position determination is worse than for the horizontal case, the reason of course mainly being the presence of atmospheric refraction. It may therefore be wise to reconsider all correction models according to their "vertical correctness" and possibly change a few.

## 5. Related Programmes.

The Survey Department of Rijkswaterstaat is very much in favour of the application of the VLBI technique to vertical (crustal) deformation studies on a European scale; one manyear of academic staff has been attributed to a feasibility study in this field during 1989/90. Therefore, we are quite willing to contribute in the planning, execution and analysis of any adopted VLBI-campaign related to the subject at hand.

In addition, mention of this possibility has also been made in the Dutch part of the proposal for the study of sea level rise to the European Community under the E.P.O.C.H.-programme (Climatology and Natural Hazards). This proposal is put forward by a consortium of research institutes from 9 countries (B, DK, D, F, GR, I, NL, UK, EIR); closing date of E.P.O.C.H. proposals is December 1, 1989. This project might give an extra dimension, - also financially - to the present EVN-proposal.

On the longer term a more continuous way of funding will be needed, but let us start with some test-experiments!!!

# **The East-Atlantic Experiments: Results For The European Stations**

Jost Vierbuchen  
Geodätisches Institut der Universität Bonn  
Nußallee 17, D-5300 Bonn 1, FRG

Nestor Zarraoa  
Instituto De Astronomía Y Geodesia  
C.S.I.C.-U.C.M., E-28040 Madrid, Spain

**ABSTRACT:** A first series of geodetic VLBI experiments in which four European stations using the Mark III system were involved, was started in 1988. The stations took part in a network called the East-Atlantic-Network (E.ATL). The VLBI experiments within the E.ATL network are part of the Crustal Dynamics Project (CDP) of NASA. The final data analysis, i.e. the determination of the stations terrestrial coordinates and of the baseline lengths has been carried out at the Geodetic Institute, University of Bonn using the Mark III Data Analysis System ("CALC/SOLVE"). Special emphasis has been placed on the European baselines because these will be used as a reference for future regular European VLBI campaigns to monitor crustal motions. Moreover, these experiments will provide a European terrestrial reference network e.g. for the Global Positioning System (GPS). The results obtained from the experiments presented here give a first impression of the repeatability and reliability of the European baseline lengths as well as of the station coordinates. The overall-accuracy of the experiments will also be discussed by comparing these results with results from IRIS-sessions.

## **1. INTRODUCTION**

At the last meeting of this Working Group in Bologna in April 1988 the growing number of operational stations for geodetic VLBI in Europe became obvious. Paying credit to this fact, the Crustal Dynamics Project (CDP) observation plan was split into the East-Atlantic (E.ATL) and the West-Atlantic (W.ATL) schedule. The E.ATL-network places special emphasis on the participating European stations, with Onsala, Wettzell, Medicina, Madrid and now Noto, which are connected to Westford and Richmond on the U.S. side (Campbell, 1988a). Based on this, the contribution of European VLBI to monitor crustal motions was discussed (Campbell, 1988b). At this meeting we can provide the "zero-epoch" data obtained from the analysis of these experiments covering a period of more than one year. Thus, the first step has been done to make VLBI data available for European geodesy, and the continuing activities in 1990 promise first results for European geodynamics.

## **2. NETWORK CONFIGURATION AND SCHEDULE OF THE E.ATL-EXPERIMENTS**

Five E.ATL sessions took place in 1988 and three were scheduled for 1989, but only two were executed; the third one was postponed to January 1990 because of the observing activities associated with the Loma Prieta earthquake in October 1989. In all, seven stations took part in at least one of the seven E.ATL experiments: Westford (E) and Richmond (R) in the United States and Onsala (T), Wettzell (V), Bologna (Medicina-L), Madrid DSS65 (M) (Rius, 1988) and Noto (N) (see fig.1 for the European part).

All of these stations are equipped with the hardware and software necessary to perform geodetic VLBI observations: a Mark III Data Acquisition Terminal, a combined S/X-band receiver, a hydrogen-maser and the Field System software.

The duration of each session was 24 hours.

Table 1 shows the observation plan for all E.ATL experiments. Due to problems with the H-maser the station Onsala could not participate in E.ATL-3/88 and Wettzell failed due to problems





Fig. 1: European part of the East-Atlantic network

Session	Date	Stations	Para	WRMS [psec]
E.ATL-1	Mar. 09, 1988	ERV T	34	77
E.ATL-2	Jun. 17, 1988	ERV TL	54	96
E.ATL-3	Aug. 31, 1988	ERV LM	49	97
E.ATL-4	Nov. 09, 1988	ER TLM	45	102
E.ATL-5	Dec. 14, 1988	ERV TLM	62	57
E.ATL-1	Feb. 20, 1989	E VTLM	81	62
E.ATL-2	Jun. 03, 1989	E VT MN	60	69

Tab. 1: Observation plan of E.ATL.  
Number of parameters solved for and weighted RMS of the group delays [picosec] for each session.

with the formatter at E.ATL-4/88. Thus, it has to be pointed out, that in none of the seven experiments the subset of stations used is the same (see tab.1).

For the first experiments (E.ATL-1/88 - E.ATL-3/88) the observing schedule has been derived from the former Cross-Atlantic schedule of CDP. From E.ATL-4/88 onwards the schedule was optimized in order to obtain the best coordinate estimates on the European side. This results in an increasing number of observations for the European stations and a better sky-coverage of the observations.

### **3. DESCRIPTION OF THE DATA ANALYSIS**

The correlation of the data was partly done at the Washington correlator and partly at the Bonn correlator of the Max-Planck-Institute for Radio Astronomy. The geodetic data analysis was performed on the HP 1000F of the Geodetic Institute of the Bonn University using the "CALC/SOLVE" software system (final F-processor version). This well-known software package allows multibaseline solutions; the results were compared with the results of single baseline solutions obtained by the OCCAM software system (see report by Zarraoa et al. in these proceedings).

#### **3.1 REFERENCE SYSTEM**

The celestial reference frame was defined by adopting the source coordinates of the Global Solution GLB 121 of the NASA-CDP data analysis - 1987 (Ryan and Ma, 1987). The station coordinates of Wettzell were taken from the same solution GLB 121 to define the terrestrial reference frame. These systems were tied together by adopting the smoothed values of the Earth rotation parameters (section 1 - final values), which are published by the International Earth Rotation Service (IERS Bull. B).

We have to bear in mind that the data sets of coordinates and ERP are not entirely consistent, but there were no better sets available to us at the time.

The precession and nutation models used in the data analysis are the J2000.0 and the IAU 1980 models, respectively (Kaplan, 1981). The geophysical and astronomical models used in CALC have been described in detail by Ma (1978).

#### **3.2 PARAMETRIZATION OF THE SOLUTIONS**

The number of geodetic VLBI observables (i.e. group delays and delay rates) in the solutions differed very much; it ranged from 523 observation pairs to about twice the number. Reasons for this are the different number of stations participating in the sessions and significant differences of performance in the individual experiments.

Additional data used in the analysis are meteorological and cable calibration data.

Regarding the parametrization of the solutions it has to be pointed out, that because of the limitations of the computing facilities the individual experiments were separately analysed. At present, our available hard- and software does not yet permit a combined so-called "global" solution. For the same reason the atmospheric delays at all sites as well as the clock-drifts could not be seen as estimated Markov processes obtained by using a Kalman filter technique (Rönnäng, 1989; Elgered et al., 1988).

Thus, the deterministic method was adopted to monitor the clock behaviour by a second-order polynomial fit and additional clock breaks, where it seemed to be necessary. The atmospheric delay offset in zenith direction was estimated by a first-order polynomial in time.

Two different atmospheric mapping functions were used: the CfA 2.2 model (Davis and Herring, 1984) and the Marini model (Marini, 1972).

In addition to these we solved for coordinates of each station except the reference-station Wettzell (in E.ATL-4/88 Onsala has been chosen as the reference) and for daily nutation offsets in longitude and obliquity, if necessary. Also, we solved for the coordinates of apparently not well-determined sources.

In table 1 the number of parameters to solve for in each experiment is given as well as the overall quality represented by the weighted RMS residuals of the group delays.

### **4. RESULTS FOR BASELINE LENGTHS**

In table 2 the computed means of the estimated baseline lengths are given together with their RMS-scatter and their  $1\sigma$ -formal errors. The RMS-scatter is equivalent to the repeatability and gives the most important criterion for the quality of the baseline length determination. It can be seen that the  $1\sigma$ -formal errors are too optimistic by a factor of about 2.

The deviations of the lengths of the individual experiments lie within a  $\pm 10$  mm range around the computed means for the European baselines, with one outlier (see fig. 2a, 2b).

Baseline	Length	$1\sigma$	RMS
	[m]	[m]	[m]
Wettzell - Medicina	522461.127	0.002	0.005
Wettzell - DSS65	1655418.172	0.001	0.002
Wettzell - Onsala	919660.991	0.001	0.002
Wettzell - Noto	1371101.056	0.003	-
Medicina - DSS65	1378852.871	0.003	0.006
Medicina - Onsala	1429470.388	0.003	0.006
DSS65 - Onsala	2205023.094	0.005	0.010
DSS65 - Noto	1711832.906	0.003	-
Onsala - Noto	2280154.883	0.004	-
Wettzell - Westford	5998325.364	0.011	0.025
Medicina - Westford	6144872.327	0.017	0.039
DSS65 - Westford	5300362.806	0.007	0.015
Onsala - Westford	5600741.490	0.008	0.019
Noto - Westford	6744637.336	0.011	-
Wettzell - Richmond	7588398.491	0.025	0.066
Medicina - Richmond	7658214.844	0.022	0.043
DSS65 - Richmond	6726067.062	0.024	0.042
Onsala - Richmond	7307152.480	0.043	0.085
Westford - Richmond	2044501.744	0.013	0.030

Tab. 2: Estimated baseline lengths,  $1\sigma$ -formal error and RMS-error in meter.

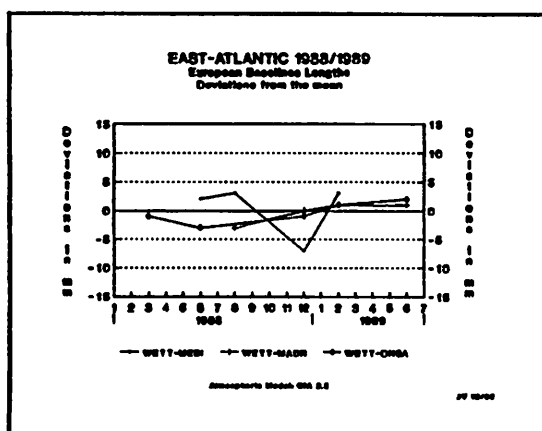


Fig. 2a: Baseline lengths estimates. Baselines to Wettzell.

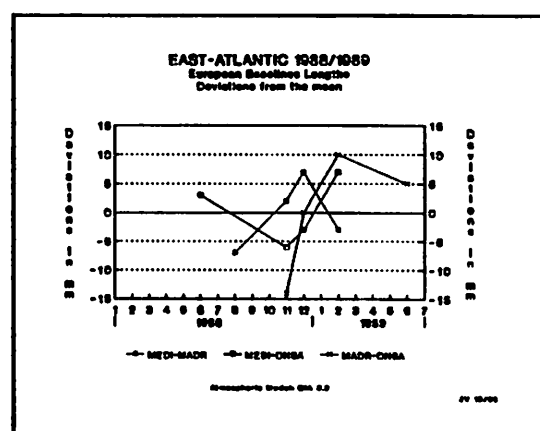


Fig. 2b: Baseline lengths estimates. European baselines.

The performance of the baselines to Westford is worse because of the much longer baselines (see fig. 2c). The maximum deviation from the mean is about 50 mm for a 6,100 km baseline. A systematic behaviour in the data can also be seen (fig. 2c) - perhaps a seasonal effect (longer baselines in winter-time than in summer).

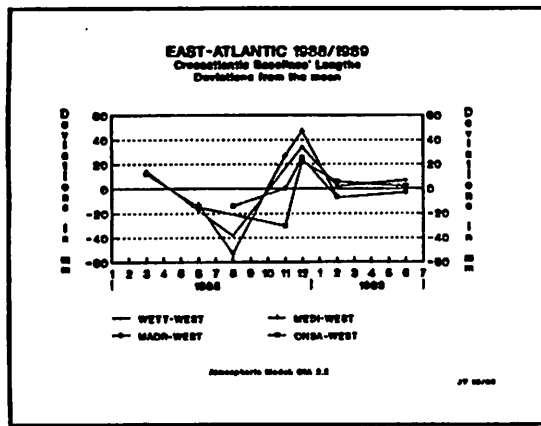


Fig. 2c: Baseline estimates. Baselines to Westford.

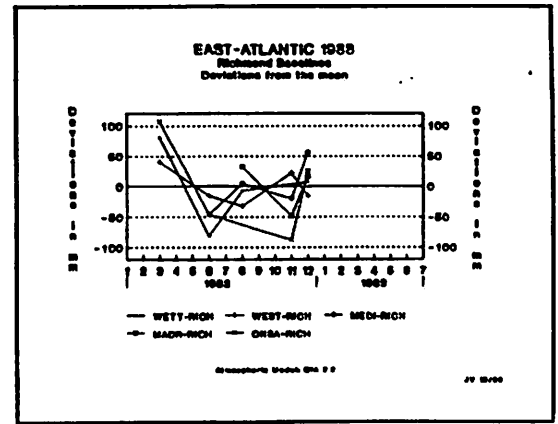


Fig. 2d: Baseline estimates. Baselines to Richmond.

Figure 2d shows the rather poor estimates for the baselines to Richmond compared with the other results. One reason for this may be the schedule, which is dominated by the European stations. The baseline repeatability, expressed by the RMS-error with respect to baseline length is plotted in figure 3. The dots represent the results for the solution using the CfA 2.2 mapping function while the bars represent those for the Marini mapping function. A relative error of  $db/b = \pm 0.5 \cdot 10^{-8}$  for the determination of the baseline lengths can be derived from this plot.

We can also see that the CfA 2.2 mapping function appears to model the atmospheric behaviour for the short baselines (<6,000 km) better than for the long baselines, compared with the Marini mapping function. We did not expect this result, because the CfA 2.2 model has been improved mainly for observations at low elevation angles, which predominate on the long baselines. The baseline length estimates are affected significantly by the differences between CfA 2.2 and Marini. Figure 4 shows these differences with respect to baseline length. The strong dependence, which has also been reported by Davis and Herring, is obvious. We found a slope of about -10 mm/1000 km (in the sense: CfA 2.2 minus Marini) which corresponds to the value of about -8 mm/1000 km estimated by Davis and Herring (1984).

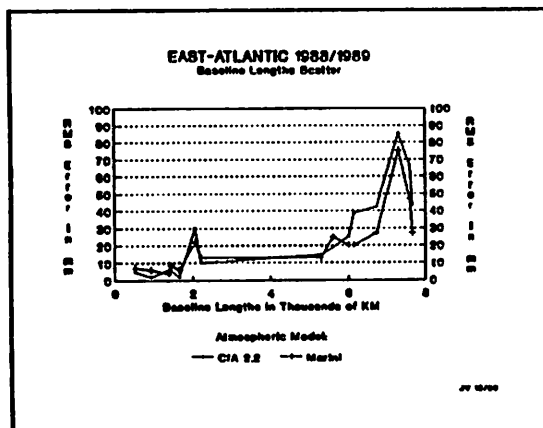


Fig. 3: Repeatability of baseline lengths.

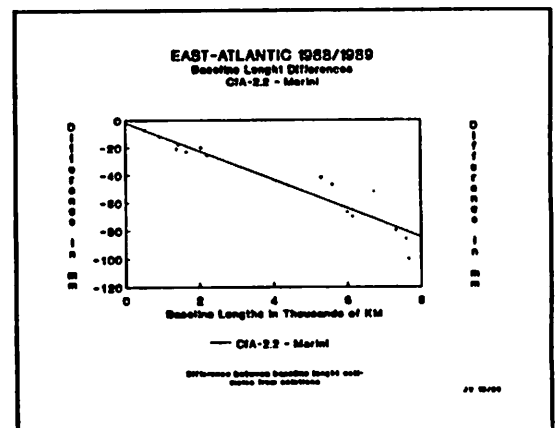


Fig. 4: Difference between baseline lengths estimates (CfA-2.2 - Marini Mapping function).

## 5. RESULTS FOR STATION COORDINATES

Table 3 gives the means of the coordinates X, Y, Z (referred to Wettzell) together with the RMS-error and their mean  $1\sigma$ -formal error. Again the scatter of coordinates expressed by the RMS-error is equivalent to the repeatability.

Station	X $\sigma$ RMS	Y $\sigma$ RMS	Z $\sigma$ RMS
Wettzell	4075541.953 - -	931734.216 - -	4801629.397 - -
Medicina	4461372.064 0.010 0.031	919595.778 0.004 0.020	4449559.226 0.011 0.061
DSS65	4849338.762 0.012 0.050	-360489.800 0.004 0.019	4114748.859 0.012 0.056
Onsala	3370608.090 0.006 0.011	711916.456 0.003 0.037	5349830.768 0.007 0.016
Noto	4934565.162 0.007 -	1321200.269 0.003 -	3806484.470 0.008 -
Westford	1492208.808 0.013 0.249	-4458131.436 0.019 0.113	4296015.717 0.019 0.102
Richmond	961260.168 0.026 0.358	-5674090.944 0.046 0.168	2740534.029 0.034 0.064

Tab. 3: X, Y, Z - coordinates,  $1\sigma$ -formal errors (2nd line) and RMS-error (3rd line) in meter. Wettzell is the reference station. All values given in meter.

Much easier to interpret than the cartesian coordinates are ellipsoidal coordinates. Therefore, we computed the RMS-scatter about the mean in a local, horizontal system of each station (see fig.5). The results for the European stations indicate that according to Herring (1986) the precision of the height determined by VLBI at each site is about  $\pm 6$  cm. The scatter of local horizontal coordinates is of course much better (with the exception of the north-component at Onsala). The results for Westford have less interpretational value due to the baseline geometry. It can be clearly seen, that the formal errors are much too optimistic, most of all for the vertical component.

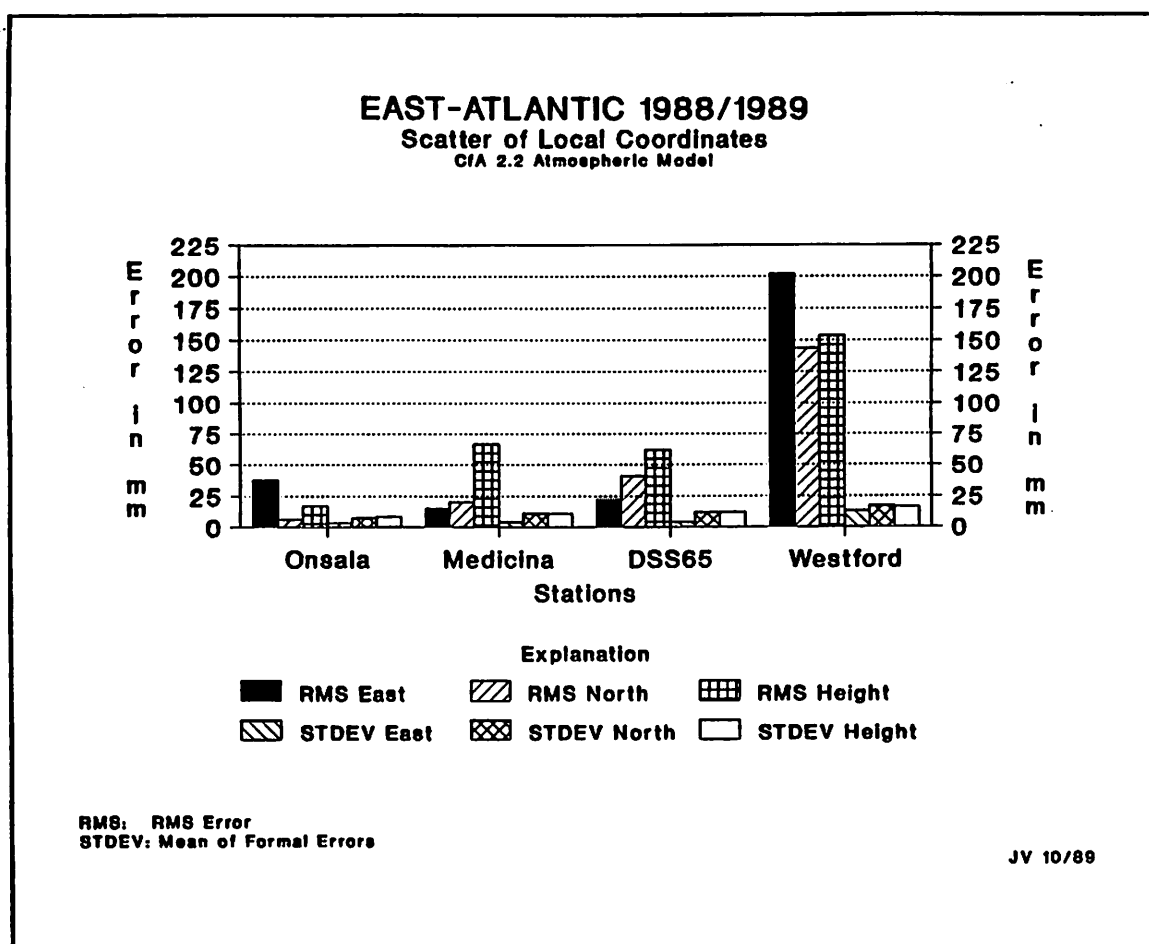


Fig. 5: RMS-error and  $1\sigma$ -formal error of coordinates expressed by local horizontal and vertical components.

## 6. ACCURACY OF EARTH ROTATION PARAMETERS DETERMINATION

Instead of solving for coordinates of the entire set of stations we performed an analysis keeping the coordinates of the well-determined stations (Westford-Onsala-Wettzell) fixed and solving for the Earth rotation parameters: dUT1,  $x_p$ ,  $y_p$  and daily nutation offsets in longitude and obliquity ( $d\psi$ ,  $d\epsilon$ ). The values listed below (see tab.4) are the computed mean values of  $1\sigma$ -formal errors compared with those, which are typical for solutions of the recent IRIS-A

NET	dUT1 msec	$x_p$ mas	$y_p$ mas	$d\psi$ mas	$d\epsilon$ mas
E.ATL	0.035	1.1	0.6	0.5	0.2
IRIS-A	0.035	0.7	0.5	0.9	0.4

Tab. 4: Comparison of Earth rotation parameters obtained by observations in the E.ATL-network with those of the IRIS-A network.

network (IRIS Bull. A). These results indicate that the overall-quality and reliability of the observations in the E.ATL-network is equivalent to those of the IRIS-A network.



## **7. CONCLUSIONS AND OUTLOOK**

In spite of the good quality of the results presented here there are some improvements to the data-analysis, which still have to be made:

- Adopt a consistent data set of source and station coordinates as well as of Earth rotation parameters as a-priori values.
- Run a global solution on all seven E.ATL experiments to obtain zero-epoch coordinates for the stations in a single least-squares fit, and compare these results with the mean values presented here.
- Use the Kalman filter technique to monitor the behaviour of the atmosphere at each station as well as the clock-drift. This method promises a reduction of the RMS-scatter in particular for the determination of local vertical components.

The main results of the analysis of the experiments in the East-Atlantic-network presented here are:

- The repeatability for European baseline lengths is less than  $\pm 10$  mm, resulting in a relative error of  $db/b = 0.5 \cdot 10^{-8}$ .
- The repeatability for European station coordinates (referred to Wettzell) is less than  $\pm 50$  mm in each component (X,Y,Z) or expressed in local horizontal and vertical coordinates better than about 60 mm for the height and much better for the horizontal components.
- The quality of the observations in this network is equivalent to that of the IRIS-A network applying the precision of the Earth rotation parameters as a standard.

Thus, the E.ATL-network will help us to establish a stable reference frame for European geodesy, in particular to give a valid set of coordinates for using the fiducial station concept in the analysis of continental GPS networks.

The final conclusion may be, that some more years of observations and data of the same quality will be necessary and sufficient to provide European geodynamics with an alternative and complement to the WEGENER/MEDLAS project:

Monitoring effects of plate motion in Europe independently by VLBI.

## **8. ACKNOWLEDGEMENTS**

The authors would like to thank the staffs at the participating stations and the members of the VLBI processing centers at Bonn and Washington correlator.

In particular the European geodetic VLBI community is grateful for the support of NASA/CDP, which made these experiments possible.

## **9. REFERENCES**

- Campbell, J.: Status of The Geodetic VLBI Campaigns in Europe. Proceedings of The 6th Working Meeting on European VLBI for Geodesy And Astrometry, April 28 and 29, 1988, Bologna, Italy, 1988a.
- Campbell, J.: The European VLBI Contribution To The Crustal Dynamics Program. Proceedings of The 6th Working Meeting on European VLBI for Geodesy And Astrometry, April 28 and 29, 1988, Bologna, Italy, 1988b.
- Davis, J. L., Herring, T. A.: New Atmospheric Mapping Function. Center For Astrophysics, Technical Memorandum No. 617 495-9279, Cambridge, Mass. 1984.

- Elgered, G., Davis, J. L., Herring, T. A., Shapiro, I. I.: The Effect of Water-vapor Radiometer Data From Onsala On The Repeatability of Baseline-length Determinations. Proceedings of The 6th Working Meeting on European VLBI for Geodesy And Astrometry, April 28 and 29, 1988, Bologna, Italy, 1988.
- Herring, T. A.: Precision of Vertical Position Estimates From Very Long Baseline Interferometry. Journal of Geophysical Research, Vol.91, No.B9, p.9177-9182, August 10, 1986.
- Kaplan, G. H.: The IAU Resolutions on Astronomical Constants, Time Scales, and the Fundamental Reference Frame. USNO, Circular No.163, Washington, 1981.
- Ma, C.: Very Long Baseline Interferometry Applied To Polar Motion, Relativity and Geodesy. NASA Technical Memorandum No. 79582, Greenbelt, Md., 1978.
- Marini, J. W.: Correction of satellite tracking data for an arbitrary tropospheric profile. Radio Science 7, p. 223-231, 1972.
- Rius, A.: Madrid Deep Space Communications Complex Status Report. Proceedings of The 6th Working Meeting on European VLBI for Geodesy And Astrometry, April 28 and 29, 1988, Bologna, Italy, 1988.
- Rönnäng, B. O.: Geodesy-VLBI Observables. Proceedings of the NATO Advanced Study Institute On The Technique and Applications of Very Long Baseline Interferometry. Castel S. Pietro Terme, Bologna, Italy, September 12-23, 1988. Published by Kluwer Academic Publishers, Dordrecht, The Netherlands, 1989.
- Ryan, J. W., Ma, C.: Crustal Dynamics Project Data Analysis - 1987. NASA Technical Memorandum No. 100682, Greenbelt, Md., 1987.
- IERS Bulletin B issued monthly by the International Earth Rotation Service (Feissel et al.), Paris, 1988-1989.
- IRIS Bulletin A issued monthly by the subcommission IRIS (J. Campbell et al.), NGS/NOAA, Rockville, Md., USA, 1989.



# **VLBI Surveying between DSS63 and DSS65**

**C. S. Jacobs  
Jet Propulsion Laboratory**

**A. Rius  
Instituto de Astronomía y Geodesia.C.S.I.C.-U.C.M.**

## **Abstract**

Using VLBI phase delay measurements, the baseline between Deep Space Station (DSS) 63 and DSS 65 has been measured at two epochs with formal uncertainties of a few millimeters (mm). A study of the internal consistency of the data has revealed systematic errors at the 10 mm level. In this paper we summarize the results obtained so far. A more detailed report is in preparation.

## **I. Introduction**

The Madrid Deep Space Communications Complex (MDSCC) is part of the NASA Deep Space Network (DSN). While the primary use of these facilities is for tracking planetary probes, time is also allocated to radioastronomical and geodynamical experiments. In order to connect the results of experiments which used different antennas a program for measuring the baseline from DSS63 to the DSS65 VLBI reference points has been started.

## **II. The interferometer setup**

Two experiments have been done: the first on 880404 and the second on 890502. Both experiments observed at S-band (2.3 GHz) and X-band (8.4 GHz) with synthesized bandwidths of 40 MHz using MarkII bandwidth synthesis switching systems. Each bandwidth was synthesized by observing three 2 MHz channels placed at the frequencies -20, +9 and +20 MHz relative to 2285 and 8440 MHz.

## **III. The observations**

We have observed sources contained in a subset of the JPL Barycentric J2000 Catalogue (Sovers et al 1988). Both observations are composed of 50 scans approximately 180 seconds long. The observing sequence was made with the objective of maximizing the azimuth and elevation coverage in the minimum time.

## **IV. Data analysis**

The correlation of the data was performed at the JPL-Caltech Block II correlator. The final observable modeling and parameter estimation was done with the JPL Masterfit Software (Sovers and Fanselow, 1987). A constant term (3 mm) was added to the measurement uncertainty which typically was in the order of 0.1 mm. This constant term was needed to account for unmodeled systematic errors.

## V. Delay model

### a) Reference frame orientation

The a priori delay model uses IRIS determinations of the Earth orientation and the celestial reference frame through the source coordinates already mentioned. Due to the short length of the baseline (0.5 Km), our results should be independent of this a priori information to less than 1 mm.

### b) Earth modeling

Maximum tidal effects are approximately:

Solid Earth tide	300 mm max
Atmospheric loading	20 mm max
Ocean loading	30 mm max
pole tide	20 mm max

Assuming that these effects vary linearly, over a 0.5 Km baseline even a 500 mm tidal effect would cause less than 0.1 mm change in our baseline. Thus these effects are negligible.

### c) Media Propagation Effects

We have used S/X dual frequency calibration for our data. For the troposphere we should take in consideration a) the fluctuation in the water vapor distribution and b) a bias due to the difference in altitudes of the two sites.

The random part a) could be considered using a stochastic model to calculate the observation covariance due to these fluctuations. In preliminary tests with an observation covariance derived from the Treuhaft and Lanyi model (Treuhaft and Lanyi 1987), the estimated baseline components changed by 0 to 3 mm with the largest change occurring in the vertical component of the baseline.

The systematic part b) could be estimated assuming, for the dry component:

- 1) a dry troposphere scale height of 8.5 Km and a zenith troposphere delay of 2.1 m
- 2) The dry component of the troposphere to be in hydrostatic equilibrium
- 3) the difference of altitude between DSS63 and DSS65 is approximately -30 m.

With these assumptions one obtains a bias in the zenith tropospheric delay of DSS 63 relative to DSS65 approximately equal to -8 mm.

For the wet component we have adjusted the DSS63 wet zenith troposphere relative to a fixed DSS65. The estimated biases were -3.4 +/- 0.8 mm and -0.8 +/- 0.8 mm on 880404 and 890502 respectively.

## VI. Receiving system

Because the geometric and media propagation effects are small on short baselines, the receiving system will produce, in this case, the large part of the error budget. Here, we will discuss the two aspects required for explaining our results: Thermal expansion and subreflector motion in the axial direction.

### Thermal expansion

Assuming a standard value for the mean linear dilatation coefficient the relative vertical displacement of both antennas is less than 0.25 mm /deg C. The air temperatures for the two experiments were as follows:

Experiment	Temperature range
880404	3 to 8 deg C
890502	16 to 23 deg C

Therefore we expect intra-experiments thermal expansions effects in the order of 1 mm. Between the 2 experiments, the 14 deg C temperature change gives a 2.9 shift in the local vertical component of the baseline.

### Subreflector motion in the axial direction

Because antenna structures deform as they change orientation in a gravity field, the subreflector position may be adjusted in order to compensate for changes in the antenna focal length. For the S/X cones of the DSN 70 m antennas, Slobin and Bathker (1988) calculate that:

$$d(\text{path delay})/d(\text{shift along the Z direction}) = 1.67$$

$$d(\text{path delay})/d(\text{shift orthogonal to Z direction}) = 0.044$$

where path delay is the path delay averaged over the reflector and the Z direction is the axial direction. The same authors report an experimental verification to 5 % for both expressions.

Using these expressions and the model for the subreflector motion we obtain the following pathlength change due to autofocusing:

$$77 \text{ mm} * \sin(\text{elevation}) - 54 \text{ mm}$$

To detect this effects the observation 890502 was splitted in two parts: one with the subreflector fixed and the second with the subreflector in autofocus mode.

## VII Baseline Results

The solution which serves as the reference for all the variations is the corresponding to the data from 890502 with the subreflector fixed to its nominal position for 45 deg elevation:

X(m)	Y(m)	Z (m)
244.114+/-0.004	-308.293+/-0.002	-360.320+/-0.003

The estimates corresponding to 890502 with the subreflector in autofocus gives a shift in local East-North-Vertical (ENV) coordinates given by:

E(m)	N(m)	V(m)
0.003+/-0.003	0.001+/-0.002	-0.067+/-0.005

This confirms the the predicted effect of the 70 m antenna gravity deformation discussed earlier.

As a test of the consistency of our measurements, we compare the estimates from the experiment 880404 with the reference solution: Experiment 880404 was performed with the subreflector in a fix position, but the phase cal tones were not available. The estimates were:

	E(m)	N(m)	V(m)
SX	0.001+/-0.002	-0.002+/-0.002	0.017+/-0.006
X	0.001+/-0.002	-0.003+/-0.002	0.017+/-0.006
S	-0.006+/-0.002	-0.001+/-0.002	0.009+/-0.006

For the SX and X solutions the horizontal baseline components (E,N) are consistent to a few mm. However the vertical components disagree by almost 3 sigma. The simple model for the thermal expansion discussed before could not explain this variation. For S-Band the east baseline components disagree by 3 sigma while the vertical component differ by only 1.5 sigma. The most likely explanation for this discrepancy seems to be uncalibrated receiving system effects.

#### Acknowledgements

We thank K. M. Liewer and C. D. Edwards for their work in developing the JPL modeling and software for phase delay data. We thank D. N. Fort and E. H. Sigman for their work on the JPL-CIT Block II correlator and J. L. Galvez and R. Robles for performing various test on the DSS 65 phase calibrator. The work of one of us (A.R.) has been partially supported by the CICYT under contract PB88-0021.

#### References

- S. D. Slobin and D. A. Bathker, 'DSN 70- Meter Antenna Gain, Phase and Pointing Performance' JPL TDA Progress Report 42-95, pp 237-245, July-September 1988
- O. J. Sovers and J. L. Fanelow, 'Observation Model and Parameter Partials for the JPL Parameter Estimation Software "MASTERFIT 1987', JPL publication 83-39 revision 3, 15 December 1987.
- O. J. Sovers et al, 'Astrometric Results of 1978-1985 Deep Space Network Interferometry: The JPL 1987-1 Extragalactic Source Catalog', Astronomical Journal, vol 95, num 6, June 1988.
- R. N. Treuhaft and G. E. Lanyi, 'The Effect of the Dynamic Wet Troposphere on Radio Interferometric Measurements', Radio Science, 22, 251-265, 1987.

# ACCURATE SPACE VLBI STATION POSITION DETERMINATION

PROF. STANISŁAW GORGOLEWSKI

TORUŃ RADIO ASTRONOMY OBSERVATORY  
UL. CHOPINA 12/18, 87-100 TORUŃ, POLAND

## ABSTRACT

In order to simplify the space VLBI Station position determination the use of VLBI signals instead of special space navigation techniques is proposed. The VLBI signals contain a number of coherent frequencies which are followed with phase-locked ground station oscillators. Three ground based data acquisition stations are required for this purpose, which have simultaneous space VLBI Station visibility. The principle of operation is based on the use of several coherent VLBI " signal " frequencies (in order to avoid ambiguity) and phase tracking by three ground data acquisition stations. In principle the anticipated position accuracy can reach centimetric accuracy limited mainly by the atmospheric and ionospheric irregularities. This kind of accuracy greatly improves the use of space VLBI Station for astrometric and geodetic purposes.

## INTRODUCTION.

In order to be able to fully utilise the longer baselines that shall become available by space VLBI one needs to maintain baseline determination accuracies that have been achieved by ground based VLBI Stations. The ground based VLBI stations remain fixed relative to each other, whereas the space VLBI Station is moving very quickly ( velocities can even reach about 8 km/sec at perigeeum ). A review of spacecraft position measurement methods has been presented at the " SIX WORKING MEETING ON EUROPEAN VLBI FOR GEODESY AND ASTROMETRY " ( Bologna, Italy 1988 ). This included the three station phase tracking method utilising the VLBI signals. It was further developed in Budapest at the " Discussion Meeting on the RADIOASTRON Project " ( Budapest, Hungary 1989 ).

The kind of signals that I'm going to consider here are based on the design consideration of the MK III System, VLBA, QUASAT,

## RADIOASTRON and the Canadian Data Recording System for Radio Astronomy.

The principle of operation of the accurate space VLBI Station position determination is relatively very simple and makes use as much as possible of the existing hardware on the Space VLBI Station as well as on the ground VLBI Stations. For the sake of simplicity and clearness of presentation, I shall go right into the heart of the matter. Let us then first consider the most demanding requirements which are incorporated into the Canadian Data Recording System ( CDRS ) i.e. 256 Mb/s. Thus we'll have a  $f_{\text{max}} = 256 \text{ MHz}$  in this system ( CDRS is meant to be compatible with all the existing or planned ground or space VLBI systems ). The frequency of 256 MHz corresponds to a  $\lambda = 117.19 \text{ cm}$ . If we could measure the phase at this  $\lambda$  with one degree accuracy our range resolution would be equal to 3.26 mm ! I assume of course that the data transfer from the space VLBI Station takes place in real time and the recording takes place at the ground data acquisition station. Such high range resolution is not attainable due to the ionospheric and atmospheric effects. To resolve the range ambiguity we need also lower frequencies where the phase rate shall be lower. One such frequency also planned for the QUASAT and RADIOASTRON stations is 32 MHz i.e.  $\lambda = 937.5 \text{ cm}$  and one degree phase accuracy = 2.6 cm ! Thus we see that centimetric range accuracy is feasible if we use sampling frequencies within the 32 -256 MHz frequency range. These are of course the frequencies which have to be provided for on the space VLBI Station for its normal operation as well as on all the ground VLBI Stations. The Data, Signal and Control module ( DSC ) in the Canadian System now supports 128 Mb/s max. data rate ( 9.8 mm range accuracy ) it provides also a separate 128 Kb/s ( corresponding range resolution at this  $\lambda = 2343.75 \text{ m}$  with  $1^\circ$  phase resolution is 6.51 m which is less than the 32 MHz  $\lambda = 9.375 \text{ m}$ . Thus we see that in principle only the two frequencies 128 kHz and 32 MHz are theoretically sufficient to get 2.6 cm range accuracy with the initial knowledge of the orbit with kilometric accuracy.

. This extremely simple idea may need some safety measures to avoid confusion in case of adverse propagation conditions. Adding

one more frequency between 128 kHz and say 128 MHz let it be 4 MHz since it is close to the geometric mean of the two frequencies. We now get very much less critical situation because we measure now the phase with only about  $11^\circ$  instead of  $1^\circ$  accuracy. There is however a problem with the highest frequency i.e. 128 MHz one gets about 7.2 cm accuracy with about  $11^\circ$  phase resolution. If we can reliably measure the phase at 128 MHz to single degrees we get single cm range accuracy. The situation is a factor of two better at 256 MHz and correspondingly better if we can send higher frequencies (harmonics of the highest sampling frequency) from the spacecraft to the three ground stations. We need at least 3 ground stations for spacecraft position determination. For highest accuracy we need large ground baselines also in N-S directions, thus southern hemisphere data acquisition stations are also needed. Ideally 3 southern and 3 northern hemisphere data acquisition stations would serve best the purpose, with  $120^\circ$  station separation in longitude on each hemisphere and  $60^\circ$  relative phase shift between the two hemispheres.

Resuming in ideal case 6 data acquisition stations and 3 frequencies: 128 kHz, 4 MHz and 128 MHz are required for this spacecraft positioning system for better than 10 cm accuracy. We can also get doppler information for better orbit parameter measurements. For highest accuracy the spacecraft carrier frequency in the GHz range is most suitable.

Measurements of the range are accomplished with orthogonal i.e. sine and cosine pairs of phase detectors for each of the 3 frequencies recorded. Phase detector signals are derived from the ground station atomic frequency standards. Such signals are generated at the VLBI stations by the Mark III, VLBA and the CDRS terminals. It is therefore advisable to place the data acquisition stations at the VLBI station sites for the sake of equipment simplicity.

Doppler information along with the 3 pairs of phase measuring systems should be used over many orbits of the space VLBI station for highest accuracy. Of course other independent methods of orbit determination can and should also be used in the initial stage of the space VLBI observations. The other methods should not be needed after the time of mastering of the above proposed very

simple spacecraft positioning system which is both passive and all weather operating system requiring only next to none additional equipment. It is very simple and thus reliable system that should also be considered in the space VLBI plans.

Aknowledgement:

This work has been supported by the:

Polish Academy of Sciences

NICOLAUS COPERNICUS ASTRONOMICAL CENTER,

Bartycka 18, 00-716 Warsaw, P O L A N D

Research Problem: CPBF-01.11. gr. t. 7.



On the Optimization of VLBI Observing Schedules  
Heinz Steufmehl

Geodetic Institute of the University of Bonn  
Nußallee 17

**ABSTRACT:** In order to achieve a high accuracy in the determination of parameters with VLBI, optimized observing configurations are needed. These observing configurations must represent a good compromise between logistical and geometrical conditions.

In the work presented here an optimization algorithm has been developed in order to create schedules, which represent the best solution with respect to the geometrical conditions, not yet looking at logistics.

The optimization process is divided into two parts. In the first part a pool of possible observing subconfigurations for all observing points of time is created, while in the second part the algorithm selects the observations for scheduling using this pool. The stations, the sources, the day and the starttime of the experiment must of course be fixed beforehand.

When this process is finished, the schedule consists of the best combination of observing subconfigurations according to a specially defined optimization criterion.

Finally, a schedule of the IRIS-A network is examined and compared with 3 optimized schedules, showing significant improvements over the original IRIS-A schedule. Alternative sources and alternative antenna mount types are chosen for further simulations in order to show that the best results will be achieved if the local station sky regions do not show empty areas.

## 1. THE OPTIMIZATION ALGORITHM

The optimization process will be explained using figure 1, which gives a general overview of the computations.

The stations, the day and starttime and the participating sources are selected beforehand. The possible station subnetting solutions and the sources are combined and tested for valid observing subconfigurations. The station subnetting box in fig. 1 contains just 3 examples out of a large number of observing subconfigurations for one point of time. They can be regarded as basic elements of a typical 24 hour experiment such as the IRIS-A experiment. For one observing point of time only one subconfiguration can be selected from this pool of possibilities.

For each configuration the contribution matrix to the matrix of normal equations is computed according to the chosen parameterization. These contribution matrices are symbolized in fig. 1 by the upper boxes. In order to simplify the computations, observations are taken in a fixed time interval. So, in this example a new computation of the upper boxes will be made every 12 minutes. These 12 minutes represent a buffer zone for telescope slewing time or tape change.

The next part contains the actual algorithm for scheduling, which depends on the computations done in the first part. It

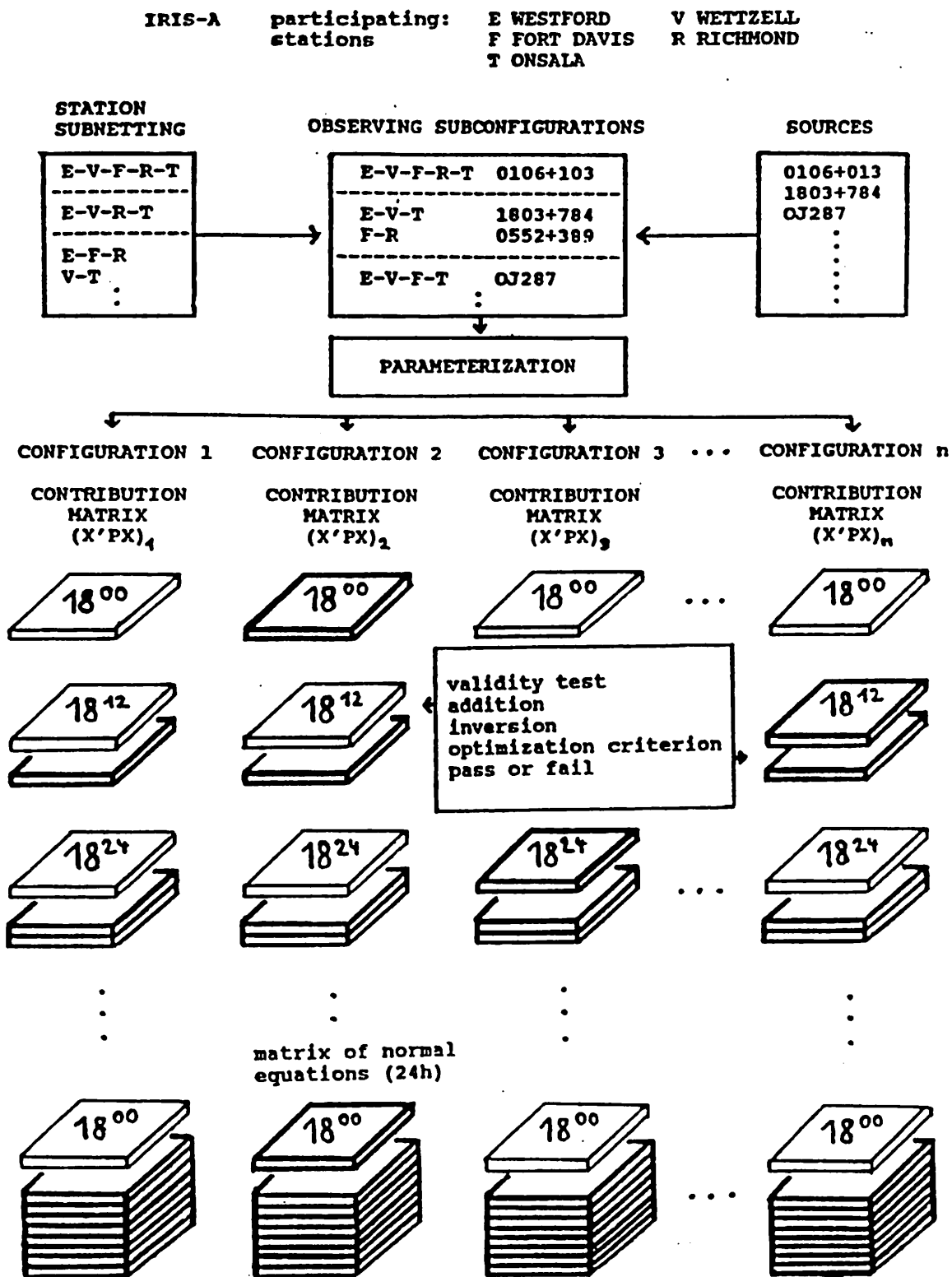


fig. 1 : The optimization algorithm

consists of the following 5 steps:

1. validity test: examination if the sources of the current subconfiguration have not been observed by the same telescope within the last 2 observing points of time, else the subconfiguration is not used for scheduling.
2. summation: addition of the contribution matrix to the already existing matrix of normal equations.
3. inversion: inversion of the newly created matrix.
4. optimization criterion:

$$\max(1/u \sum_{i=1}^u ((\sigma_n)_i - (\sigma_{n+1})_i) / (\sigma_n)_i)$$

where

$u$  is the number of unknown parameters, and

$(\sigma_n)_i$  is the standard deviation of the parameters before the addition of the subconfiguration.

$(\sigma_{n+1})_i$  is the standard deviation of the parameters after the addition of the subconfiguration.

The percentual decrease of the standard deviation of the unknowns will be maximized.

5. pass or fail: The configuration, which best fulfills the optimization criterion will be selected for scheduling, the others fail.

So, the first observing subconfiguration of the schedule must be fixed beforehand and is really arbitrary. This is symbolized by the bold box in the first line. This bold box turns into the lower ones in the second line and so on. In the last line there is the symbolized matrix of normal equations after 24 hours, only containing the bold boxes, respectively the selected subconfigurations. As a whole they represent the best combination of subconfigurations according to the optimization criterion.

## 2. RESULTS

Now an original schedule of the IRIS-A network with 5 stations will be compared with 3 optimized schedules. The numbers in table 1 are the standard deviations of the unknown parameters, computed for the original IRIS-A schedule of March 1989. The pole components and DUT 1 are estimated, furthermore every six hours new atmospheric parameters and clock polynomial coefficients.

Then the optimization algorithm is applied to the same 15 sources and the same 24 hours of observations as in the original schedule. The main result is (tab. 1): The standard deviations of the most interesting parameters, this means the earth rotation parameters, decrease by 6 %. This is remarkable, because the original IRIS-A schedule has been improved continuously over the years.

For the next simulation, the sources were changed. In fig. 2 the dots represent the source positions of the original IRIS-A schedule, whereas the circles represent the alternative positions in the celestial reference frame. So, more southern sources can be observed, but the same number (15) as in the original schedule was retained.

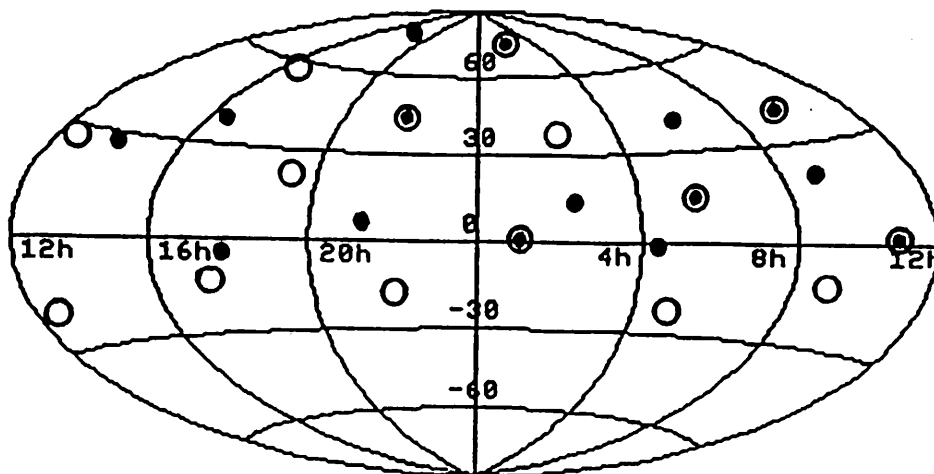


fig. 2 : Sources of the original and the optimized schedule

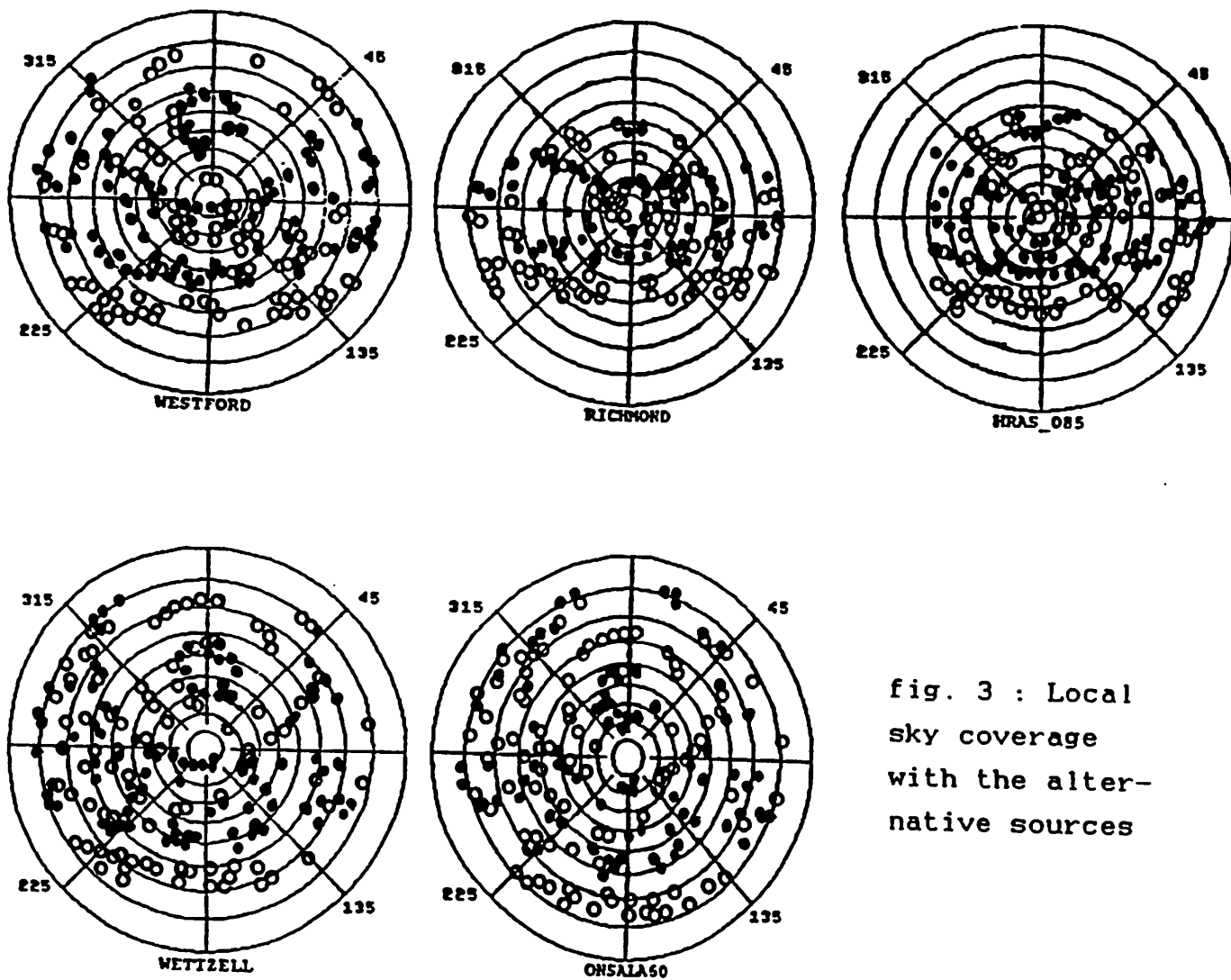


fig. 3 : Local  
sky coverage  
with the alter-  
native sources

Applying the algorithm again, the result is a decrease of 15% as regards the standard deviations of the earth rotation parameters (tab. 1).

Figure 3 shows the local sky coverage with observed source positions for each station and for 24 hours of scheduling. The different circles represent different lines of elevation. The dots are the observed positions in the original schedule, whereas the small circles are those in the optimized schedule. It is obvious, that the optimization algorithm frequently selects the southern sources as can be seen in the southern regions.

But the telescopes of Richmond and Fort Davis are not able to observe sources with low elevations in the northern direction. This is due to the antenna mount type (polar mount). So, for the next simulation, Richmond and Fort Davis are assumed to have an alt-azimuth-mount.

Now the standard deviations decrease again with respect to the original schedule, this time by 25%! (tab. 1)

Looking at the distribution of the observations (fig. 4), it becomes obvious, that no local sky regions may be excluded from observation in order to have the best geometrical conditions. At Richmond and Fort Davis the polar mounts prevented observations in the northern part of the local skies.

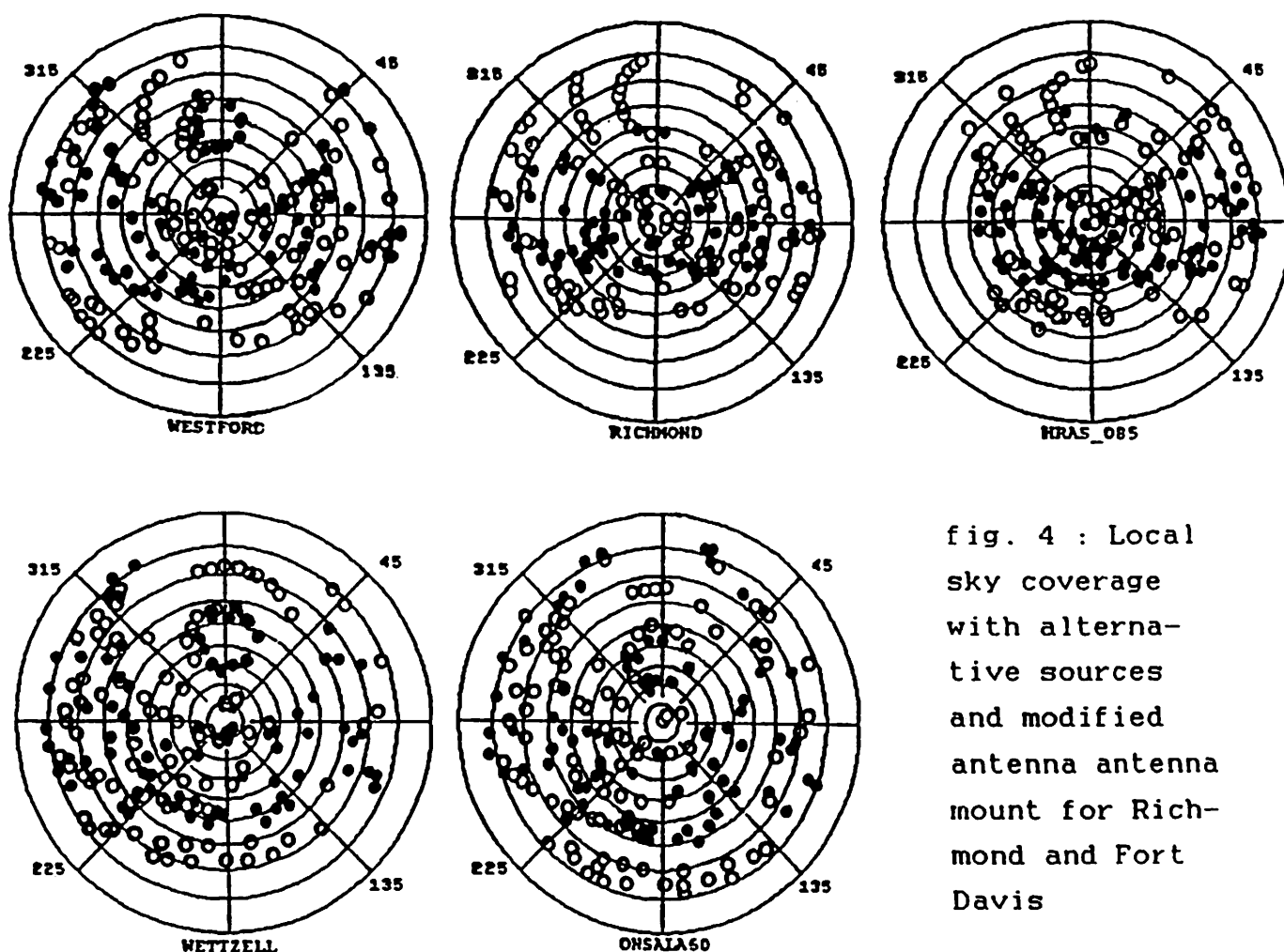


fig. 4 : Local sky coverage with alternative sources and modified antenna mount for Richmond and Fort Davis



	original schedule	optim. schedule	altern. sources	altern. sources, antennas
numb. of obs	854	886	803	925
mean corr.	.164	.158	.156	.153
XP (as)	.6246D-03	.5961D-03	.5344D-03	.5036D-03
YP (as)	.5265D-03	.4830D-03	.4661D-03	.4008D-03
DUT1 (s)	.2708D-04	.2578D-04	.2192D-04	.1836D-04
atm1 WF (m)	.3003D-02	.3613D-02	.3142D-02	.3270D-02
atm2 WF (m)	.2494D-02	.3496D-02	.3853D-02	.3541D-02
atm3 WF (m)	.2693D-02	.3416D-02	.3075D-02	.2694D-02
atm4 WF (m)	.3080D-02	.3814D-02	.3795D-02	.3688D-02
atm1 WZ (m)	.2523D-02	.3919D-02	.3846D-02	.4041D-02
atm2 WZ (m)	.2390D-02	.3073D-02	.3757D-02	.3497D-02
atm3 WZ (m)	.3097D-02	.3118D-02	.3422D-02	.3618D-02
atm4 WZ (m)	.3179D-02	.3533D-02	.4000D-02	.3819D-02
atm1 FD (m)	.4006D-02	.7711D-02	.5380D-02	.3097D-02
atm2 FD (m)	.3517D-02	.4856D-02	.3307D-02	.2674D-02
atm3 FD (m)	.3212D-02	.5449D-02	.5232D-02	.2757D-02
atm4 FD (m)	.4983D-02	.4103D-02	.5066D-02	.3234D-02
atm1 RM (m)	.7290D-02	.3960D-02	.3475D-02	.3108D-02
atm2 RM (m)	.4798D-02	.5075D-02	.5253D-02	.2930D-02
atm3 RM (m)	.5270D-02	.4175D-02	.4340D-02	.2380D-02
atm4 RM (m)	.4153D-02	.4420D-02	.4099D-02	.3450D-02
atm1 ON (m)	.2823D-02	.3938D-02	.3207D-02	.3539D-02
atm2 ON (m)	.2914D-02	.3256D-02	.4311D-02	.3503D-02
atm3 ON (m)	.2783D-02	.3201D-02	.3266D-02	.3150D-02
atm4 ON (m)	.3365D-02	.3687D-02	.4038D-02	.4810D-02
tau WZ (s)	.6593D-10	.6777D-10	.6857D-10	.6366D-10
tau1 WZ	.2279D-14	.2391D-14	.2476D-14	.2404D-14
tau2 WZ (/s)	.2527D-19	.2638D-19	.2779D-19	.2720D-19
tau FD (s)	.5158D-10	.6803D-10	.5749D-10	.5150D-10
tau1 FD	.2208D-14	.2673D-14	.2497D-14	.2309D-14
tau2 FD (/s)	.2502D-19	.2868D-19	.2751D-19	.2534D-19
tau RM (s)	.5568D-10	.4803D-10	.4499D-10	.4613D-10
tau1 RM	.2377D-14	.2141D-14	.2216D-14	.2221D-14
tau2 RM (/s)	.2564D-19	.2508D-19	.2548D-19	.2520D-19
tau ON (s)	.6468D-10	.6580D-10	.6410D-10	.5950D-10
tau1 ON	.2266D-14	.2313D-14	.2386D-14	.2301D-14
tau2 ON (/s)	.2531D-19	.2591D-19	.2785D-19	.2676D-19

table 1 : Standard deviations of the unknown parameters

#### 4. CONCLUSIONS

The advantages of the optimization algorithm presented here consist of a fast optimization for any type of observing program, profound examination of geometric relations and a good evaluation of networks for geodetic VLBI. With more telescopes joining the networks every year, the need for efficient schedule optimization programs will become ever more obvious. The next to do will be the further refinement of the present version, ready to be included in the program SKED. Then also the logistical aspects will be fully taken into account.

#### 5. REFERENCES

Ma, C. : Very Long Baseline Interferometry applied to Polar Motion, Relativity and Geodesy. Chapter IV.C ,1978

SKED Reference Manual. Interferometrics Inc. Greenbelt, Md, USA

# **Determination of Correlation Coefficients between VLBI-Observables**

H. Schuh and A. Wilkin  
Geodetic Institute  
University of Bonn  
Bonn, W.-Germany

**ABSTRACT.** At present no a priori correlations between the observables of a VLBI-experiment are taken into account in the least squares fit. The causes of such correlations are pointed out, which are in particular due to imperfections of the models which are used in VLBI data analysis. Empiric correlation coefficients have been determined from the residuals of first (uncorrelated) solutions of 19 VLBI-experiments. Significant correlations were found, in particular between simultaneous observations on two baselines with a common station and also between all observations of the same radio source from each particular baseline.

## **1. INTRODUCTION**

Usually the least squares method is used for the analysis of a geodetic VLBI experiment, i.e. the determination of the unknown parameters such as station coordinates, Earth rotation parameters or clock parameters.

The complete model of least squares adjustment contains the full variance-covariance matrix of which the elements of the main diagonal can be computed from the a priori errors  $\sigma$  of the observables and the off-diagonal elements can be derived from the  $\sigma$ 's and from the correlation coefficients  $\rho$  between each pair of observations.



However, in all present standard VLBI solutions, only the variances of the observations are used whereas the covariances are set to zero. Even more, none of the existing VLBI programs which provide the highest accuracies like the US software packages SOLVE and MASTERFIT or the Bonn VLBI Software System BVSS allow the inclusion of a priori correlation coefficients. Although this would need slightly more sophisticated software and more CPU time for the execution of the programs, the main reason is that we do not have any knowledge about the size of the a priori correlation coefficients.

## 2. REASONS FOR CORRELATIONS BETWEEN OBSERVABLES

In this paragraph we want to point out what could cause a priori correlations between the VLBI observables (see also Schuh, 1986).

### - geometric correlation

Usually during a VLBI experiment made with a network of several stations a radio source is observed simultaneously from all or from most of the participating stations. Thus, observables (delays and delay rates) from geographically close stations, in particular made on baselines which have one common station will be correlated stronger than from baselines which are far apart.

### - correlation due to short time difference

The usual duration of a geodetic VLBI experiment is 24h - 48h. Due to similar external influences, like the slowly varying atmospheric conditions, observations which are made close in time will be correlated stronger than observations which are far apart in time. But there may also occur periodic changes of the correlation coefficients due to periodic influences on the stations which are caused by the Earth tides and the ocean tides or influences on the observables, for instance because of a quasi-periodic behaviour of the meteorological parameters.

- correlation between all observables of the same radio source  
Observations of the same radio source may be correlated, too, due to systematic influences of the structure of the source or because of errors of the source positions which show up in the residuals if the position is not solved for in the least squares adjustment.
- technical and other reasons  
There may also be reasons of 'technical' nature for a correlation between observables. For example all observables which have been obtained simultaneously by the physical process of correlation at the correlation center may be mathematically correlated. The delays and the corresponding delay rate observables which are determined by a common process in the Fringe program may be correlated, too.

Almost all of these probable causes of correlations mentioned above can be put down to still existing imperfections of the models which are used in VLBI data analysis and are not 'real' correlations between the measurements. However, even these dependencies which are due to common errors of the models have to be considered in the mathematical model of the least squares fit as well as correlations which are caused by the condition of the hardware during the time of observations.

### 3. THE DETERMINATION OF A PRIORI CORRELATION COEFFICIENTS

A method which is often used for the determination of the full variance-covariance matrix is the variance-covariance component estimation (Koch, 1988). This method needs the introduction of a priori variances and covariances to start with, which then will be improved by an iterative process. However, because we do not have any idea about the size of the a priori correlations it is doubtful whether this method will be successful in the case of VLBI data analysis.

The second (and pragmatic) method is the determination of empiric correlation coefficients which can be computed between each two groups of residuals of a first uncorrelated solution according to the equation:

$$\rho = \frac{[e_i \cdot e_j]}{\sqrt{[e_i^2] [e_j^2]}} \quad (1)$$

$e_i, e_j$  = residuals of the two groups of observables .

For the use of equation (1) the following conditions must be checked first:

- normal distribution of observables,
- linearity between  $e_i$  and  $e_j$ ,
- no external influences on the data which cause a special correlation model.

This method has been applied by Qian (1985) to analyze the residuals of a few VLBI experiments. According to Wolf (1975) the significance of the correlation coefficient  $\rho$  which is obtained by eq. (1) can be tested by a t-test with

$$t = \frac{[e_i \cdot e_j] \sqrt{(n - 2)}}{\sqrt{([e_i^2] \cdot [e_j^2] - [e_i \cdot e_j]^2)}} \quad (2)$$

$e_i, e_j$  = residuals of the two groups of observables,  
 $n$  = number of summands .

#### 4. EXPERIMENTS

Table 1 shows all VLBI experiments of which the residuals have been analyzed with respect to the possible reasons of correlations by using equations (1) and (2). We looked at the residuals of 19 intercontinental VLBI experiments of different networks such as IRIS-A, IRIS-S, IRIS-P and the CDP networks (ATLANTIC, POLAR, PACIFIC). The duration of these experiments usually is between 24h - 48h and they have at least 500 observations. This guarantees a

statistically sufficient number of products which are summed up in the equations (1) respectively (2).

For the VLBI data analysis, i.e. the first (uncorrelated) least squares fit we used the software package CALC/SOLVE as installed at the Geodetic Institute of the University of Bonn. This software contains all models which are given in the MERIT Standards (Melbourne et al., 1983). Standard least squares adjustments have been performed solving for relative station coordinates, atmospheric parameters and clock parameters.

## 5. RESULTS

Since the delay observables play a much more important role in the VLBI solutions than the delay rates we place our main interest on the correlations between the delays.

### - Correlations between simultaneous delay observables on different baselines ('geometrical correlation')

For the correlations between delay observables which have been simultaneously observed in a network we obtained the following results.

Table 2 shows the average absolute values of the correlation coefficients for all combinations of baselines which have one common station and which are almost orthogonal, i.e. which include a spherical angle around 90 degrees. It can be noticed that all of them got a correlation coefficient of about 0.3.

Table 3 however contains the average absolute values of the correlation coefficients for those baselines which have a similar direction, i.e. which include a spherical angle of less than 15 deg. A significantly higher correlation coefficient of up to 0.7 or even more can be seen. In particular when the length of the baselines is about the same as for instance Westford-Onsala and Westford-Wettzell. Then, the elevation angles at the two stations Wettzell and Onsala are about the same and the influence of tropospheric refraction will be similar due to similar weather conditions at those two stations.

type	experiments	dura- tion	number of obs.	stations	reference station
IRIS	86MAR19	24 h	529	WES,WET ONS,RIC, HRA	WES
	86MAY13		504		
	86JUN17		521		
	86SEP15		472		
	86OCT15		448		
	86DEC09		459		
ATLANTIC	86MAY14	36 h	1283	WES,WET ONS,MOJ, HRA	WES
	87APR09		1243		
	87MAY04		1172		
POLAR	85JUN19	36 h	973	WET,WES, ONS,GIL, MOJ,KAS	WES
	85NOV21		950		
	86JUN18		1029		
	87JUN24		999		
PACIFIC	85JUL06	48 h	1482	GIL,KAS MOJ,VND, KAU,KWA	KAU
	85JUL20		1502		
	85JUL27		1415		
	85AUG10		1511		
	86JUL05		1918		
	86AUG02		2129		

GIL = Gilcreek (Alaska, USA)	= GILCREEK
HRA = Fort Davis (Texas, USA)	= HRAS 085
KAS = Kashima (Japan)	= KASHIMA
KAU = Kauai (Hawaii, USA)	= KAUAI
KWA = Kwajalein (Micronesia)	= KWAJAL26
MOJ = Mojave (California,USA)	= MOJAVE12
ONS = Onsala	= ONSALA60
RIC = Richmond (Florida, USA)	= RICHMOND
VND = Vandenberg (California, USA)	= VNDNBERG
WES = Westford (Massachusetts, USA)	= WESTFORD
WET = Wettzell (Bavaria, W.-Germany)	= WETTZELL

**Table 1: VLBI experiments of which the residuals were used to determine empiric correlation coefficients**

baseline	spheric angle between baselines [°]	correlation
Wes-Wet Gil-Wes	86	0.30
Wes-Ric Hra-Ric	92	0.27
Hra-Wet Hra-Moj	99	0.26
Hra-Ons Hra-Moj	94	0.28
Wes-Moj Gil-Moj	86	0.29
Wet-Kas Moj-Kas	86	0.32
Moj-Wet Moj-Kas	85	0.32
Kas-Ons Moj-Kas	81	0.33
Moj-Ons Hra-Moj	85	0.29
Gil-Moj Gil-Kwa	98	0.27
Gil-Kas Kas-Kwa	99	0.26
Moj-Kas Moj-Vnd	83	0.30
Moj-Kwa Kas-Kwa	95	0.28
Moj-Vnd Kas-Vnd	90	0.28

Table 2: Average absolute values of the correlation coefficients between observations on baselines which have a common station and which are almost orthogonal

baseline	spheric angle between baselines [°]	correlation
Wes-Wet Wes-Ons	9	0.68
Wes-Wet Hra-Wet	11	0.64
Wes-Wet Ric-Wet	8	0.68
Wes-Ons Ric-Ons	5	0.68
Wes-Ons Hra-Ons	15	0.62
Ons-Wet Gil-Wet	4	0.62
Wes-Ric Ric-Ons	14	0.58
Ric-Ons Ric-Wet	8	0.70
Hra-Wet Hra-Ons	6	0.70
Hra-Wet Moj-Wet	12	0.67
Hra-Ons Moj-Ons	12	0.67
Wes-Hra Wes-Moj	18	0.61
Wes-Kas Gil-Wes	8	0.61
Wes-Kas Gil-Kas	8	0.62
Wet-Kas Kas-Ons	6	0.70
Moj-Wet Moj-Ons	4	0.72
Gil-Wet Gil-Ons	1	0.73
Moj-Kwa Kau-Moj	7	0.65

Table 3: Average absolute values of the correlation coefficients between observations on baselines which have a common station and a similar direction

Fig. 1 now shows the absolute values of the correlation coefficients of all baseline combinations which have been analyzed with respect to the spherical angle between the baselines. A clear decrease can be observed from 0.72 down to 0.3 for the orthogonal baselines. For the observations on baselines which include an angle larger than 100 deg the correlation coefficients even increase slightly which means that observations on baselines which have the same orientation but opposite direction are stronger correlated than those on orthogonal baselines.

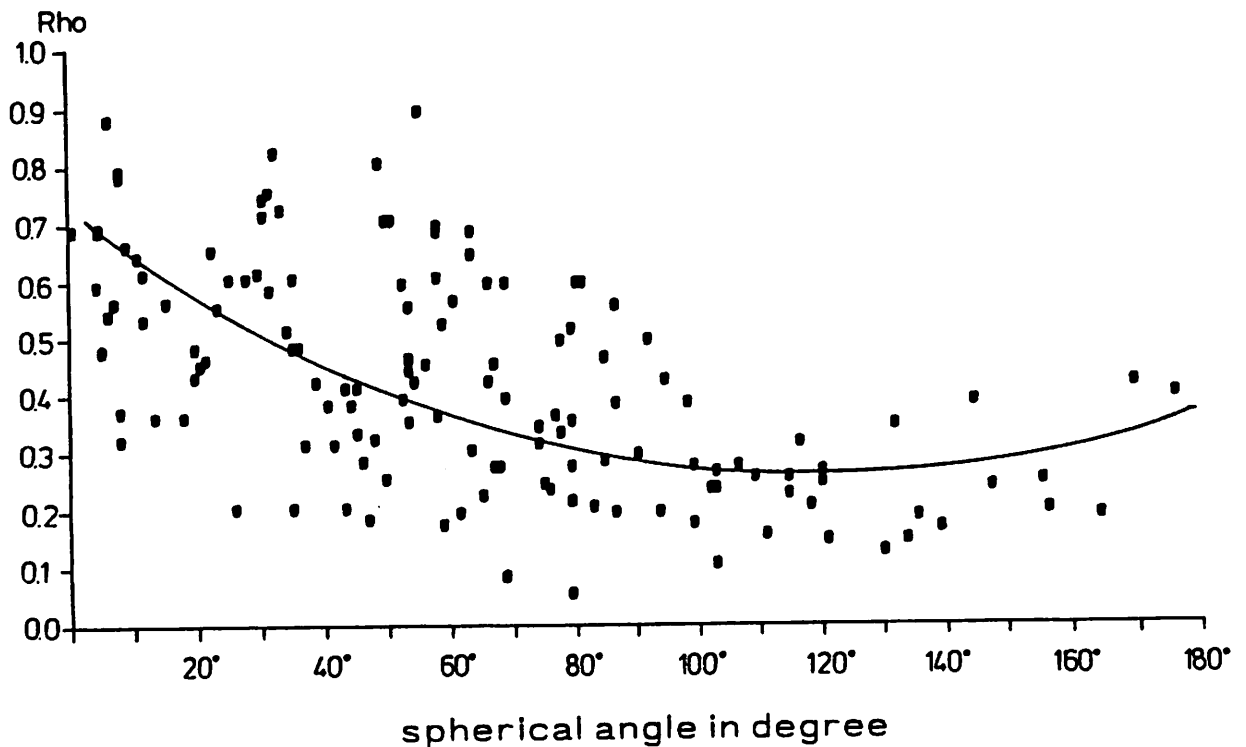


Figure 1: Absolute values of the correlation coefficients between simultaneous observations on baselines with a common station as a function of the spherical angle between the baselines and a parabola fitted through the data.

A parabola has been fitted through the data shown in fig. 1 to obtain a functional description of the dependence of the correlation coefficient on the angle between the baselines.

For the function

$$\rho = a + b \cdot \alpha + c \cdot \alpha^2 \quad , \quad (3)$$

$\alpha$  = sperical angle (deg) between the two baselines,  
the parameters have been determined to:

$$a = + 0.72284 \quad ,$$

$$b = -0.007810777 \quad ,$$

$$c = +0.000032774 \quad .$$

This will allow in the future to compute approximate 'theoretical' absolute values of the correlation coefficients only as a function of the angle between the two baselines.

#### - Correlations between observations close by time

We calculated the autocorrelation function of the residuals to have some idea about the correlation coefficients between observations on the same baseline with respect to the difference of the observing times. As this requires equidistant data the observing time corresponding to each residual was shifted to the next half-hour time step on the time axis. Fig. 2 shows as a typical autocorrelation function that of the residuals on the baseline WEST-FORD-WETTZELL of the POLAR-experiment from 86JUN18. No obvious trend or periodicities can be seen in fig. 2 neither in most of the other autocorrelation functions. But all of them start with a correlation of 0.3-0.4 between observations which are closer in time than one hour. For the second hour we usually had correlation coefficients of about 0.2 decreasing to zero for all observations which are further apart in time than 3 hours. Thus, an obvious but small correlation coefficient for all observations which are closer in time than 3 hours should be applied.



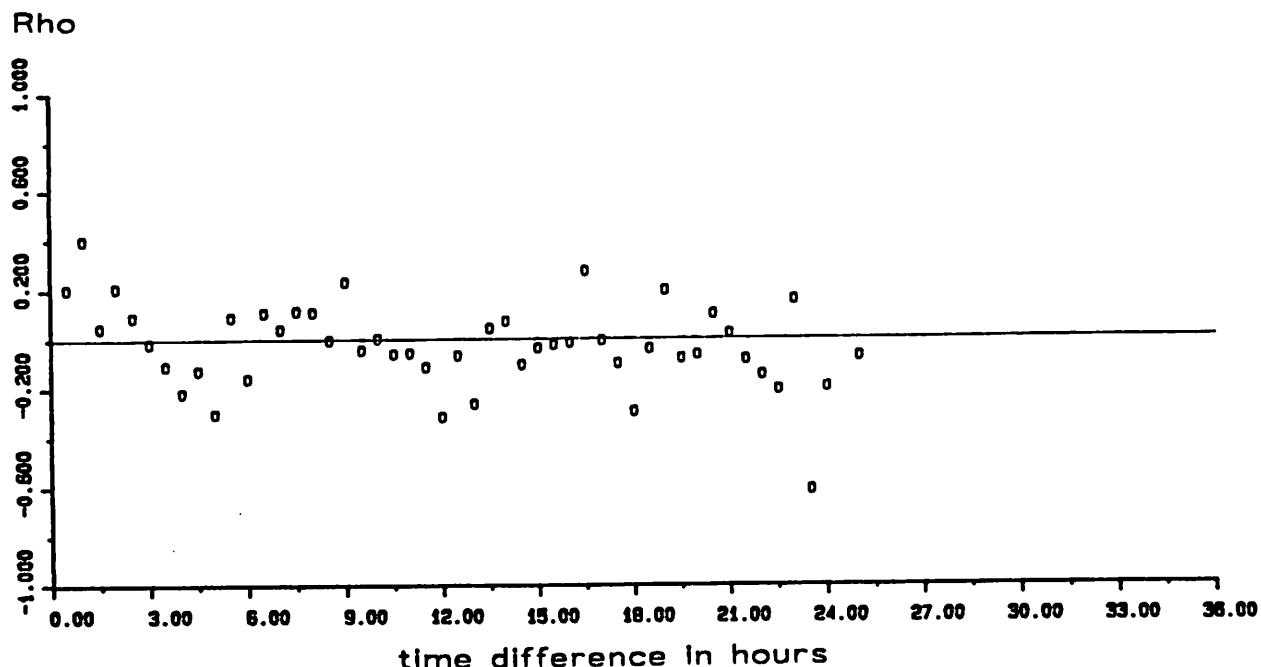


Figure 2: Autocorrelation function of the residuals on the baseline WESTFORD-WETTZELL of the POLAR-experiment from 86JUN18

#### - Correlations between observations of the same radio source

The residuals of all observations of a radio source on a particular baseline were picked out and multiplications of all possible combinations of residuals were performed. The sum of these products was used as denominator of eq. (1) and the correlation coefficient between the observables of this individual source is obtained.

As an example, table 4 shows the correlation coefficients related to each radio source observed on the baselines which were part of the POLAR-experiment on 24th of June, 1987. If a source has been observed successfully less than 5 times on a baseline, the number of multiplications becomes too small to determine a reliable correlation coefficient. These cases are marked with --- in table 4. From this example as from other experiments we could at least partially recognize some systematic and repeatable correlation coefficients for observations of a particular radio source. For instance, we see in table 4 that the source 1803+784 produced corre-

lations close to zero on all of the baselines whereas the observations of the source 1144+402 yielded correlation coefficients almost always higher than 0.7 and even up to 0.98 on the baseline Mojave-Onsala. However, up to now the number of computations which have been carried out is not sufficient to derive final results which may be applied as a priori correlation coefficients to the observations of each particular radio source.

Basislinie	WES-	WES-	WES-	MOJ-	GIL-	GIL-	GIL-
Radloquelle	ONS	KAS	MOJ	ONS	ONS	MOJ	KAS
3C345	-0,25	-0,19	--	-0,25	-0,09	0,54	-0,20
3C273B	--	--	-0,07	--	--	-0,03	--
OJ287	--	0,23	-0,12	--	--	0,222	0,111
1803+784	-0,05	-0,05	-0,04	-0,09	-0,03	-0,03	-0,04
0552+398	0,20	0,82	0,80	0,49	0,16	0,40	-0,13
1502+106	0,64	--	0,40	--	--	0,67	0,97
1749+096	0,17	--	--	--	--	-0,29	--
1144+402	0,08	0,79	0,85	0,98	0,93	0,82	0,73

Table 4: Correlation coefficients between all observables of a radio source on the baselines of the POLAR-experiment on 24th of June, 1987

#### - Correlation between delay and delay rate observables

We also computed the correlations between each simultaneous delay and delay rate observables from the residuals. For all experiments and on all baselines we obtained correlation coefficients smaller than 0.14 which means that there is no significant dependence between those different types of observations.

## 6. FINAL CORRELATION COEFFICIENT

Now, the problem arises to compute the final correlation coefficient for a pair of observations for which two or more causes of correlation exist. This may be for instance between two observations of the same radio source which are closer by time than one hour. We have not found any reference about the combination of empiric correlation coefficients and we suggest to compute as a first approach the final covariance from the individual correlation coefficients  $\rho_i$ ,  $i=1,2,\dots,n$ , by

$$\rho = \sqrt{\rho_1^2 + \rho_2^2 + \dots + \rho_n^2} \quad (4)$$

Different signs of the individual correlation coefficients are not considered in eq. (4). Thus, it will just help to get some idea about the maximum size of the final correlation coefficient and the question how to combine coefficients with different signs is still unsolved. In any case, if necessary the correlation matrix has to be normalized to contain only elements  $\leq 1$  because no correlation coefficient may be  $> 1$ .

In future, a multidimensional approach is needed, i.e. observations for which several causes of correlations exist have to be treated separately.

## 7. CONCLUSION

With the results obtained in the previous paragraph and by using equation (4) it is possible to compute the total 'theoretical' correlation coefficient between each pair of observations of a VLBI-experiment.

Then, the next step will be to include such a correlation matrix in a VLBI least squares fit and to repeat the solution, now with the full variance-covariance matrix. The new results should show even higher stability and reliability than those from the present solution because of the better consistency between 'real world' and the statistical model of the least squares fit.

## 8. REFERENCES

KOCH, K.-R.: Parameter Estimation and Hypothesis Testing in Linear Models, Springer-Verlag, Berlin/Heidelberg/New York/London/Paris, 1988

MELBOURNE et al.: Project MERIT Standards. U.S. Naval Observatory, Circular No. 167, Dec. 1983 (Update #1, Dec. 1985)

QIAN, ZHI-HAN: The Correlations on VLBI Observations and its Effects for the Determinations of ERP, Columbus, Proc. Vol.1, p. 369-365, 1985

SCHUH, H.: Die Radiointerferometrie auf langen Basen zur Bestimmung von Punktverschiebungen und Erdrotationsparametern. DGK Reihe C, Nr. 328, München 1987

WOLF, H.: Ausgleichungsrechnung, Dümmlerbuch 7835, Ferdinand-Dümmler-Verlag, Bonn 1975

**OCCAM: A COMPACT AND TRANSPORTABLE TOOL  
FOR THE ANALYSIS OF VLBI EXPERIMENTS**

N. Zarraoa, A. Rius, E. Sardón  
Instituto de Astronomía y Geodesia, CSIC-UCM  
MADRID, SPAIN

H. Schuh, J. Vierbuchen  
Geodetic Institute, University of Bonn  
BONN, F.R.G.

**Abstract**

Based on the Bonn VLBI Software System, a new package for the analysis of geodetic VLBI experiments is being developed in the environment of an IBM XT or AT or compatible under MS-DOS. A new data handling structure has been designed, the BVSS FORTRAN code has been reallocated into different subprograms that perform the different tasks of a geodetic VLBI analysis. New code has been added to fulfill the requirements generated by the new structure and to introduce new features in the program. We present this new product, designed for compact and time-optimized processing of full experiments, baseline by baseline. We analyse its structure, its new features and the expectations for a future development. We include first comparisons with another standard VLBI package.

**1. Introduction**

The characteristics of the Bonn VLBI Software System, (BVSS), (Schuh, 1987) make it an appropriate tool for development and testing of new models in VLBI analysis. On the other hand it has not been designed for massive data processing. When we started thinking about improving BVSS package, one of our aims was to combine both features; an easy structure to help the installation and testing of new models and a system with reasonable processing speed. Now we have developed a package that keeps a modular structure in every step, with an easy access to the databases that ensures a

total transparency on data handling. It is running on one of the most popular, cheap and simple computer environment, an IBM AT or compatible under DOS, so full transportability is guaranteed.

The package is able to run automatically full experiments from beginning (NGS format data file) to end (adjusted values for the parameters) in short time, depending on the number of stations. It takes less than one hour the processing of an experiment with 5 stations - 10 baselines - 24 hour on an standard AT (8 MHz).

The name we have given to the package, OCCAM, refers to William of Ockham, XIV century's English philosopher who stated that from all possible answers to a question, the right one is the simplest one. Our aim is to get the simplest solution for VLBI analysis and research, and OCCAM is the first result.

## 2. Program Requirements and Capabilities

The program has been written for an IBM AT environment under DOS and the language employed has been the most standard FORTRAN 77 in order to optimize the transportability of the program into other software and hardware environments. Hardware and software requirements are listed in table 2.1.

---

IBM XT, AT or fully compatible systems
DOS version 3.2
512 Kbytes RAM (640 Kbytes recommended)
Hard-disk (Minimum available space, 3 Megabytes)
HP LaserJet Printer or HP Plotter
FORTRAN compiler supporting the standard FORTRAN 77

---

*Table 2.1. Minimum Hardware and Software Requirements*

One of the limitations of the package capabilities is generated by the small amount of memory that DOS system can handle. This problem affects the development of a multi-station analyser on this environment. A solution under study is given by the use of 386 or 486 based processors and operating systems able to address a larger RAM memory, like UNIX.

The processing capacity of OCCAM package for a single run covers experiments up to 45 baselines (10 stations) with a maximum of 250 scans each, which represent normally more than 24 hours of observing time. These figures show that the program capacity stands perfectly with almost any geodetic VLBI experiment. A complete list of the package limitations is shown on table 2.2.

---

10 stations
45 baselines
40 sources
250 observations per baseline
Solve for 31 parameters per baseline

---

*Table 2.2. OCCAM processing capabilities*

### 3. Program Structure and Data Flow.

The package is divided in two main parts. In the first part, all the calculations and corrections related to the different models applied are performed. The second part performs the least squares fit of the observed values minus the computed theoretical values, in order to get a solution for the experiment. Figure 3.1 shows the data flow in OCCAM system from beginning to end.

The computation of theoreticals and partial derivatives contains the basis for a multibaseline extension of the program. All the information computed there, i.e. partial derivatives, corrections to a priori values and the theoretical delays and delay rates, is stored in binary files for further use.

Although this information is now used for a single-baseline fit, the computations have been designed thinking on a multibaseline extension, the partial derivatives are computed with respect to station and not to baseline coordinates. All the corrections to the geometry of the interferometer are applied to stations and sources, not to baselines. All the information for an experiment is stored so only one single run of this part is necessary.

The different kind of computations involved in this stage made us divide it into four independent programs, each of them related to

a different item. Independent files to store different kinds of information are created. The package generates three main data files and some auxiliary files (table 3.1).

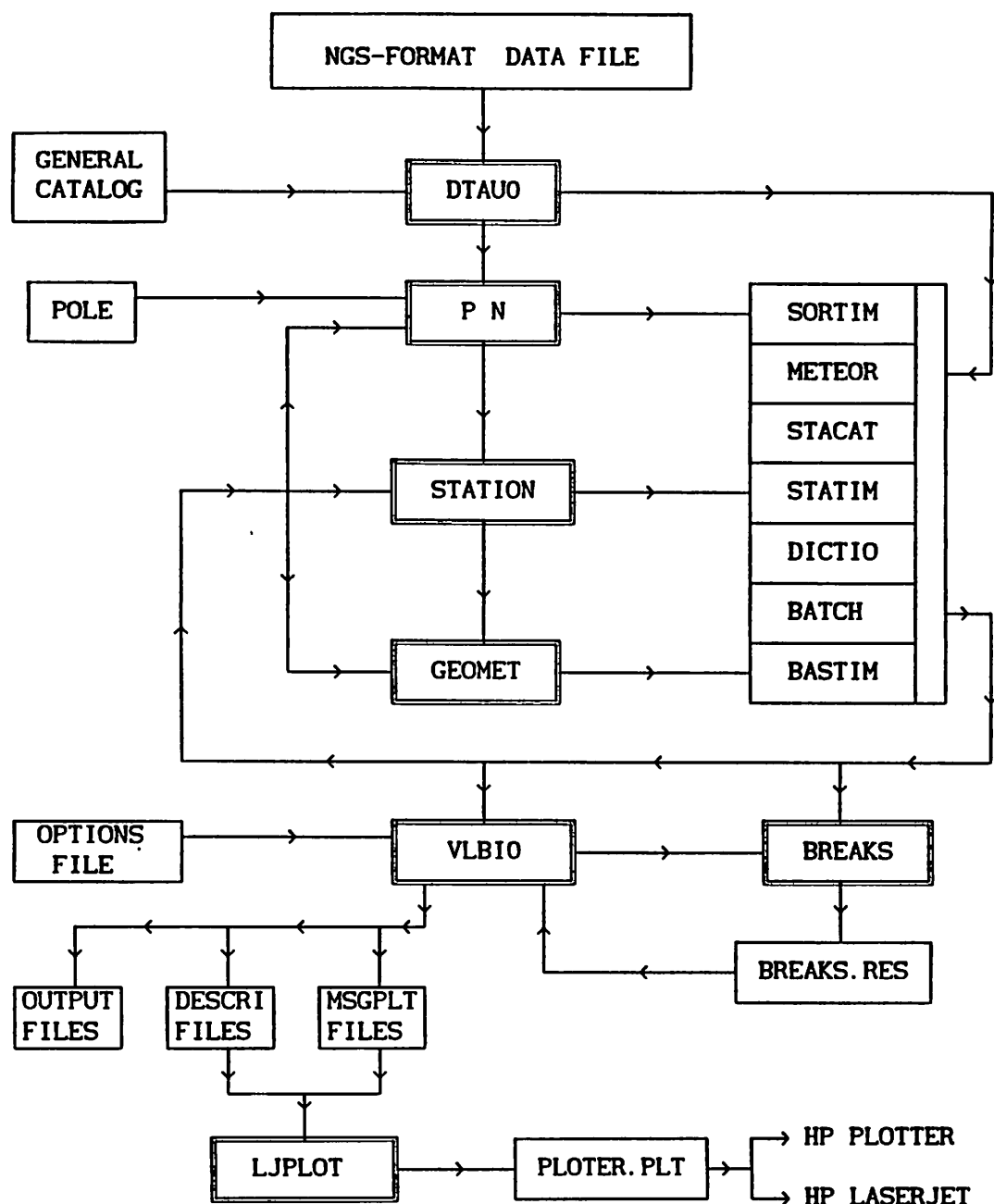


Figure 3.1. Data flow in OCCAM package

### Data Handling

A program named DTAUO reads original input for the experiment, a NGS-format data file, and distribute the information contained there between the standard data files. The analyst can choose whe-



ther external information like ionospheric or cable calibration data should be included or not and which baselines he wants to process. The program creates the standard data files using information from a general catalogue of station and source coordinates, and the observed values read from the NGS-format file.

---

SORTIM	Source vs. time information
STATIM	Station vs. time information
BASTIM	Baseline vs. time information
DICTIO	Directory of the data storing information
STACAT	Local experiment catalogue
METEOR	Meteorological data
BATCH	List of baselines

---

*Table 3.1 Standard File list*

DTAUO is the only link with the input NGS-format data file. If a different input file were to be used, a new Data Handling program should be made, but the rest of the package would not be changed.

#### *Source Dependent Information*

Some corrections that OCCAM applies do not depend on the station or the baseline considered. A program called PN applies all these corrections and stores them on the file SORTIM.

First, a conversion from 2000 epoch to date apparent coordinates for each source at each time must be performed. The precession and nutation model employed is the standard given by IERS (1989). The baricentric position, velocity and acceleration of Earth are also computed and the a priori Earth rotation parameters are interpolated for each observing time.

#### *Station Dependent Information*

Most of the partial derivatives used in the least squares fit and different corrections to the delays and delay rates or to the geometry of the interferometer are computed in this step by the pro-

gram STATION. This information is stored on the file STATIM:  
The program STATION includes models for some effects that change the station coordinates. These models are:

- Earth Tides. A short (93 constituents) harmonic development extracted from the complete model ETMB 85 (Buellesfeld, 1985)
- Ocean Loading. The standard model described by IERS (Goad, 1980) is used here for the three components of the Ocean Loading.
- Atmospheric Loading. (Rabbal & Schuh, 1986)
- Pole Tide. (Yoder, 1984; Wahr, 1985)

Also the Polar Motion produces a rotation of the station position that must be considered.

The hour angle of a source can also be slightly changed by some effects that are modelled in OCCAM

- Short UT1 Variations (Yoder, 1981)
- Ocean M2 Tide effect (Baader, 1983; Brosche, 1989)

The tropospheric models available in OCCAM are the following:

- Chao Model. No external data needed. (Chao, 1974)
- Marini Model. Atmospheric data (temperature, pressure and humidity) needed. (Marini, 1972)

The program can compute corrections due to antenna axis offsets for Azimuth-Elevation and Equatorial mountings. Also the special case of Richmond's antenna is considered in the model.

The program computes the partial derivatives with respect to station coordinates, source coordinates, tropospheric zenith delay and Love numbers (not checked). Most of the total time of running OCCAM is spent at this step.

#### *Baseline Geometric Model*

Finally, the package computes the geometric model in the program GEOMET. Baseline vector coordinates are needed to compute the theoretical delays and delay rates, so they must be computed for all baselines at all times in which they take part.

The relativistic model used to compute the theoretical delays is given by Finkelstein et al. (1985). The model suggested by the IERS standards (Zhu & Groten, 1988; Hellings, 1986) is also available. The delay due to the gravitational bending of the light is given by Finkelstein and the partial derivative with respect to gamma (relativistic PPN factor) is computed. The information is stored in the file BASTIM. Theoretical delay rates are computed using numerical differentiation.

### *Least Squares Fit*

The second part of the program comprises the least squares fit of the different parameters selected. A single program called VLBI0 uses all the information already included in the standard files, applying the corrections and generating the design matrix for the adjustment. The results of the fit are stored on different output files. Plots with the results and the residuals of the fit for each baseline can be generated using a program called LJPLOT. The user can select what parameters should be solved for, which tropospheric model should be applied and if any reweighting must be applied to the observables. A clock model for the stations involved can be included. Ambiguities on single baselines can be automatically eliminated by the program.

---

Global initializing
Read Options and Parametrization
Starting the Loop for running full experiments
Read clock breaks model for each baseline
Read standard data files
Correct the data with the theoretical models
Generate the Design Matrix
Run Least Squares twice to neglect outliers
Generate plot information files
Generate standard output file
Go back for the next baseline or quit if completed

---

*Table 3.2 VLBI0 steps*

The program incorporates a new least squares fit routine, that allows the use of rank deficient design matrices, non diagonal weighting matrix and constraints for the different parameters. Constraints are available for the continuity of the clock model when there is no evidence of a jump.

The design matrix can include up to 31 parameters. The model for the clock breaks is read from an independent file that can be generated automatically by a different program called BREAKS that detects the time of the clock breaks from the residuals of the adjustment (Sardón et al, 1990). Table 3.2 shows the different steps of the program VLBI0.

#### 4. Results obtained from a comparison with the MarkIII Data Analysis System CALC/SOLVE

We have made a first set of comparisons between OCCAM and one of the most standard VLBI analysis packages, CALC/SOLVE, in the version installed at the Geodetic Institute of Bonn University. Up to now only the baseline length results have been compared.

We have used the results of CALC/SOLVE for five experiments of the project Eastern-Atlantic, with similar schedules and network and one of the Western-Atlantic, with different sources and sites (Vierbuchen & Zarraoa, 1990).

The results show an agreement between both programs for European baselines with a maximum difference below two centimeters, being the average discrepancy of less than one centimeter. The formal error obtained from OCCAM for these baselines is less than one cm. For transoceanic baselines the discrepancy increases but in most of the cases it is below the formal error level of OCCAM, around three centimeters. However, we have found significative discrepancies in some trans-oceanic baselines that are now under study. Figure 4.1 shows the difference between one solution from OCCAM and other from CALC/SOLVE for the experiment E.ATL-1 of January 1989.

The conditions in which the comparisons have been performed are not equivalent for OCCAM and CALC/SOLVE. This one produces a global multibaseline solution, and not a single baseline solution as OCCAM does. Also Earth orientation parameters or nutation offsets have been estimated by CALC/SOLVE, and not by OCCAM.

The conclusions we can directly draw from these comparisons are optimistic. The program shows a good consistency on European baselines, with a remarkable agreement with CALC/SOLVE solutions in spite of the different conditions mentioned above. For the inter-continental baselines OCCAM produces weaker solutions than those from CALC/SOLVE but they agree inside the formal error range.

## 5. Future expectations

OCCAM package is still under development. Some of the existing models must be refined or new models implemented. The performance of the program should also be optimized in speed and easy-usage. Exhaustive comparisons with other standard packages must be made. One of our aims is getting a multibaseline and multiexperiment analyser software. To reach this we have studied two different approaches. A first possibility is to use the baseline vectors that have been independently solved for a single experiment. This could lead us to a further combination of these results and their variance-covariance matrix to get an adjustment of the station coordinates. Atmosphere and clock behaviour should be modeled and corrected by VLBI0 in advance.

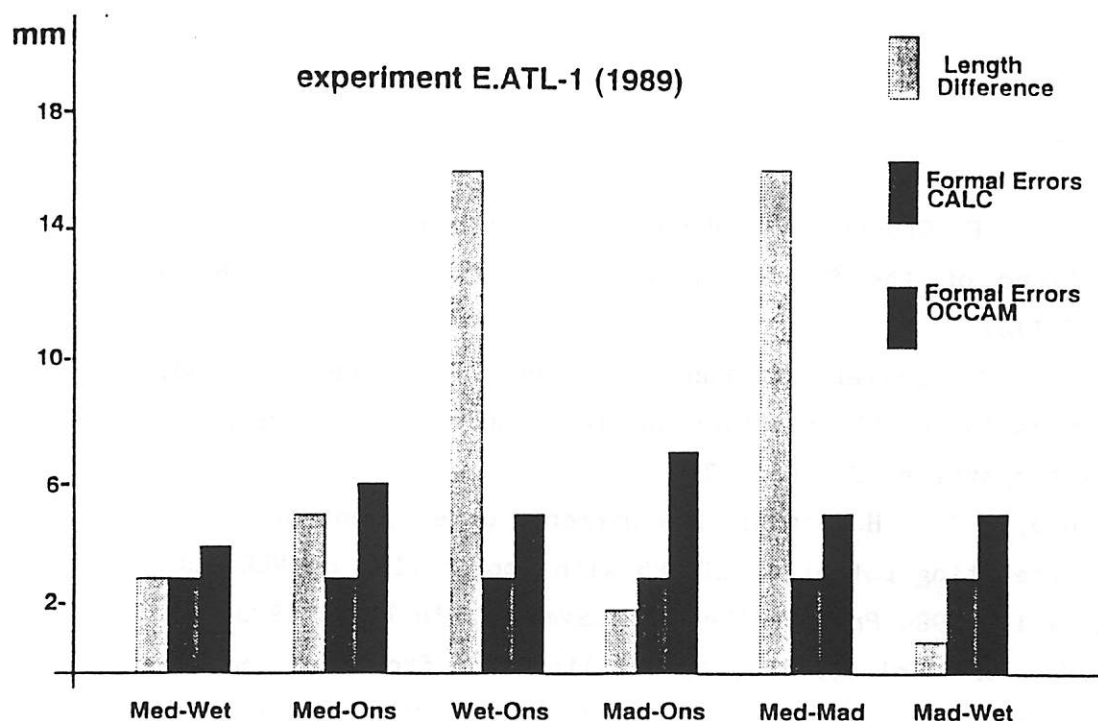


Figure 4.1

Comparison of OCCAM and CALC baseline estimates

The second approach would be to perform the least squares fit with all the observables for all the baselines involved as a single set. This way requests the implementation of new features in the program to solve for new parameters or to include new models and the possibility of using a computer with larger memory capacity.

The package could be improved in its independence from any other system but the correlator. Up to now, the only input it admits is a NGS-format data file which should already contain the information of the ionospheric or cable calibration corrections. OCCAM should be able to compute the ionospheric calibrations from S-Band (2.3 GHz) and X-Band (8.4 GHz) delays and delay rates.

We can foresee different fields in which this package could be an useful tool even in its present state. These fields range from the easy access for testing new models for VLBI analysis, to the fast computations of ambiguities and clock models. It has an extremely low cost and provides easy handling for VLBI processing due to the simple environment in which it has been designed, with fully transportability that can easily be extended to any other environment able to compile FORTRAN 77 code. These advantages make OCCAM an useful tool for educational and training purposes.

The I.A.G. members have carried out the present work with the support of CICYT under contract no. PB88-0021. N. Zarraoa acknowledges Caja Madrid for the financial support provided.

## References

- Baader, H.R., P. Brosche & W. Hövel; "Ocean tides and periodic variations of the Earth's rotation", 1983, *J. of Geoph.* 52 (140-142)
- Brosche, P., U. Seiler, J. Sündermann and J. Wunsch; "Periodic changes in Earth's rotation due to oceanic tides", 1989, *Ast. & Astrophysics*, 220 (318-320).
- Buellesfeld, F.J. & H. Schuh; "New Harmonic development of the Tide-Generating potential ETMB85 with application on VLBI data analysis", 1986, *Proc. of the X Int. Symp. Earth Tides* (933-942).
- Chao, C.C.; "A Model for troposph. calibration from daily surface and radiosonde balloon measurements", 1972, *JPL T.M.* (301-350).

- Finkelstein, A.W., V. Kreinovich & S.N. Pandey; "Relativistic reductions for radiointerferometric observables", 1983, *Astrophysics and Space Science* 94 (233-247).
- Goad, C.C.; "Oceal Loading site displacements", 1983, Appendix 7 in: *Project MERIT Standards*.
- Hellings, R.H., "Relativistic effects in astronomical timing measurements", 1986, *The Astronom. J. Vol. 91 No. 3* (650-659).
- IERS Technical Note 3, IERS Standards 1989, D.D. McCarthy (ed.)
- Marini, J.W.; "Correction of satellite tracking data for an arbitrary tropospheric profile", 1972, *Radio Science* 7 (223-231).
- Rabbel, H. & H. Schuh; "The influence of atmospheric loading on VLBI-experiments", 1986, *Journal of Geophysics* 59 (164-170).
- Ryan, J.W. & C. Ma; "Crustal Dynamics Project Data Analysis, fixed station VLBI geodetic results", 1985, *NASA Tech. Memo. 86229*.
- Sardón, E., N. Zarraoa & A. Rius; "Automatic modeling of clock breaks in geodetic VLBI analysis", 1990, *This volume*.
- Schuh, H.; "Die Radiointerferometrie auf Langen Basen zur Bestimmung von Punktverschiebungen und Erdrotationsparametern", 1987, *Ph. D. Thesis, Deutsche Geod. tische Kommission* 328.
- Vierbuchen, J. & N. Zarraoa; "The East-Atlantic experiments: results for the European stations", 1990, *This volume*.
- Wahr, J.M.; "Polar Motion induced gravity", 1985, *Proc. Int. Conf. on Earth Rotation and Terr. Ref. Frame, Vol. 2* (736-741).
- Yoder, C.F., J.G. Williams & M.E. Parke, "Tidal variations of Earth Rotation", 1981, *J. of Geophys. Research*, 86 (881,891).
- Zhu, S.V. & E. Groten; "Relativistic effects in VLBI time delay measurement", 1988, *Manuscripta Geodaetica* 13 (33-39).

# **AUTOMATIC MODELLING OF CLOCK BREAKS IN GEODETIC VLBI ANALYSIS**

**E. Sardón, N. Zarraoa and A. Rius**

**Instituto de Astronomía y Geodesia, C.S.I.C.-U.C.M.**

**Madrid, Spain**

## **ABSTRACT**

**This paper describes an automatic method for detecting sistematic trends -clock breaks- in the delay residuals obtained in a geodetic VLBI analysis, based on statistical analysis of these residuals. We include a description of the algorithms used as well as applications to recent experiments.**

## **INTRODUCTION**

The clock modelling is traditionally done with one of these two methods:

- the analyst estimates the clock breaks situation by inspection of the delay residuals, introducing a subjective element in the analysis.
- the clock behaviour is estimated every certain amount of time (1, 2, hours), increasing the number of estimated parameters.

In order to improve these situations we have developed an automatic method based on the study of the effect of the clock breaks on the residuals. Besides, this method reduces greatly the time neccesary to model the clock breaks and offers two kinds of clock break detections: in stations or in baselines.

## **EFFECTS OF THE CLOCK BREAKS ON THE RESIDUALS**

An ideal behaviour of the clock means that the difference between the two clocks in a baseline has a simple ( $2^{\text{nd}}$  order) polynomial trend. In general, the clock for each station can suffer deviations relative to the ideal situation at least by two causes: 1) variation of the clock offset,



2) variation of the clock rate. Each of them will produce different effects on the residuals.

In figure 1 different possible clock behaviours and the corresponding effects on the residuals are shown. We denote by  $t_b$  the time in which the clock break takes place. In the first column, the line of dots represents the linear model of the clock behaviour. In the second column the VLBI observable residuals appear as the difference between the estimated straight-line and the clock behaviour values.

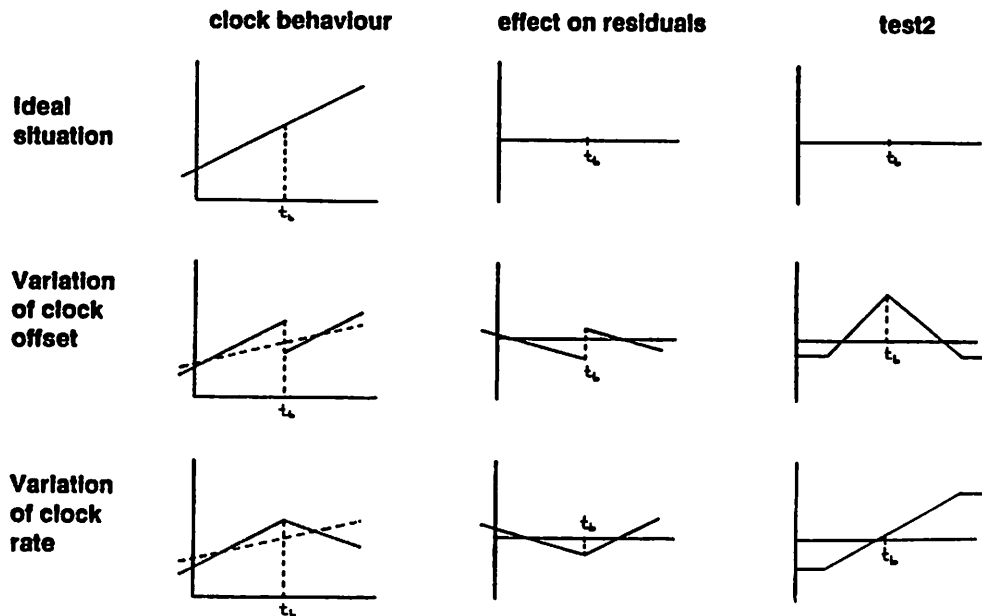


Figure 1

## DETECTION OF THE CLOCK BREAKS

We consider the residuals of one single baseline. For each observation on it we form a group with the  $N$  previous residuals:  $A_1$  and another group with its residual and the  $M-1$  following ones:  $B_1$ . Let  $T_{A1}$  and  $T_{B1}$  be the corresponding times for those residuals ( $T_{B1}$  will be the time of the observation itself).

**TEST0.** - Fitting a straight-line with the first group without  $A_1$  and another with the second group without  $B_1$ , this algorithm checks if these two lines intersect in a point close to  $B_1$ . If this does not occur, this algorithm indicates a higher probability that the clock has changed its offset (clock jump). Besides, the time of the clock break should coincide with the instant in which the TEST0 fails.

Assuming that the straight-lines adjusted by least squares are

$$y_A = a_1 * t + a_2, \quad y_B = b_1 * t + b_2$$

and their variances:

$$\sigma_{a1}, \sigma_{a2}, \sigma_{b1}, \sigma_{b2}$$

What this algorithm checks is if the intervals:

$$\left[ x - 3 \sigma_x, x + 3 \sigma_x \right] \quad \text{and} \quad \left[ T_{AN}, T_{B2} \right]$$

intersect each other, where:

$$x = \frac{b_2 - a_2}{a_1 - b_1} \quad (\text{x-coordinate of the cut point})$$

$$\sigma_x^2 = \left[ \frac{1}{a_1 - b_1} \right]^2 \left[ \sigma_{a2}^2 + \sigma_{b2}^2 \right] + \left[ \frac{x}{a_1 - b_1} \right]^2 \left[ \sigma_{a1}^2 + \sigma_{b1}^2 \right]$$

TEST2.- In this method this is the principal algorithm. This algorithm is the Student's test for comparison of means of two populations with equal variances. This algorithm reacts to both kind of breaks (variation of clock offset, variation of clock rate) with different behaviour for each of them. Looking at the figure 1, we can see that in the case of clock offset variation, the time of the clock break should coincide with the instant of the extreme value of test2 (like in test0) while in the case of clock rate variation, the instant of the clock break does not coincide with the instant of the extreme value of the algorithm, but this extreme occurs N observations after the real break. Then it is necessary to discern in which case we are. We can do it in the following way: we use the values of test2 to identify clock breaks and the values of test0 to assign the correct type and time for the breaks found. If test0 fails the clock offset has changed at that precise instant. If test0 does not react the break is a rate variation that took place N observations before.

What this algorithm computes is:

$$\text{TEST2} = \frac{\bar{B} - \bar{A}}{S} \frac{1}{\sqrt{\frac{1}{N} + \frac{1}{M}}} \quad (\text{T-STUDENT})$$

where  $\bar{A}$  and  $\bar{B}$  are the mean value of  $A_1$  and  $B_1$  and  $S$  is the standard deviation of  $(A_1, B_1)$ .

### SYNTHESIS OF THE CLOCK BREAKS

#### a) For each station

When a clock break happens in one of the stations of a VLBI experiment, it perturbs all the baselines in which this station participates. So, when analysing only one baseline we cannot assign the clock fail to any of the two stations of this baseline. But, we have an algorithm that give a value for each observation of each baseline. To identify the "guilty" station at a determinate instant we do the following steps:

- For each baseline, we assign the algorithm value to the first station with its sign and to the second station with the opposite sign.
- For each observation and each station, we compute the sum of these values (with the corresponding sign) and we consider only the station with the highest sum in absolute value.

The next step is the analysis of the information for each station along the experiment. This is done looking for the maxima values of sums of test2 in groups that have the same sign for these sums. These maxima values indicate possible clock breaks. To discern if this bad behaviour we have assigned to the station is caused by a clock break occurred at that moment or it is a product of a clock break occurred before, we use a criteria of minimum time span between two test failures to be considered as two different clock breaks (around two hours).

b) For each baseline

In this case, the process is basically the same that in the case of stations. The only difference is that now we do not look for a "guilty" station at each instant, we only work with each baseline looking for clock breaks along the experiment, independently of the other baselines.

## RESULTS

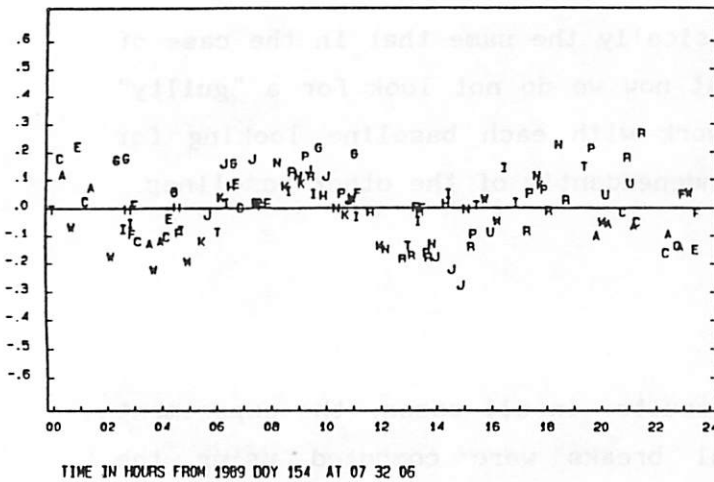
We present some comparison of results. In all cases, the experiment analysed is E.ATL-2/89. The manual breaks were computed using the residual plots obtained with the package CALC & SOLVE (GSFC VLBI Group). The automatic clock breaks were obtained with the method presented here using the residuals from the package OCCAM (N. Zarraoa et al). Table 1 shows the clock break times.

	<u>Manual breaks</u>		<u>Automatic breaks</u>	
DSS65	Reference		89/06/03	11:44
				21:15
			89/06/04	3:40
WETTZELL	89/06/03	17:17	89/06/03	11:02
		22:30		20:57
			89/06/04	1:21
ONSALA60	89/06/03	15:00	89/06/03	18:35
		22:30		
NOTO	89/06/03	12:50	89/06/03	14:06
		22:30	89/06/04	3:33

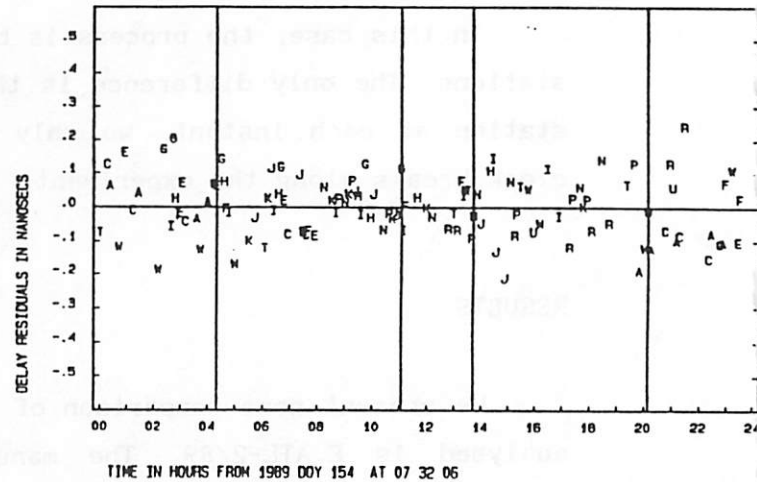
TABLE 1

Figure 2 shows the residuals obtained by OCCAM with automatic clock modelling and without clock modelling. We can see how the sistematic behaviour has been removed.

Without modelling



Automatic model



EXPERIMENT 89EATL2C BASELINE DSS65 -ONSALA60

Figure 2

Comparison of OCCAM baseline estimates obtained using Manual and Automatic Breaks

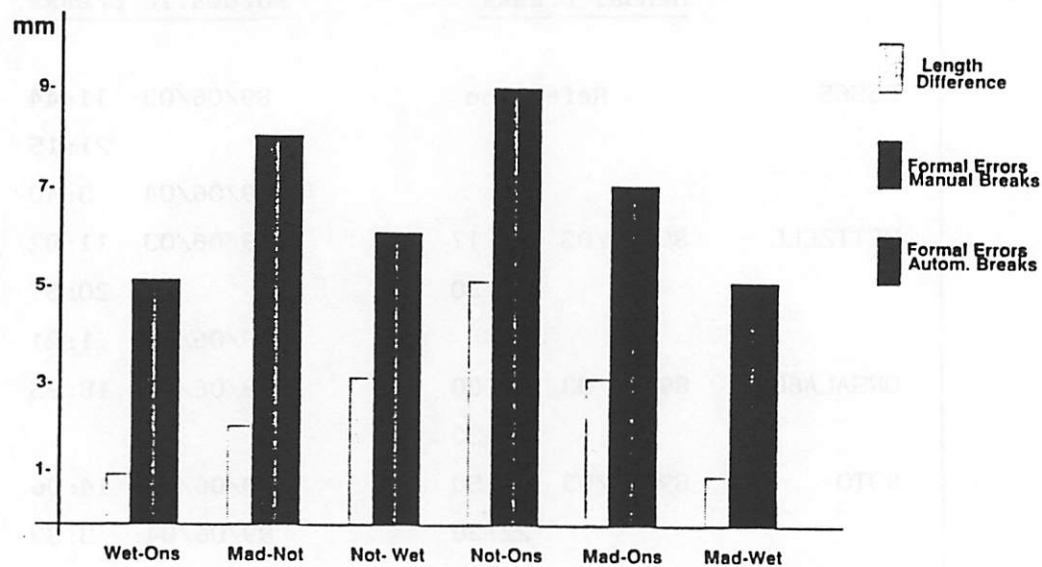


Figure 3

A comparison has been done between the baseline results of OCCAM package obtained with manual and with automatic breaks (Figure 3). In this case, the manual clock breaks obtained using the package CALC were applied into the OCCAM package to obtain the results with manual clock

breaks. We can see in this figure that the baseline length difference between the manual and the automatic method is, for all the European baselines, well under the formal error. Then we can consider that both solutions are equivalent.

## CONCLUSIONS

By the moment, all the tests we have performed make us be optimistic about the usefulness of this method, though some points still have to be refined. The most important of these points is: transportability to other VLBI analysis packages.

In any case, the method, in its present stage, gives a very good tool for the analysis of VLBI experiments, saving time and avoiding personal errors, in the modelling of the clock behavior, or any other phenomena which produces analogous effects on the residuals.

This work has been partially supported by the CICYT under contract PB88-0021. Nestor Zarraoa acknowledges the support given by Caja Madrid.

## REFERENCES

N. Zarraoa, A. Rius, E. Sardón, H. Schuh, J. Vierbuchen, "OCCAM: A Compact and Transportable Tool for the Analysis of VLBI Experiments", 1989.

GSFC VLBI Group, "CALC Version 6.0", Goddard Space Flight Center, Greenbelt, Maryland, 30 jan. 1985.

# SPECTRAL ANALYSIS OF THE "WET" DELAY: PRELIMINARY RESULTS

G. Elgered  
Onsala Space Observatory  
Chalmers University of Technology  
S-43900 Onsala, Sweden

## ABSTRACT

Microwave radiometry has been used to estimate the propagation delay of radio waves due to atmospheric water vapor ("the wet delay"). Time series of microwave radiometer measurements have been transformed into the frequency domain. These spectra are used to study the variations in the wet delay itself, the instrumental noise, and possible variations introduced by measuring in different directions on the sky.

## 1. INTRODUCTION

Measurements of the atmospheric emission at 21.0 and 31.4 GHz made with a water vapor radiometer (WVR) have been used to estimate the propagation delay caused by atmospheric water vapor (see *e.g.* Johansson *et al.*, 1987). The WVR at the Onsala Space Observatory has been used since 1980 to correct for the wet delay during geodetic radio interferometry campaigns. In this paper a short theoretical background is given and, thereafter, inferred spectra of the wet delay are presented and discussed.

## 2. BACKGROUND THEORY

The wet delay can be written as:

$$\Delta L_w = (1762 \pm 20) \times 10^{-6} \int_0^{\infty} \frac{a_v(z)}{T(z)} dz \quad (1)$$

where  $a_v$  is the water vapor density in  $\text{g/m}^3$ ,  $T$  is the temperature in K, and  $z$  is the coordinate along the path through the atmosphere.

A discussion on the spectral density of the wet delay has been given by Thompson *et al.*, 1986.

## 3. RESULTS AND DISCUSSION

All WVR data spanning a time period larger than 24 hours and taken during geodesy VLBI experiments have been transformed into the frequency domain. In total 76 such data sets of the equivalent zenith wet delay were analyzed. An example of the obtained "Power Spectral Density" (PSD) is shown in Figure 1. Let us assume that the PSD can be written as:

$$S(f) = a \times f^b \quad (2)$$

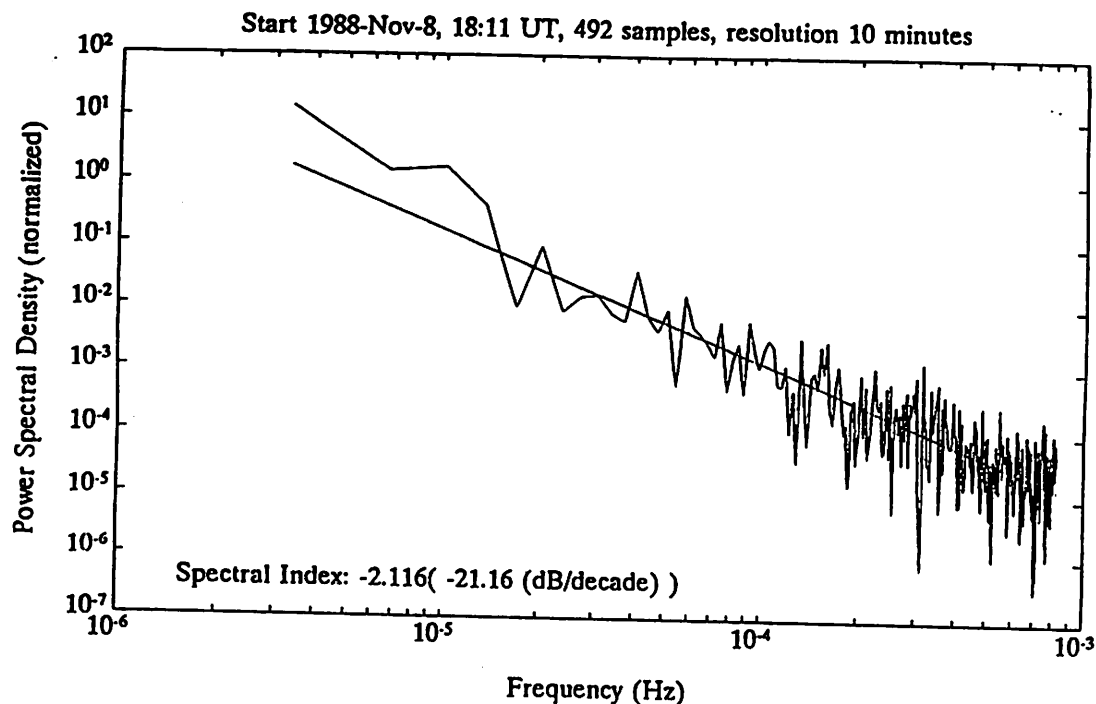


**Figure 1.** Estimated power spectral density of the wet propagation delay measured with microwave radiometry during three contiguous geodetic VLBI experiments in November 1988.

The constant  $b$  is often referred to as the spectral index. Figure 2 shows the estimated spectral indices for all 76 data sets. The mean is equal to -1.95. For a fully developed Kolmogorov turbulence in the atmosphere the spectral index is expected to be equal to  $-8/3$  (Thompson *et al.*, 1986). In order to study the influence of noise a Monte-Carlo study has been carried out. The result obtained when white noise of 3 mm (RMS) was added to the time series of the wet delay is presented in Figure 3. We note that the mean is now decreased to -1.3. The error bars give the one sigma scatter obtained from 20 estimates of the spectral index from each data set.

The same analysis was also carried out when 1 and 5 mm (RMS) white noise were added to the time series of equivalent zenith wet delays. An approximate linear relationship was obtained between the amount of added noise and the estimated mean spectral index. We conclude that if the original data includes an RMS noise of approximately 3 mm the spectral index of the fluctuations due to the variations in the atmospheric water vapour would be approximately  $-8/3$ .

## REFERENCES

- Johansson, J.M., G. Elgered, and J.L. Davis, *Geodesy by Radio Interferometry: Optimization of Wet Path Delay Algorithms Using Microwave Radiometer Data*, Res. Rept. No 152, Onsala Space Observatory, Sweden, 1987.
- Thompson AR, Moran JM and Swenson GW Jr, In: *Interferometry and Synthesis in Radio Astronomy*, Wiley & Sons, 1986.



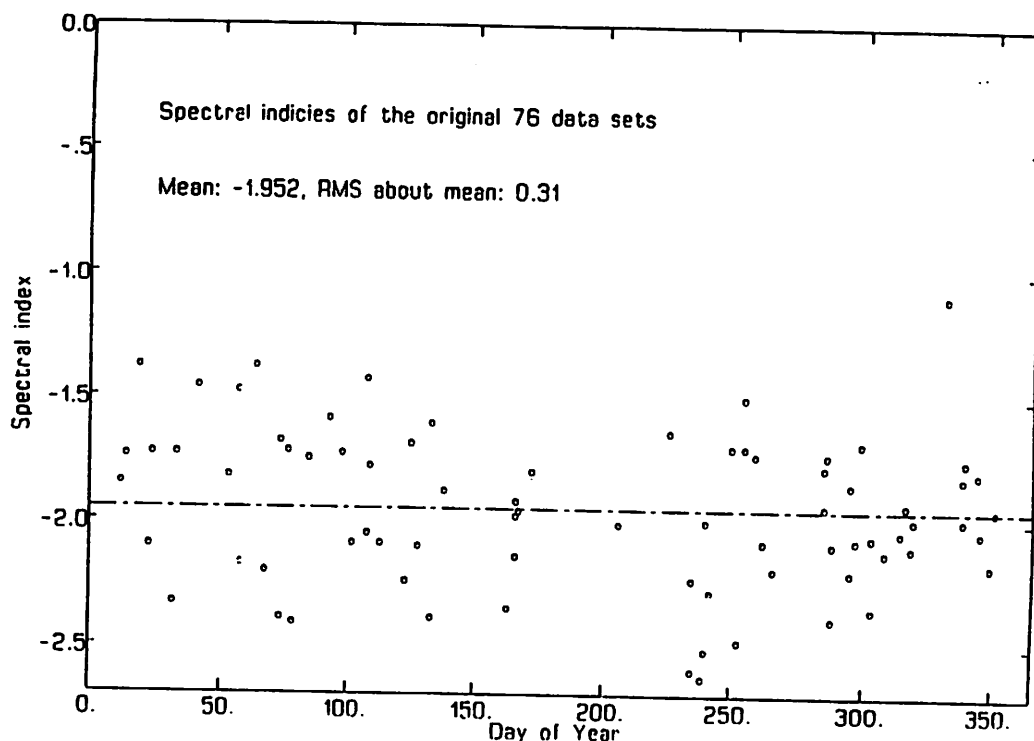


Figure 2. Estimated spectral indices of 76 data sets of the wet propagation delay measured with microwave radiometry.

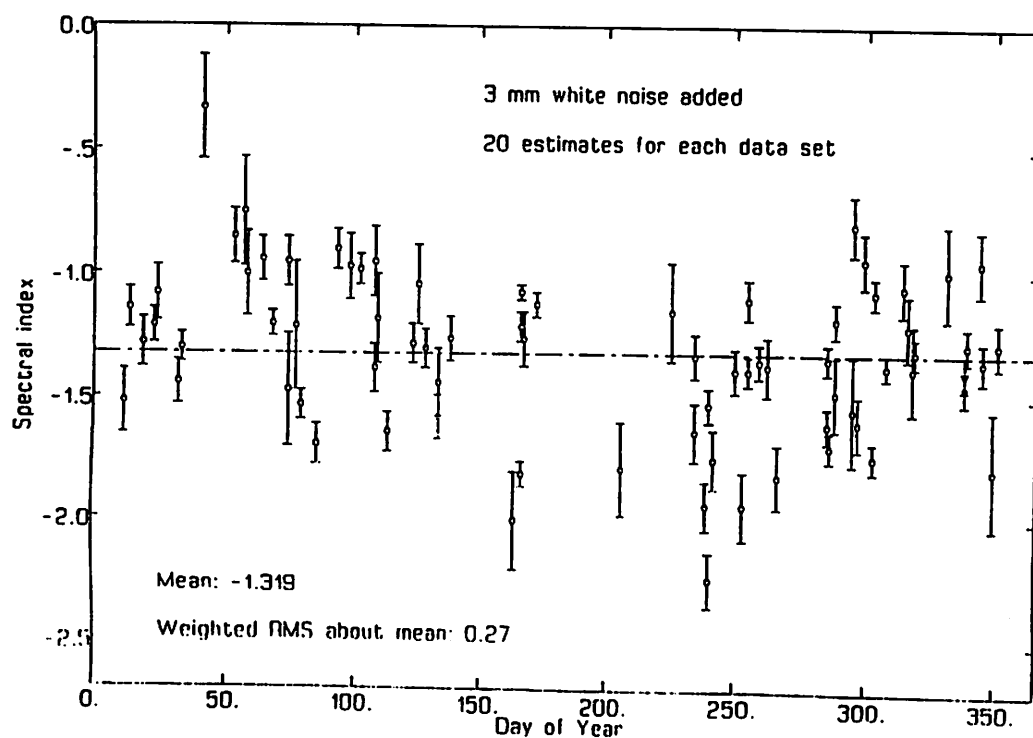


Figure 3. Estimated spectral indices of 76 data sets of the wet propagation delay when an extra white noise of 3 mm (RMS) is added to the measured time series.

# **GALACTIC MASERS AS A TOOL TO RELATE THE RADIO AND OPTICAL CELESTIAL REFERENCE FRAMES**

by

**B.O. Ronnang**

**Onsala Space Observatory  
Chalmers University of Technology  
S-439 00 ONSALA  
Sweden**

**Abstract.** Ground based optical astronomy, astrometry satellites, and Very Long Baseline Interferometry (VLBI) provide completely different methods to obtain very accurate celestial positions. Unfortunately different objects, stars and cores of compact radio galaxies in the case of VLBI, are observed and as many methods as possible must be found to relate the two frames. This paper summarizes the methods, presents a new observational technique using SiO-masers, and lists suitable observatory pairs for 7 mm observations.

## **The extragalactic and the optical reference frame.**

Radio astrometry has made great progress in the past ten years in making accurate positional measurements over large sky angles. Currently Very Long Baseline Interferometry (VLBI) produces the most accurate positions of celestial bodies with formal errors of conventional celestial coordinates approaching a milliarcsecond (mas) and for a small selection of sources as small as 0.3 mas (Ma 1988). The extragalactic radio sources, i.e. the compact radio cores of active galaxies and quasars, make excellent reference points for establishing a reference frame as they should display little or no detectable proper motion thanks to the great distance to these objects. One of the most important goals in this field is to get a more even distribution of sources in the northern and southern hemisphere. Most sources are presently in the northern sky as seen from figure 1. The reason is of course that all but a few of the existing VLBI antennas are far north of the equator. The JPL 1986-3 catalogue, less accurate due to Mark II recording, is the only one based on data from a southern hemisphere telescope (Sover and Treuhaft 1988).

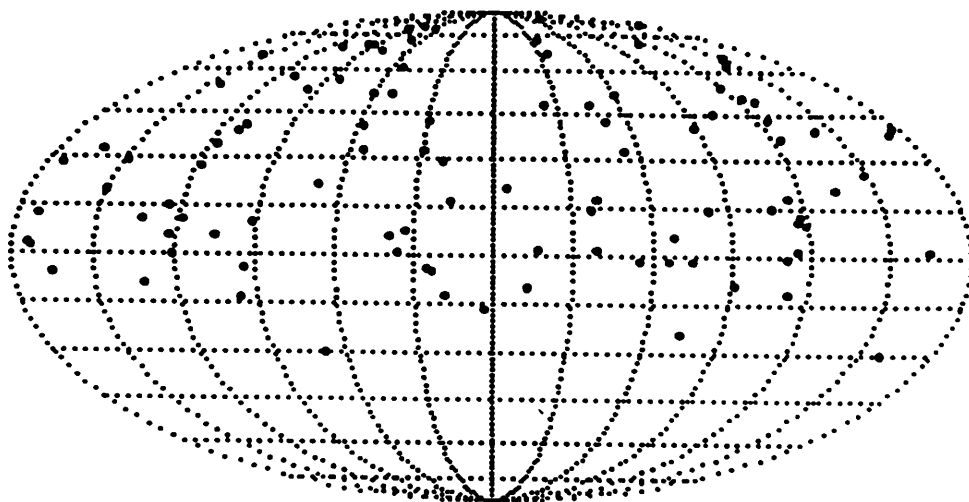


**Figure 1.** The sky distribution of the compact extragalactic radio sources (mainly Seyfert galaxies and quasars) forming the extragalactic reference frame. Some of the 114 included sources have been observed with VLBI more than 15,000 times and are marked with circles. Notice that most sources currently are in the northern sky.

One of the fundamental difference between the extragalactic and stellar reference frames is the proper motion of the objects that defines the frame. Most stars have proper motions of the order arcseconds to milliarcseconds while no significant proper motions have been detected for extragalactic objects. The accuracy of any stellar position is therefore time dependent, decreasing with increasing time from the mean epoch of observations. The most accurate present star positions are in the FK5 catalogue containing about 5000 stars. The positions are believed to be known to 30 mas at the mean epoch of 1986 and with proper motion uncertainty of less than 1 mas/year. In principle, ground based astrometric technique have the potential to reach 10 mas accuracy in sky fields of less than 10 degrees. The fundamental problem is with large arcs where the refractive properties of the earth's atmosphere limits the accuracy. The solution is the future space based techniques.

The ESA astrometry satellite HIPPARCOS, the unfortunately failed to reach its final orbit after the launch in July 1989, was designed to make precise measurements of the positions, parallaxes, and proper motions of about 120 000 selected stars brighter than magnitude 13. Accuracies of the order of 2 mas were expected for positions and parallaxes, and 2 mas/year for proper motions. In addition a separate Hipparcos experiment called "Tycho" would have produced a lower precision, but larger, catalogue of approximately 500 000 stars brighter than magnitude 11. The initial accuracy would accordingly have been almost the same as that of the extragalactic frame and as in the case of VLBI Hipparcos were designed to measures arc differences by superposition of two distant star fields on a single focal plane by means of a complex mirror.

### **Methods to relate the radio and the optical reference frames.**

The task to relate the optical and radio reference frames is by no mean trivial, but several methods exist. In the following we briefly describe two established methods and give a more detailed description of a link between the two frames based on circumstellar maser sources (Baudry et al. 1979). Especially the choice of molecular transition is discussed.

#### *Observations with the Hubble Space Telescope.*

Quasars in the extragalactic reference frame which has optical counterparts can be observed by the Hubble Space Telescope together with stars in the optical catalogues. Similar type of observations can also be done with ground based astrograph cameras. These optical counterparts are always very faint objects compared to the stars and the number of objects are limited to a few hundred. Both these facts limit the accuracy.

#### *Observation of radio stars.*

Stars which display radio emission provide a direct link if there radio positions can be determined precisely with respect to the radio reference frame using the Very Large Array in the USA or VLBI. The radio emission occurs due to the violent interaction in close multistar systems (see Lestrade et al., this publication). These systems, mostly close binary stars, are also included in the optical reference frame but the number of such objects are few.

It should once again be pointed out that both methods rely on the assumption that we can determine the location of the radio emission with respect to the optical photocenter. This weakness also applies to the amplified molecular line radio emission that occurs in the envelope of many late type stars during their mass loss evolution stage. In this case the position of the optical star, e.g. a Mira or supergiant star, is known and the radio position of the maser regions in the envelope is measured relative to the extragalactic reference frame. The next sections describe the feasibility of this method.

#### *Observations of circumstellar OH, H<sub>2</sub>O, and SiO masers.*

Cosmic masers are the most compact molecular line sources studied by radio astronomers. Thanks to the amplification of the molecular lines the received signal from a very small region becomes strong enough to be detected by the radio telescope. The masers, associated with molecules of hydroxyl (OH), water (H<sub>2</sub>O), silicon monoxide (SiO) and methanol (CH<sub>3</sub>OH), are found in star forming regions and circumstellar envelopes of late type stars. In connection to astrometry the H<sub>2</sub>O masers in star forming regions have provided an important tool to measure galactic distances in a direct way. However, our main interest is concentrated to the circumstellar masers. The central star in this case is a late type star in the mass loss evolution stage. Some of the OH-maser stars have probably evolved even further towards the planetary nebula stage. The fundamental question is if the positions of the circumstellar maser emission regions could be related to the position of the central star to provide a new method to connect the two reference frames. Let us try to answer this question by describing some of the properties of the different circumstellar masers.

In the past decade the spatial structure of the OH shells around late type stars has been studied successfully by radio interferometer techniques. For the so called OH/IR-stars,

which have spectra at the longest of the four  $\lambda = 18$  cm energy transitions dominating by two peaks with a separation of 20-40 km/s, we have a good picture of the spatial structure and the circumstellar envelope. The shape of the spectra tells us that the maser emission comes from a rather thin, uniformly expanding shell in the outermost regions of the envelope at a distance of 500-10000 astronomical units from the star. In this picture the strongest maser emission originates from the front and the backsides of the shell. The separation between the peaks is twice the expansion velocity of the shell and the stellar velocity lies halfway between the peaks. These objects are suitable for direct distance measurements in the Galaxy as the central star is a long period variable and the variability also appears in the OH radio emission (Herman et al. 1985). The distance is obtained by comparing the angular size of the thin shell and the time lag between the variations of the two peaks in the spectrum. However, this class of objects has no optical counterpart and they cannot be used to connect the two reference frames. For the more nearby OH masers associated with Mira stars the position uncertainties due to eventual nonspherical expansion in conjunction with the relatively long wavelength of 18 cm, where the ionosphere can cause problems, are the main drawbacks for astrometry.

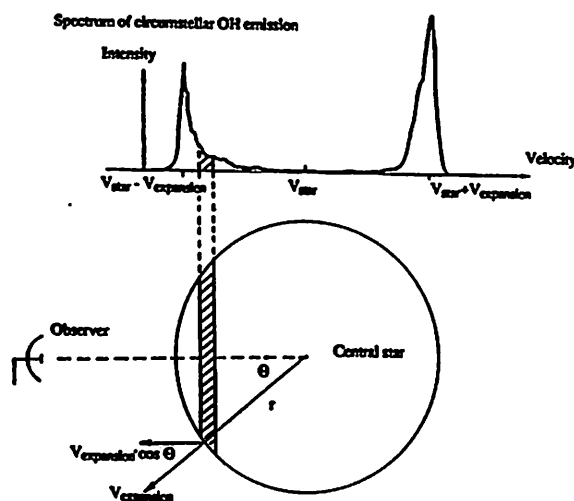


Figure 2. Thin shell model of an OH/IR maser source. For a uniformly expanding thin shell each radial velocity in the observed OH spectrum, shown above the star model, corresponds to a slice through the maser shell perpendicular to the line of sight. The strong emission at the two edges of the spectrum correspond to the regions in front of and behind the star.

Let us instead look at the emission from water vapour, which appears at the wavelength of 1.35 cm. High resolution interferometry shows that the  $\text{H}_2\text{O}$  emission occurs closer to the star than the OH emission (Johnston et al. 1985, Lane et al. 1987). The total extent of the  $\text{H}_2\text{O}$  regions of many Mira variables have been measured to be between 10 to 100 astronomical units, while the regions associated with supergiants long-period variables are several hundred astronomical unit in extent. The intensity of the signal varies rapidly and there are evidence for non-spherical geometry as expected in these warm, inner regions. The  $\text{H}_2\text{O}$  masers are thus unsuitable for astrometry as it is difficult to estimate the position of the central star.

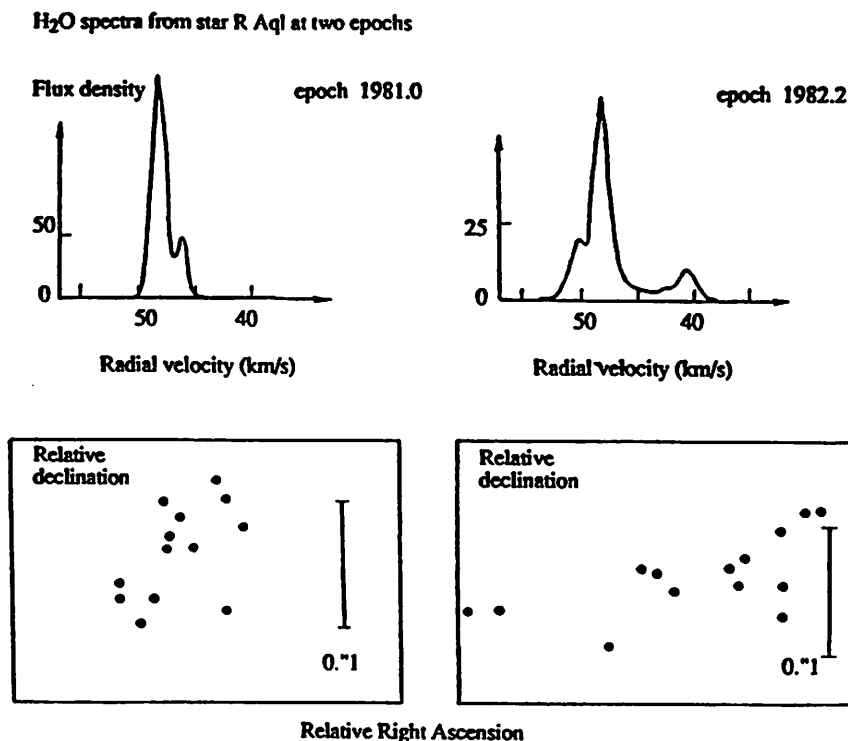


Figure 3. Spectra of water vapour emission and corresponding maps at two epochs of the compact H<sub>2</sub>O maser spots around the Mira star R Aql. Notice how fast the maser positions change which makes it difficult to locate the position of the star (from Johnston et al. 1985).

The next maser line emission, if we exclude the methanol emission, is from SiO molecules. VLBI observations at the wavelength of 7 mm (the wavelength corresponding to the lowest rotational transition of SiO) of a few Mira and supergiant stars have revealed that the SiO maser regions are very close to the photosphere of the star (Moran et al. 1979, Genzel et al. 1979, Lane et al. 1980, McIntosh et al. 1988). The emission intensity and spectral line shape varies, but only occasionally in phase with the intensity variation of the star. The mean velocity of the maser line features agrees, however, with the radial velocity of the star. There are therefore good reasons to believe that the star is in the center of a region with several compact maser spots as in figure 4. Further studies will reveal how well we can determine the position of the central star. A good guess is to better than 10 mas. Several hundreds of SiO-masers have been detected in recent searches. In many cases the objects are so far away that the optical counterpart cannot be identified but for most of the nearby sources the associated Mira or supergiant stars are known. And in some of these cases nearby extragalactic objects included in the radio reference frame can be found. We thus determine the positions of the SiO masers as accurately as possible with reference to the extragalactic reference frame using VLBI. We then try to relate the positions of the maser spots relative to the star based on the astrophysics and single telescope and/or interferometer observations. The position of the star is already known from optical catalogues and we thus have a link between the two frames. The weak part of the link is as before the connection between the maser spots and the star.

SiO spectra from the supergiant star VX Sgr

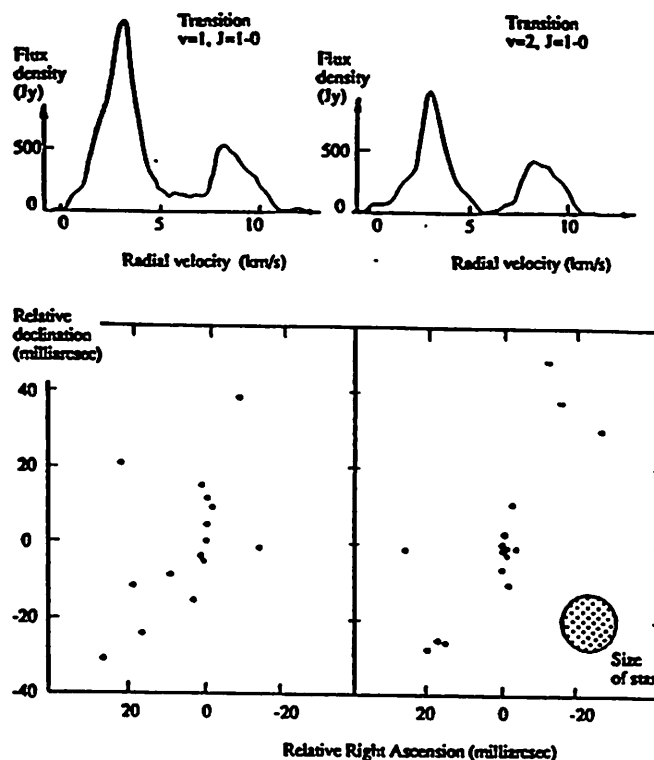


Figure 4. Two SiO spectra of the supergiant VX Sagittarii in two vibrationally excited lines about 300 MHz apart at a frequency of 43 GHz together with VLBI maps showing the relative positions of the maser spots.

The short wavelength of 7 mm has advantages as well as drawbacks. The ionosphere does not contribute to the measurements uncertainty, for example, but instead the tropospheric water vapour attenuates the radio signal. The short wavelength implies that interferometers with moderately long baselines must be used as the maser spots otherwise will be resolved. Only one suitable interferometer, permanently equipped with 7 mm receivers and H-maser, exists in the world, namely the Nobeyama-Kasima interferometer in Japan with its 170 km long baseline. This baseline was successfully used at the wavelength of 7 mm in November 1989 (M.Inoue, private communication). The Onsala-Effelsberg baseline has been used several times since 1986 and proven to be too long for most sources. However, a suitable combination of data from the Onsala-Effelsberg, Nobeyama-Kasima baselines and the shorter Yebes-Pico Veleta baseline in Spain (when Pico Veleta is equipped with a H-maser and a 7 mm receiver) should give interesting results.

Let us also look at the necessary and available sensitivity in the VLBI observations of SiO masers where the coherent observing time is limited by the frequency stability of the atomic frequency standard and the instabilities in the troposphere. With a mean telescope size of 30 m and state-of-the-art low noise receivers an acceptable signal to noise ratio is obtained for SiO masers stronger than about 10 Jansky and for extragalactic compact sources stronger than about 1 Jansky. The SiO sources as well as the compact extragalactic objects are time variable. Available surveys indicate, however, that at least 50 sources of both kinds should be available simultaneously.

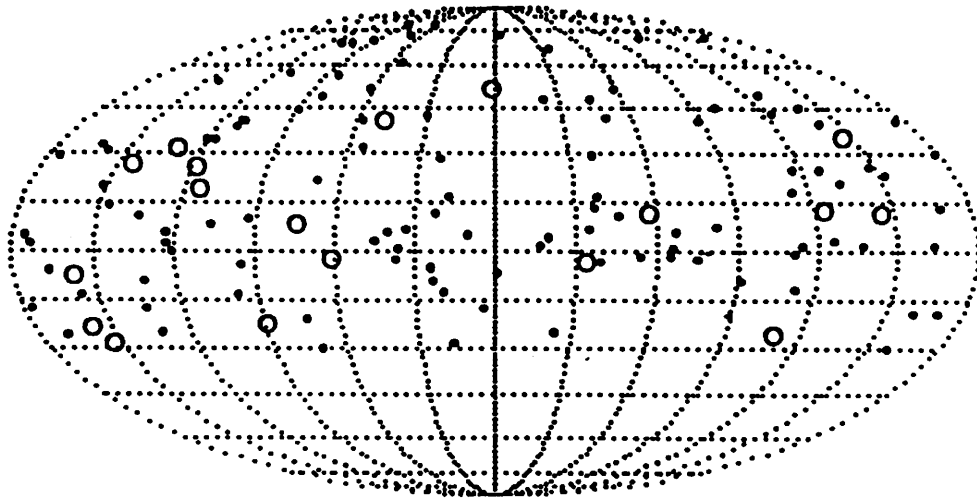


Figure 5. A sky map showing positions of compact extragalactic sources observed to be stronger than 1 Jy at the wavelength of 7 mm (dots). From Owens et al. 1978, Owens et al. 1980, Edelson 1987. Some SiO-masers suitable for position measurements are also included (circles).

The radio techniques to reference the position of spectral line sources to extragalactic objects many degrees away in the sky is not straightforward and new method has to be tested. The technical development in mm-wave astronomy is remarkably fast. There are therefore good hopes that an extensive observational program with thorough data analysis will give acceptable accuracy within a few years, i.e. long before there is a replacement for Hipparcos. It is well worth the efforts as an unified celestial reference frame is fundamental to all kinds of precise position measurements on the earth and in space as well as for studies of the dynamics of the earth, the solar system, and the Galaxy.



## References

- Baudry A., Delannoy J., Lequeux J., *J. Optics*, **10**, p. 359, 1979
- Edelson R.A., *Millimeter-Wave Spectra and Variability of Bright, Compact Radio Sources*, *Astron. J.*, **94**, pp. 1150-1155, 1987.
- Genzel R., Moran J.M., Lane A.P., Predmore C.R., Ho P.T.P., Hansen S.S., Reid M.J., *VLBI Observations of the SiO Maser in Orion*, *Ap.J.*, **231**, L73-L76, 1979.
- Herman J., Baud B., Habing H.J., Winnberg A., *VLA Line Observations of OH/IR Stars*, *Astron. & Astrophys.*, **143**, pp.122-135, 1985.
- Johnston K.J., Spencer J.H., Bowers P.F., *The Circumstellar H<sub>2</sub>O Maser Emission Associated with Four Late-Type Stars*, *Ap.J.*, **290**, pp.660-670, 1985.
- Lane A.P., Ho P.T.P., Predmore C.R., Moran J.M., Genzel R., Hansen S.S., Reid M.J., *VLBI Observations of the  $v=1$  and  $v=2$  SiO Masers in W Hydra and VX Sagittarius*, in B.H. Andrew (ed.), *Proceedings of the IAU Symposium 87, "Interstellar Molecules"*, Reidel, Dordrecht, 1980.
- Lane A.P., Johnston K.J., Bowers P.F., Spencer J.H., Diamond P.J., *H<sub>2</sub>O Masers in Circumstellar Envelopes*, *Ap.J.*, **323**, pp.756-765, 1987.
- Ma C., *The VLBI Celestial Reference Frame of the Nasa Crustal Dynamics Project*, in A.K. Babcock (ed.), *Proceedings of IAU Symposium 128, "The Earth's Rotation and Reference Frames for Geodesy and Geodynamics"*, Kluwer Academic Publishers, Dordrecht, 1988.
- McIntosh G.C., Predmore C.R., Moran J.M., Greenhill L.J., Rogers A.E.E., Barvainis R., *VLBI and Polarimetric Observations of the SiO Masers in R Cassiopeia*, *Ap.J.*, **337**, 934-944, 1988.
- Moran J.M., Ball J.A., Predmore C.R., Lane A.P., Huguenin G.R., Reid M.J., Hansen S.S., *VLBI Observations of SiO Masers at a Wavelength of 7 Millimeters in Late-Type Stars*, *Ap.J.*, **231**, L67-L71, 1979.
- Owen F.N., Porcas R.W., Mufson S.L., Moffett T.J., *Observations of Radio Sources with Flat Spectra*, *Astron. J.*, **83**, pp. 685-696, 1978.
- Owen F.N., Spangler S.R., Cotton W.D., *Simultaneous Radio Spectra of Sources with Strong Millimeter Component*, *Astron. J.*, **85**, pp. 351-362, 1980.
- Sovers O.J., Treuhaft R.N., *Radio Reference Frame Stability from VLBI Data*, in M.J. Reid and J.M. Moran (eds.), *The Impact of VLBI on Astrophysics and Geophysics*, Kluwer Academic Publishers, Dordrecht, 1988

# RADIOASTRONOMICAL ANALYSIS OF IRIS-EXPERIMENTS:

## Status Report

Schalinski, C.J.<sup>1,2</sup>, Witzel, A.<sup>1</sup>, Alef, W.<sup>1</sup>,  
Campbell, J.<sup>2</sup>, & Alberdi, A.<sup>1,3</sup>

<sup>1</sup>: Max-Planck-Institut für Radioastronomie, Bonn, F.R.G.

<sup>2</sup>: Geodätisches Institut der Universität Bonn, F.R.G.

<sup>3</sup>: Instituto de Astrofísica de Andalucía, Granada, Spain

In the early eighties a transcontinental geodetic VLBI-network began to operate at 8.4GHz and 2.4GHz (X/S-band) using the MkIII-system in Mode C (Carter et al., 1985). Purpose of the *IRIS-Project* (*International Radio-Interferometric Surveying*) is the monitoring of earth rotation parameters (UT1, polar motion) by the weekly observations of 15 extragalactic radio sources. From the beginning it was obvious that the sources are *not pointlike* but display structure on the milliarcsecond("mas")-scale. In order to *minimize* the influence of structural phases  $\psi_s$  on the primary observables (phase and group delay) it was suggested not to observe the minima of the *Visibility* (Thomas, 1980). Since structural variability is not negligible - the source list contains some of the wellknown *superluminals* - *monitoring* of the source structure is required.

We started an interdisciplinary project with the aim to study the structures and kinematics of the IRIS-sources with *mas*-resolution and to investigate the applicability of structural phases for the improvement of geodetic parameters. Here we report on the status of the radioastronomical analysis with emphasis on the structural evolution at 8.4GHz. Details of the calibration procedure which is the essential step to obtain reliable maps from the *snap-shot*-data, and the maps prior to 1986 are given in Schalinski et al. (1986) and Schalinski et al. (1987). Recent results of the geodetic analysis are reported by Campbell & Zeppenfeld (this volume).

Table 1 shows that 10 epochs between 1983.35 and 1987.7 of *1803+78* are analyzed. The dynamic range of the maps at 8.4GHz presented in Fig. 1 exceeds 50:1. At this frequency the source consists of two components. Regression analysis gives a separation rate of  $0.004 \pm 0.028$  mas/yr ( $0.09c \pm 0.61c$  with  $H_0 = 100$  km/s/Mpc,  $q_0 = 0.5$ ). The corresponding value at 5GHz based on three epochs with a maximum timescale of 6 years is  $0.006 \pm 0.046$  mas/yr ( $0.13c \pm 1.0c$ ) (Schalinski, 1990, to be subm.). Thus the components can be regarded as *stationary* within the errors. Since within the framework of the *standard relativistic jet model* subrelativistic motion is in contrast to the high  $\delta$ -factors derived by flux density variability and the deficiency of observed *inverse Compton* X-rays, additional assumptions of the physical nature of components (e.g. stationary shocks) have to be made (Witzel et al., 1988). The simple *mas*-structure consisting of two components with constant separation, and the good uv-coverage because of the frequent measurements and the high declination make *1803+78* unique among the IRIS-sources as *structural*

Tab. 1: STATUS: Hybrid Maps and/or Modelfits for 1803+78 and 0212+73

<i>Epoch</i>	$1803 + 78_{\lambda 3.6\text{cm}}^X$	$1803 + 78_{\lambda 13\text{cm}}^S$	$0212 + 73_{\lambda 3.6\text{cm}}^X$	$0212 + 73_{\lambda 13\text{cm}}^S$
1983.4	x	x	x	x
1983.9	x	x	x	x
1984.3	x	x	x	x
1984.5	x	x	x	x
1984.6	x	x	x	x
1985.8	x	x	x	
1986.2	x	x		
1986.5	x	x	x	
1986.9	x	x		
1987.7	x	x		

MkIII, Mode C, 100-400s Scans (Details s. Kilger, 1984)

STATIONS<sup>1</sup>:

WETTZELL (F.R.G.)

ONSALA (Sweden)

WESTFORD (Mass., U.S.A.)

FORT DAVIS (Texas, U.S.A.)

(RICHMOND (Florida, U.S.A.))

<sup>1</sup>: 1983.4: EFFELSBURG, MADRID, ONSALA, HAYSTACK, FORT DAVIS

*calibrator* for this geodetic network at 8.4GHz.

The use of a structural calibrator is necessary esp. for the sources in the IRIS-schedule with lower declination, because these sources are less frequently observed so that there are not sufficient data points to apply amplitude selfcalibration algorithms. We checked the calibration of 1803+78 versus the quasar 4C39.25. The maps at two epochs (Schalinski et al., 1988) are reliable above the 2% level. The apparent superluminal velocity derived from these data is consistent with the number obtained at 10.7GHz (e.g. Marcaide et al, 1988). The results of the investigation of recent epochs of this source are presented by Alberdi et al. (this volume).

In addition we used the 1803+78-data for the calibration of the source 0212+73. This source is ideal to check the calibration because it appears as often in the schedule as 1803+78. Fig. 2 shows the maps of 0212+73 at 1983.35 and 1986.94. The maps display a  $45^\circ$  change in p.a. close to the core confirming the elongation of the core at 23GHz measured with a snap-shot experiment. The source has a secondary component at a separation of about 1.0mas w.r.t. the core. The analysis of 4 epochs with a timebase of 3.5 years (1983.4-1986.9) yields a separation rate of  $0.05 \pm 0.04$  mas/yr ( $2.2c \pm 1.7c$ ) (Schalinski, 1990, to be subm.). This is in perfect agreement with the value obtained from the analysis of 3 epochs at 5GHz (timebase: 5.4 years):  $0.05 \pm 0.06$  mas/yr ( $2.2c \pm 2.6c$ ). Obviously, in case of welldefined components the data from IRIS-experiments can be used for the kinematic analysis. The resolution at 8.4GHz (0.5mas) in comparison with

lower frequency data gives reduced errors combined with a shorter timebase.

The data presented here demonstrate that geodetic VLBI-experiments with their special observational characteristics - switched observations between many sources, irregular uv-coverage etc. - can be used for the study of the *mas*-structures of extragalactic radio sources and their evolution, if a source with simple, nonvarying structure is available, which allows to establish a consistent calibration that is applied to the other sources. In view of the huge database already available (about 60 VLBI-experiments = 900 maps between 1983 and 1989 were correlated at MPIfR) the next steps are obvious: use of the calibration scheme for the reduction of more epochs, production of maps of the other sources at selected epochs, and optimization of the procedures to achieve quasi-automatic data reduction. Further improvements of the dynamic range of the maps being expected because of the participation of additional sensitive VLBI-telescopes (Medicina, Noto, Madrid) require flux density monitoring at the epoch of the IRIS-runs.

## References:

- Carter W.E., Robertson D.S., Mackay J., 1985: *Journ. of Geophys. Res.*, **90**, p. 4577
- Kilger, R., 1984: *Veröff. d. Bayer. Komm. f. d. Intern. Erdm., Astron.- Geod. Arb.*, Heft Nr. 45, München 1984, p. 73
- Marcaide, J.M., Alberdi, A., Elósegui, P., Jackson, N., und Witzel, A., 1989: *Astron. & Astrophys.* **211**, L23
- Schalinski C.J.<sup>\*</sup>, Alef W., Campbell J., Schuh H., Witzel A., 1986: *Die Arbeiten des SFB 78 Satellitengeodäsie der TU München 1984 und 1985*, ed. M. Schneider (München: Bayerische Akademie der Wissenschaften), p. 292
- Schalinski C.J., Alef W., Witzel A., Campbell J., Wynands R., Schuh H., and Zeppenfeld G., 1987: *Proceedings of the 5th Working Meeting on European VLBI for Geodesy and Astrometry*, held at Wettzell, F.R.G., on 7/8 November 1986; in: *Mitteilungen aus den Geodätischen Instituten der RWU Bonn*, Nr. 71, ed. J. Campbell and H. Schuh, Bonn 1987, p. 103
- Schalinski, C.J., Alberdi, A., Elósegui, P., und Marcaide, J.M., 1988: IAU Symposium 129, *The Impact of VLBI on Astrophysics and Geophysics*, ed. Reid M.J. & Moran J.M. (Dordrecht: Kluwer), p. 39
- Thomas, J.B., 1980: JPL Publication 80-84
- Witzel, A., Schalinski, C.J., Johnston, K.J., Biermann, P.L., Krichbaum, T.P., Hummel, C.A., und Eckart, A., 1988: *Astron. Astrophys.* **206**, p. 245

Fig. 1: Hybridmaps of 1803+78 at 8.4GHz from geodetic IRIS-Experiments. The separation between A and B is 1.4 mas.

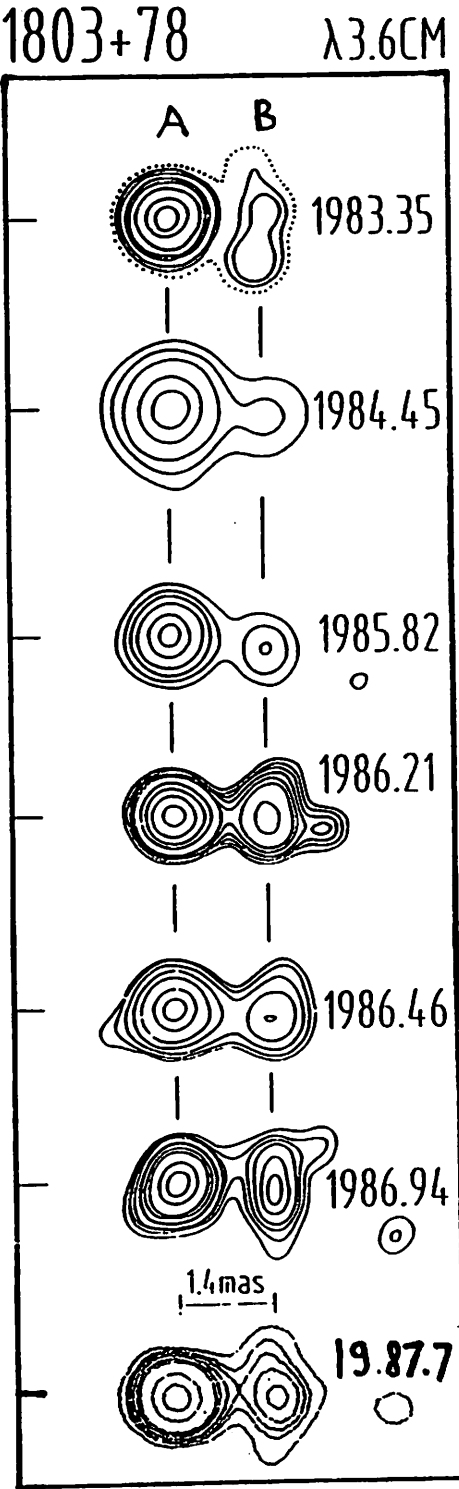
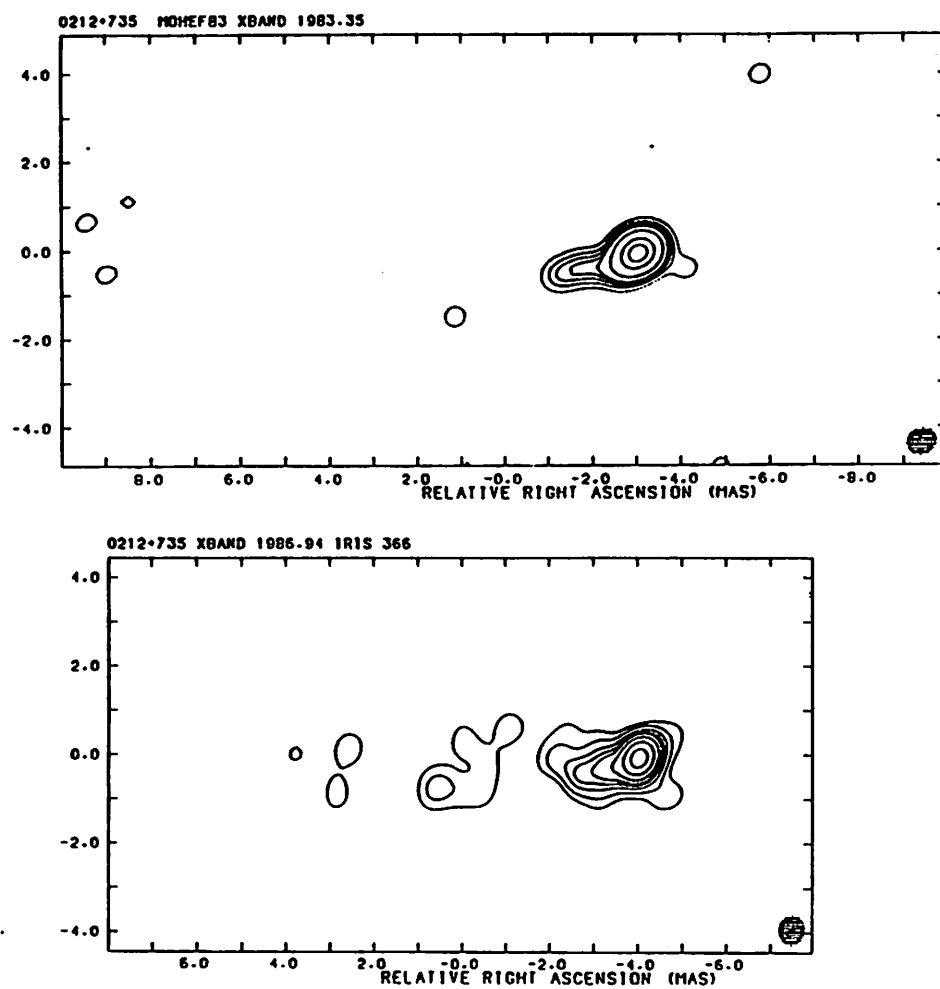


**Fig. 2: Hybridmaps of 0212+73 at 8.4GHz from geodetic VLBI-Experiments at 1983.35 and 1986.94. Contour levels (in percent of the peak flux density) are: 2,4,6,8,10,20,50,80% .**



# TESTING THE COMPUTATION OF SOURCE STRUCTURE DELAY

G. Zeppenfeld  
University of Bonn  
Bonn, Germany

## ABSTRACT

This contribution reviews methods to verify the computation of delay corrections caused by source structure effects. After a short introduction in how to compute source structure delay corrections a description of selfcalibration and hybrid mapping using the closure technique is given. In the next step two methods are explained to calculate closure phase and closure delay on a direct and on an indirect way. Finally some results are presented.

## 1. INTRODUCTION

For some years several VLBI groups have been involved in the computation of delay corrections due to source structure effects. The German VLBI-Group at the University of Bonn also developed a software module **STRUC** which can be linked to our geodetic VLBI program **BVSS**. Before starting to implement this software we had to verify our computations.

## 2. COMPUTATION OF SOURCE STRUCTURE CORRECTIONS

The effect of source structure on the geodetic VLBI-observable group delay is defined as the derivative of fringe phase with respect to angular frequency:

$$d\tau = \frac{d\phi}{d\omega} \quad (1)$$

The fringe phase is given by this expression:

$$\tan \phi = \frac{\text{Im } V(u,v)}{\text{Re } V(u,v)} \quad (2)$$

where  $V(u,v)$  is the complex visibility function of the observed source calculated from a given brightness distribution using a two dimensional Fourier Transformation:

$$\begin{aligned} V(u,v) &= A(u,v) \cdot e^{i\phi(u,v)} \\ &= \iint H(x,y) \cdot e^{-2\pi i \cdot (ux + vy)} dx dy \end{aligned} \quad (3)$$

We are not interested in phase computation only, but also in the variation of phase with respect to frequency. To compute these values we expand equation 1 into two parts and then we obtain this new expression:

$$\begin{aligned}
 d\tau &= \frac{d\phi}{d\omega} = \frac{d\phi}{du} \cdot \frac{du}{d\omega} + \frac{d\phi}{dv} \cdot \frac{dv}{d\omega} \\
 &= \nabla\phi \cdot \frac{\vec{B}_s}{\omega \lambda}
 \end{aligned} \tag{4}$$

where  $\nabla\phi$  is the gradient of phase with respect to the coordinates  $u$  and  $v$ ,  $\omega$  denotes the observed frequency,  $\lambda$  is the wavelength and  $\vec{B}_s$  represents the baseline projection into the plane of sky.

The phase derivative with respect to the coordinates  $u$  and  $v$  will be computed using the following equation:

$$\frac{d\phi}{du} = \frac{\frac{d\text{Im } V(u,v)}{du} \text{Re } V(u,v) - \frac{d\text{Re } V(u,v)}{du} \text{Im } V(u,v)}{\text{Re } V(u,v)^2 + \text{Im } V(u,v)^2} \tag{5}$$

with a similar expression for phase derivative with respect to  $v$ .

So if we want to compute delay corrections in this way, we need a map of DELTA FUNCTIONS representing the brightness distribution  $H(x,y)$  of a source in the plane of sky (THOMAS 1980).

Figure 1 represents the significant structure of source 3C454.3. The map was produced by Pauliny-Toth at 8.4 GHz observed in 1983:

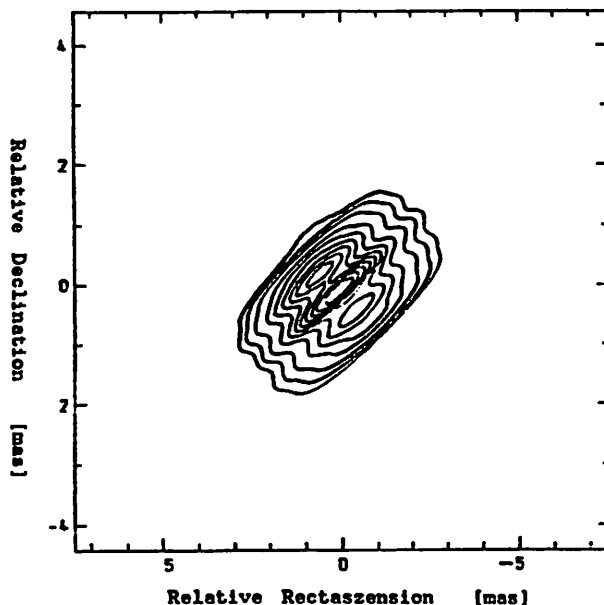


figure 1

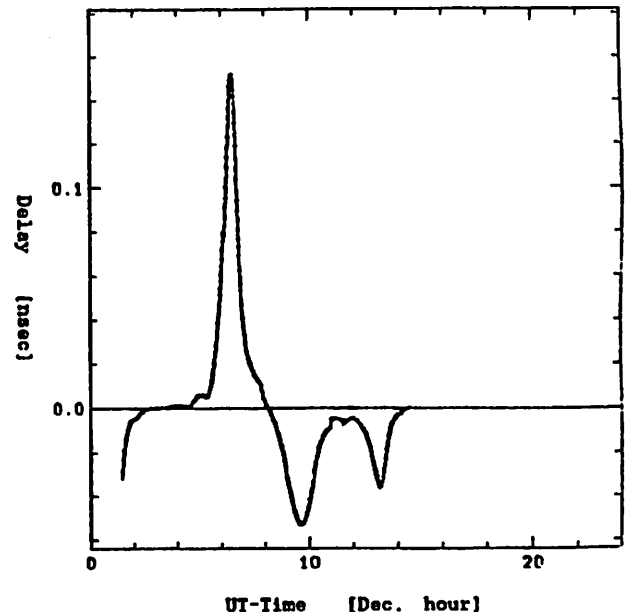


figure 2

Figure 2 shows the results we obtain computing delay-corrections for baseline WESTFORD-WETTZELL using the above equations (1-5).

An important piece of information in this result is the fact, that the delay corrections are greater than 120 psec which corresponds to 4cm, a level, which can not be neglected in doing millimeter VLBI.



### 3. SELFCALIBRATION, HYBRID MAPPING AND CLOSURE TECHNIQUE

The complex visibility (PHASE and AMPLITUDE) measured by a radio interferometer consisting of one baseline is a single Fourier component of the sky brightness distribution of the observed source. So a map of this source can be made by using Fourier synthesis to combine measurements obtained with different interferometer baselines. This is the so-called "aperture synthesis".

A common problem in source mapping is the fact that the phase of the complex visibility is badly corrupted by instrumental and other effects. A part of the lost phase information can be recovered by forming combinations of measured visibility phases the so-called "closure phases" (PEARSON and READHEAD 1984).

This partial information together with the constraint that the source brightness must be positive can be used to recover the full phase information. This method is called "selfcalibration or hybrid mapping" (READHEAD and WILKINSON 1978).

Closure phases are calculated by summing the phases around a closed loop of baselines (i.e. a triangle). The results must be zero, because nearly all effects known today (atmospheric, clock-offsets, ...) except source structure effects are associated with individual antennas (PEARSON and READHEAD 1984).

### 4. CLOSURE QUANTITIES: THE FINAL CHECK

In the reverse order, if we use closure phases for source imaging we should also be able to compute closure phases from the obtained map. Provided that all computations are based on the same experiment and same frequency the closure phases derived from the map should agree with the observed data to within the noise level. We cannot expect identical results, because the mapped brightness distribution is not the real one but very similar, because of uncertainties in observations and mapping algorithms.

For closure delays we expect the same results as for closure phases, because source structure is the only reason for delay misclosures.

The comparison between the predicted closures (obtained from maps) and the observed closures will be the "FINAL CHECK" in computation of delay corrections based on source structure effects.

### 5. COMPUTATION OF PHASE AND DELAY CLOSURES

Now a new problem arises: How to compute the observed closure quantities from a given DATA-BASE in an easy way?

The computation of measured closure quantities may be done in two different ways obtaining the same results:

#### a) Direct computation

We consider a network of three stations A, B, C, and, for simplicity we suppose that all clocks in this network are exactly synchronized.

Now, a wavefront, which arrives at station A at time  $t = 0$  will arrive at station B at time  $t = \tau_{AB}^t$ . But in this time the delay from station B to C will have increased by an amount of  $\tau_{AB}^t \cdot \dot{\tau}_{BC}^t$ .  $\dot{\tau}_{BC}^t$  is the delay rate of station C with respect to station B with the assumption that it is constant over the time  $\tau_{AB}^t$ . Finally the wavefront arrives at station C at time  $t = \tau_{BC}^t + \tau_{AB}^t \cdot \dot{\tau}_{BC}^t$ . This must be equal to the delay of station A and C:

$$\tau_{AB}^t + \tau_{BC}^t + \tau_{AB}^t \cdot \dot{\tau}_{BC}^t = \tau_{AC}^t \quad (6)$$

In this theoretical case the closure delay will be given by:

$$\tau_{AB}^t + \tau_{BC}^t - \tau_{AC}^t + \tau_{AB}^t \cdot \dot{\tau}_{BC}^t = 0 \quad (7)$$

But in practical work we encounter difficulties such as station clock offsets or source structure as mentioned above. If we assume that station A will be the clock reference station in this triangle, the delay closure error will be given by:

$$\tau_{AB} + \tau_{BC} - \tau_{AC} + (\tau_{AB} - \delta t_{AB}) \cdot \dot{\tau}_{BC} = \Delta \tau_E \quad (8)$$

where  $\delta t_{AB}$  means the apriori clock offset at baseline AB.

The computation of closure phase based on the observed total phase  $\phi_{IJ}$  will be given by a similar expression (theoretical case):

$$\phi_{AB} + \phi_{BC} - \phi_{AC} + \tau_{AB}^t \cdot \tau_{BC}^t \cdot F_0 = 0 \quad (9)$$

In reality we obtain a closure phase error caused by source structure effects:

$$\phi_{AB} + \phi_{BC} - \phi_{AC} + (\tau_{AB} - \delta t_{AB}) \cdot \dot{\tau}_{BC} \cdot F_0 = \Delta \phi_E \quad (10)$$

An important point in computing the closures according to the above procedures is the fact, that we have to compute a correction term consisting of apriori clock offset, clock rate and for phase computation frequency information. The disadvantage of this method is the fact, that we have to look for the same computation order (reference point) for station A, B and C as set by the correlator. If we don't use the same station order we get a wrong correction term and badly corrupted misclosures (WHITNEY 1974).

#### b) Indirect computation

An alternative method to compute the closure delay uses the difference between observed and theoretical delay (HERRING 1983):

$$v_{IJ} = \tau_{IJ} - \tau_{IJ}^t \quad (11)$$

In this case we are able to sum the differences around a closed loop of baselines without any information about the order of computation:

$$\Delta \tau_E = v_{AB} + v_{BC} - v_{AC} + \dot{v}_{AB} \cdot \tau_{BC}^t + \dot{v}_{BC} \cdot \tau_{AB}^t \quad (12)$$

The last two terms are very small. They can be neglected without loss of accuracy.

The advantage of this method is the independence in selecting the reference point within the triangle, because the order of computation is no longer important. But there is one important disadvantage: In this method we need the theoreticals calculated from CALC.

An alternative to compute phase closures is the use of the "earth centered phase  $\gamma$ " computed and corrected with respect to the center of the earth by program FRINGE:

$$\Delta \phi_E = \gamma_{AB} + \gamma_{BC} - \gamma_{AC} \quad (13)$$

This equation needs no correction term like equation 10, because the earth centered phase does not produce such a term.

## 6. RESULTS

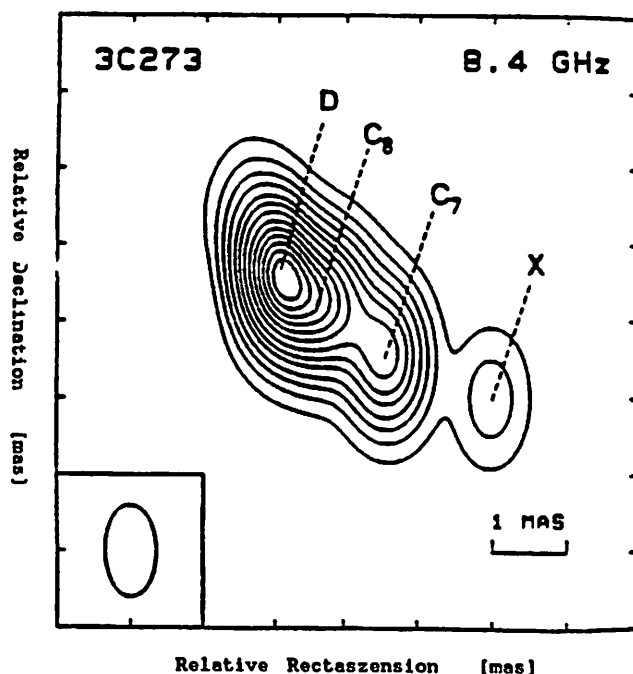


Figure 3 shows the examined map (contour level plot) of source 3C273 obtained from the North - Pacific 1 experiment MAY 1985 (participating station: Gilmore Creek, Hatcreek, Kauai, Kashima Mojave, Vandenberg). The map was produced by P. Charlot at 8.4 GHz and shows significant structure (CHARLOT 1989).

figure 3

The FINAL CHECK was first computed at the triangle GILCREEK-KAUAI-HATCREEK (figure 4) and there is a very good agreement between the measured closure delays with their uncertainties and the calculated closure delays obtained from the map. The computed closure delays

in this example reaches a dimension about 100 psec corresponding to a 3 cm level.

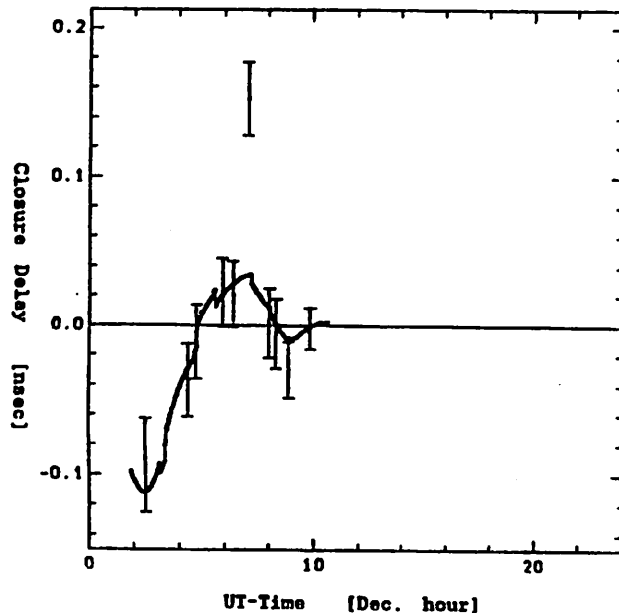


figure 4

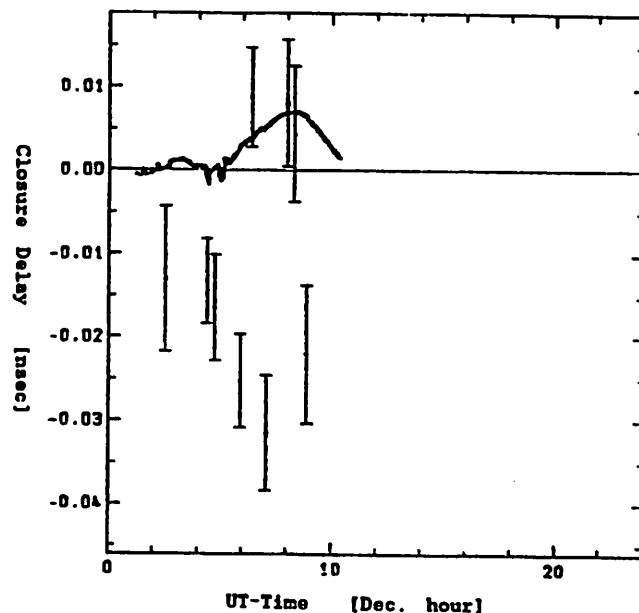


figure 5

The next example (figure 5) is based on the same source 3C273 but on a different triangle. It does not show such a good agreement between measured and calculated closure delays, because we use a triangle (Gilmore Creek-Hatcreek-Mojave) with two similar baseline lengths and orientations. In this case the two similar baselines give similar source structure delay errors. They cancel if we sum the delays around the closed baseline loop and only the third short baseline contributes in closure delay.

## 7. CONCLUSIONS

The comparison between the calculated and measured closure quantities is of particular importance and should be used more extensively. However we had to select the observed triangle very carefully, because closure delay depends on triangle form. We did not obtain significant source structure effects using two similar baselines, because the closure delay error level is at 50 to 80 psec (Mark III accuracy). We can expect significant closure effects only on triangles with baselines of equal lengths but different orientations. The results shown here confirm the thesis, that delay errors due to source structure can not be neglected for millimeter accuracy in VLBI.

## 8. FUTURE

In the future we plan to do more testing of new experiments and more comparison with other groups computing source structure corrections. We are now starting to implement the source structure software package in our geodetic VLBI program BVSS and, in a different way, also in the present CALC/SOLVE version.

## References

- Charlot, P., 1989: Thèse de doctorat: Structure des sources radio extragalactiques dans les observations VLBI d'astrométrie et de géodynamique. Soutenue à l'Observatoire de Paris
- Herring, T.A., 1983: Doctor Thesis: Precision and Accuracy of Intercontinental Distance Determinations using Radio Interferometry, P. 114ff. Massachusetts Inst. of Technology, Camb. USA
- Pearson, T.J. and Readhead, A.C.S., 1984: Image Formation by Self-Calibration in Radio Astron., Ann. Rev. Astron. Astroph. P. 97f
- Readhead, A.C.S. and Wilkinson, P.N., 1978: The Mapping of Compact Radio Sources from VLBI DATA, The Astroph. Journal 223: P. 25ff
- Thomas, J.B, 1980: An Analysis of Source Structure Effects in Radio Interferometry Measurements, JPL Publ. 80-84, Pasadena, California, USA
- Walker, R.C., 1989: Very Long Baseline Interferometry, Techniques and Applications, Felli, M. and Spencer, R.E. (eds.) (Dordrecht: Kluwer), P. 141ff.
- Whitney, A.R., 1974: Doctor Thesis: Precision Geodesy and Astrometry via VLBI, P. 276ff. Massachusetts Inst. of Technology, Cambridge USA
- Wilkinson, P.N., 1989: Very Long Baseline Interferometry, Techniques and Applications, Felli, M. and Spencer, R.E. (eds.) Dordrecht: Kluwer), P. 183ff.
- Wilkinson, P.N., 1989: Very Long Baseline Interferometry, Techniques and Applications, Felli, M. and Spencer, R.E. (eds.) Dordrecht: Kluwer), P. 69ff.
- Zeppenfeld, G., Campbell, J., Schuh, H., 1988: IAU Symposium 129, The Impact of VLBI on Astrophysics and Geophysics, Reid M.J. & Moran J.M. (eds.) (Dordrecht: Kluwer), P. 427f.
- Zeppenfeld, G., 1988: Diploma Thesis, University of Bonn

Evidence for the Effect of Source Structure  
in Geodetic and Astrometric VLBI

G. Petit  
Institut Géographique National  
2, Ave. Pasteur  
94160 Saint Mandé FRANCE

P. Charlot  
Jet Propulsion Laboratory MS 238-332  
California Institute of Technology  
4800, Oak Grove Drive  
Pasadena, Ca, 91109 USA

**ABSTRACT.** The effect produced by the structure of the radio sources on the Band Width Synthesis (BWS) delays measured in geodetic and astrometric VLBI is significant: Its value can be as large as 100 picoseconds (ps) on the average for some sources. We present an analysis of this effect in a set of 9 IRIS experiments conducted between August and October 1985. Hybrid maps of 4 sources for the epoch September 1985 have been used to correct the VLBI observables of these sources. Applying the structure correction improves the Root Mean Square (RMS) of the post-fit BWS delay residuals by as much as 15% and leads to changes of up to 2 cm in the estimated station coordinates.

## 1. INTRODUCTION

At the milliarcsecond level, most of the extragalactic radio sources used for geodetic and astrometric VLBI applications exhibit extended structures which are variable in both time and frequency. It has been shown that the effects produced by these structures on the BWS delay VLBI observable are significant: They are typically at the level of 100 ps for some sources (Charlot et al. 1988, Charlot 1989a). Therefore, they should be accounted for when high-precision geodetic/astrometric VLBI data are analysed.

An algorithm has been implemented to calculate source structure corrections for the BWS delays and phase rates, in order to refer the position of each source to a specific feature of its morphology, for example its core (Charlot 1989b). Both 8.4 and 2.3 brightness distributions should be known for this calculation. We have analysed a set of 9 IRIS experiments conducted between August and October 1985, and derived structure corrections for the 4 sources which are known to have the most extended structure. For the calculation of the structure effects, hybrid maps of September 1985 (Charlot 1989a) have been used. We discuss the improvement of the RMS of the post-fit BWS delay residuals as well as the variation of the geodetic parameters estimated in our analysis, when structure corrections are applied.

## 2. OBSERVATIONS AND DATA PROCESSING

Our data set includes the IRIS experiments 48 to 56 of the year 1985 (from the end of August to the early October), with 4 stations, Westford, Fort Davis, Richmond and Wettzell, forming a network with three intercontinental "long" baselines and three US "short" ones.

About 3300 delay observations and as many delay rates measured on 14 sources have been analysed with the MASTERFIT software (Sovers and Fanselow 1987). The Earth Orientation Parameters were adopted from the IRIS bulletin of the National Geodetic Survey and 266 parameters were estimated: 9 station coordinates (Westford fixed), 27 source coordinates (right ascension of 3C273 fixed), 36 zenith troposphere delays (one per day per station) and 194 clock parameters (about 3.5 linear segments per day per station, except Westford). The RMS of the post-fit residuals for this solution is 89.4 ps for the delays and 0.083 ps/s for the rates.

A similar solution, but with structure corrections applied to the observations on four sources, has also been computed. These sources (3C273, 3C345, 3C454.3 and 4C39.25) have an extended structure which is changing on a time scale of a few months, and maps of September 1985 were used (Charlot 1989a). The other 10 sources have less structure but their effect should nevertheless be accounted for. We plan to do this in the future using maps of May 1985 (Charlot 1989c). Applying the structure corrections slightly decreases the global RMS of the delay residuals from 89.4 to 88.6 ps. It should be kept in mind that this result has been obtained with a correction applied to 25% of the data set only. The variation of the RMS of the delay residuals of each of the four sources corrected is studied in the following section. As expected, no difference can be seen in the rate residuals, as the effect of the structure is in general much smaller.

## 3. INFLUENCE OF THE STRUCTURE ON THE RMS OF THE DELAY RESIDUALS

a) The influence of the structure of the sources can be seen from table 1, which shows the RMS of the delay residuals of our standard solution for each source, for the intercontinental baselines on one side, and for the US baselines on the other side. The sources have been classified into three subsets, according to their structure: Four sources with large structure, six with intermediate structure and four with small structure.

The four sources with an expected large structure actually have larger residuals: On long baselines the RMS of their delay residuals is 107 ps compared to 92 for the other 10 sources. Even more evident is the comparison of the RMS on the intercontinental baselines and the RMS on the US baselines, for the three subsets of sources: The former is 30% larger than the latter for the sources with large structure and 10% for the intermediate group. On the contrary no significant difference is found for the sources with the smallest structure.

	Source	Intercont. baselines	US baselines
Sources with large structure	3C 273	127.1	87.7
	3C 345	100.3	76.9
	3C 454.3	93.2	67.4
	4C 39.25	106.1	84.8
	Average	106.7	79.2
Sources with moderate structure	OQ 208	110.7	92.3
	1803+784	88.0	102.7
	VRO 42.2	124.1	104.3
	2134+004	97.7	83.5
	0106+013	103.8	73.6
	0212+735	90.8	101.8
	Average	102.5	93.0
Sources with small structure	DA 193	75.9	88.8
	OJ 287	86.9	78.3
	0229+132	72.0	72.4
	0528+134	66.4	82.2
	Average	75.3	80.4

**Table 1:** RMS of post-fit delay residuals (ps) for intercontinental and US baselines

b)Applying the structure correction tends to decrease the RMS of the residuals on long baselines for the four sources with large structure (see table 2). It is not very important for 3C 273 for which practically no gain is reported (0.3ps). It is of the order of 3% for 3C 345 (2.5ps) and 4C 39.25 (3.3ps), and it reaches 14% for 3C 454.3 (12.7ps). This seems to be related to the value of the computed visibilities for those sources: The average X-band visibility is about 0.1 for 3C273, 0.3 for 3C345, and reaches 0.4 for 4C39.25 and 3C454.3. This indicates that it is more difficult



than average to compute the structure correction when the visibility is poor. Thus the computed visibility is a way to estimate the error on the computed correction.

Source	Intercontin. baselines		US baselines	
	without	with	without	with
3C 273	127.1	126.8	87.7	85.5
3C 345	100.3	97.8	76.9	72.4
3C 454.3	93.2	80.5	67.4	64.7
4C 39.25	106.1	102.8	84.8	85.4

**Table 2:** RMS of post-fit delay residuals (ps) for the solutions without and with structure correction

In order to test this hypothesis we have performed a similar analysis of the data, without applying the structure correction, after removing from the data set the 37 observations for which the X-band visibility is smaller than 0.1 (28 of them concern 3C273, the other 9 concern 3C345). The RMS of the delay residuals is 88.8 ps, which indicates that those 37 observations had larger residuals (a mean value of 135 ps) than the other ones. Moreover, a similar solution, with the structure correction applied, gives a value of 87.9 ps for the RMS of the delay residuals and, in that case, the gain in the RMS of the residuals for 3C273 on intercontinental baselines is 14.7 ps. This confirms the fact that, in the case of very low visibility, the dynamic range of hybrid maps is not high enough to properly model the structure effect, as it has been shown in (Charlot 1989b).

It is also possible that the structure of the source changed significantly during the 40-day period of our data, which makes the structure correction inadequate for the whole data set. This possibility will be further studied, for example by splitting the data set into several subsets.

c) The structure correction provides also a slight improvement on the US baselines: Although it is not the case for 4C39.25 (0.6ps worse), it reaches 6% for 3C345 (4.5ps), 4% for 3C454.3 (2.7ps) and 3% for 3C273 (2.2ps). In that case the visibilities are higher (0.6 to 0.8) and, although the structure effects are much smaller, they must be more precisely modeled.

#### 4. INFLUENCE OF THE STRUCTURE EFFECTS ON THE ESTIMATED PARAMETERS

In our analysis we can only evaluate the influence of the structure corrections on the station coordinates. The source positions themselves are affected but, because the point that has been chosen as reference in the models of each source will not coincide with the centroid of the source (which position is computed when no correction is applied), it has no meaning to draw any conclusion from the differences in the computed source positions. Only if several models at different epochs were used to analyse a long data set could the computed solution show evidence of the variation of the structure with time.

Table 3 shows the variation of the station coordinates when applying the structure corrections. They can reach 2 cm and several of them are significant with regard to the formal errors. This effect is larger than would have been suspected from the values of the computed corrections (a few tens of picoseconds average on 25% of the scans). This may be due to the IRIS schedule, which repeats itself at each session in our data set, and prevents the corrections to be averaged. This will be further studied for other schedules.

Station		Standard error(mm)	Variation (mm)
Ft Davis	X	4	- 2
	Y	10	+ 19
	Z	10	- 6
Richmond	X	3	- 4
	Y	8	+ 1
	Z	12	+ 4
Wettzell	X	16	+ 7
	Y	11	- 6
	Z	19	- 20

**Table 3:** Variation of the station coordinates when applying structure corrections to the BWS delays

## 5. CONCLUSIONS

The study of structure effects in a set of 9 IRIS experiments conducted in 1985 shows that these effects are significant. It has been found that the RMS of the post-fit BWS delay residuals calculated source by source depends on the size of the structure. In the data set analysed, it is 30% larger for sources with large structures than for sources with small structures. Similarly, the RMS of the BWS delay residuals is 30% larger on intercontinental baselines than on US baselines for the large structures, whereas no significant difference is found between the two subsets of baselines for the small structures. By applying structure corrections derived from hybrid maps, the RMS of the BWS delay residuals can be reduced by as much as 15% on intercontinental baselines for sources with large structures. Though significant, this improvement is lower than one might expect from the comparison of the RMS of the residuals on intercontinental and US baselines for these sources (difference of 30%). It is possible that a few observations have improper structure corrections that lessen the improvement of the RMS. This is the case for observations in low-visibility regions of the u-v plane because structure effects are difficult to model with hybrid maps for these observations (Charlot 1989b). In high-precision geodesy and astrometry, such observations should be avoided by an appropriate scheduling.

Structure effects have also a significant influence on the geodetic parameters estimated. In the IRIS data set analysed, the changes of the station coordinates are up to 2 cm when structure corrections are applied to the observations. Such analysis should be extended to several epochs in order to study the influence of these corrections on long term astrometric/geodetic solutions. However, this single example shows that for centimeter-level geodesy structure effects should be included in the theoretical model used to compute the BWS delays. In the future, improvements of mapping techniques and the use of larger VLBI arrays (e.g. the Very Long Baseline Array) should yield more accurate maps and therefore more accurate structure corrections, especially in the low-visibility regions of the u-v plane. Applying these corrections should then reduce the RMS of the BWS delay residuals on intercontinental baselines by at least 30% for sources with large structures.

## 6. ACKNOWLEDGEMENTS

We thank the US National Geodetic Survey for providing the IRIS data used in this analysis. We are indebted to J-F. Lestrade for stimulating discussions and to O.J. Sovers for his assistance with the analysis software.

## 7. REFERENCES

Charlot, P., Lestrade, J-F., Boucher, C., 1988: 3C273 and DA193 mapped with Crustal Dynamics VLBI data, in IAU Symposium 129, The Impact of VLBI on Astrophysics and Geophysics, Ed. by M.J. Reid and J.M. Moran, Kluwer Academic Pub., Dordrecht, p. 33

Charlot, P., 1989a: Structure des sources radio extragalactiques dans les observations VLBI d'astrométrie et de géodynamique, Thèse de Doctorat de l'Observatoire de Paris, France

Charlot, P., 1989b: Radio source structure in astrometric and geodetic Very Long Baseline Interferometry, Astron. J. (in press)

Charlot, P., 1989c: Fourteen extragalactic radio sources mapped with a 24-hour Crustal Dynamics Program VLBI experiment, Astron. Astrophys. (in press)

Sovers, O.J., Fanselow, J.L., 1987: Observation model and parameter partials for the JPL VLBI parameter estimation software MASTERFIT-1987, JPL Publication 83-39, Rev. 3

## **Size and Position of SgrA\***

**J.M. Marcaide, A. Alberdi, P. Elósegui, M.J. Rioja**  
Instituto de Astrofísica de Andalucía, C.S.I.C.

**M.I. Ratner, I.I. Shapiro**  
Harvard-Smithsonian Center for Astrophysics

### **Abstract**

**We have determined the sky position of the compact non-thermal radio source at the Galactic Center, commonly referred to as SgrA\*, in the reference frame of the extragalactic radio quasars for epoch J2000.0. We have also determined the size of the source at 1.3, 3.6 and 13cm wavelengths and found that the source size increases proportionally to the observing wavelength squared, as expected from source size broadening by interstellar scattering.**

## I. Introduction

Our galaxy harbours a compact radio source at its center (Balick and Brown, 1974) and in its neighborhood energetic events take place. The situation is not unlike that of many similar galaxies (i.e. M81, Bartel et al. 1982) although in our Galaxy the energies involved are lower. Since our distance to the Galactic Center is small (i.e. Reid et al., 1987) the various phenomena taking place there can be studied in great detail. In particular, NeII maps (Serabyn and Lacy, 1985) show complex high velocity motions of the ionized gas, indicating the existence of a concentration of mass at the center. The origin of these motions is uncertain as they can be due to a massive and compact stellar cluster or to a black hole. It has always been assumed that IRS16 is the core of the central stellar cluster and marks the dynamical center of the galaxy. Evidence may be recently emerging that the components of IRS16 are simply young stars. In such a case, the positional offset between IRS16 and the compact radio source would not have any major significance. On the other hand, the lack of an association of a luminous source with the compact radio source does not preclude the possibility of the existence of a massive black-hole since the actual accretion process is highly uncertain.

The nature of the compact radio source, commonly referred to as SgrA\* as we will do hereafter, would be best revealed by detailed high-resolution studies of its morphology and by its proper motion. Unfortunately, until now these studies have been plagued by many difficulties, some of which may soon be overcome: the major VLBI capabilities have only existed on the northern-hemisphere and there have been very few sufficiently short baselines on which the source is not completely resolved. The latter factor has been worsened by a fact which was soon recognized (Davies et al., 1976), that is, that the actual size of the compact source has a  $\lambda^2$  dependence and that what can be observed at centimeter wavelengths is the interstellar-scattering-broadened source and not the actual source. Going to shorter and shorter wavelengths, i.e. 7mm, is essential to eventually minimize the interstellar scattering effects and determine the actual intrinsic source structure.

Differential proper-motion measurements of SgrA\* have been made with the Very Large Array (VLA) by Backer and Sramek (1987). The VLBI technique has not been exploited yet for astrometric purposes for lack of appropriate baselines. The position determination which we present in this paper, being the first one achieved by VLBI and referred to the extragalactic radio source reference frame, is still too coarse to be useful in any proper motion study.

## II. Observations

We report on VLBI observations of SgrA\* made at the wavelengths of 3.6 and 13 cm in May 1983 and at 1.3 cm in February 1985. The recording instrumentation used was MkIII. The 3.6 and 13cm observations took place simultaneously. The source was only detected in the baseline DSS14 (Goldstone)- OVRO at these frequencies.

At 1.3 cm we only had the baseline Haystack-Green Bank. After correcting for coherent losses, the data were calibrated in a standard manner using the system and antenna temperatures measured during the experiment and/or antenna gain calibration information. The *a priori* antenna gain information was much improved in the 3.6 and 13cm observations profiting from the fact that the SgrA\* observations were made in the same run as synthesis observations of the quasars 4C39.25 and 1038+528A,B and for these quasars the relative antenna gains could be accurately determined with the self-calibration method. We used the Caltech package for the mapping of these quasars and for the modelfitting of the SgrA\* data. The determination of the total flux density of SgrA\* in our modelfitting is about 5% accurate. We have modelfitted our data at all wavelengths with circular gaussian models. Before modelfitting the 13cm data in the baseline Goldstone-OVRO we excluded the non-detections in order not to bias the fit.

Conveniently spaced in time among the SgrA\* observations we observed the astrometric calibrator source NRAO530. We also observed four more extragalactic astrometric calibration sources (NRAO150, 4C39.25, 1642+690, and BL Lac) in a global run where the observations of NRAO530 and SgrA\* were included. The positions of these calibrator sources have been accurately determined in global astrometric/geodetic observations (IERS Annual Report, 1990. Goddard Space Flight Center (GSFC) Crustal Dynamics Project (CDP) VLBI Global Solution GLB622) which define the GSFC VLBI celestial reference frame. We used for OVRO the coordinates given in the GSFC VLBI Global Solution GLB622 after interpolation to the experiment day. For Goldstone (DSS14) we used coordinates obtained in the GSFC frame by a transformation from another frame. The details about this transformation will be explained elsewhere. We estimate the total uncertainty in the location of DSS14 in the GSFC terrestrial frame in about 10 cm.

Having fixed the position of the calibration sources, the coordinates of the antenna sites, the Earth's orientation parameters and chosen the values of the tropospheric zenith delays, we used the group delay and fringe rate observables to determine the position of SgrA\* and the relative behaviour of the Goldstone and OVRO clocks. The determination was made in a least-squares sense. The program we used to determine those parameters is VLBI3 (Robertson D.S., 1975) in its E version (called VLBI3E) which has been produced to incorporate the latest internationally-agreed-upon values and conventions (i.e. speed of light,...) and to use a J2000.0 ephemeris. This version of the program, like previous ones, has been cross-checked against the program CALC-SOLVE (Clark T. et al., 1985). As input to VLBI3E two tables are necessary: 1) A table with values of UT1-TAI and 2) a table with pole orientation corrections  $\omega_x$  and  $\omega_y$ . Table 1 contains the essential astrometric information we have used and the estimated position for SgrA\*.

	X(m)	Y(m)	Z(m)	Zenith Delay(ns)
OVRO	-2409598.904	-4478350.447	3838603.695	6.9
Goldstone	-2353619.392	-4641342.401	3677052.834	7.1

	(hh mm ss.ss)	( <sup>o</sup> ' ")	
NRAO530	17 33 02.7057033	-13 04 49.54802	(J2000.0)
SgrA*	17 45 40.0833 ± 0.0071	-29 0 27.489 ± 0.159	(J2000.0)

**Table 1: Astrometric information and results**

The source could only be detected simultaneously in three scans at 3.6 and 13cm wavelengths in the baseline Goldstone-OVRO which makes the correction of the ionospheric aberration difficult. We have attempted to account for the ionosphere in various ways obtaining each time a similar position for SgrA\*. The details of our procedures will be published elsewhere. It should be noted that the fact that we could only detect three times the source at 13cm is due to source size and not to interferometric sensitivity.

### III. Results

The fits of the circular gaussian component model to the data at 1.3, 3.6 and 13cm are shown in Figures 1a, b and c. The sizes determined at each wavelength are given in Table 2. The errors in the size determination correspond to formal errors once they have been scaled to give a reduced chi-squared of unity. In Figure 2a we have plotted the sizes determined as a function of the wavelength (logarithmic scale) and a straight line least-squares fit to the data. The slope of this fit corresponds to the best estimate of the exponent  $\beta$  in the power law  $\theta \sim \lambda^\beta$ , where  $\theta$  is the source size and  $\lambda$  the observing wavelength. The estimate for  $\beta$  is  $2.00 \pm 0.09$  where again the error quoted is the formal error scaled to give a chi-squared of unity. If we take our best results, that is the 3.6 and 13cm where we have an excellent relative and absolute calibration of the data, the estimate turns out to be  $1.95 \pm 0.05$ . A large set of well calibrated data at 1.3cm is essential to narrow down reliably the error. Also, we have taken all size estimates in the literature (Lo *et al.* 1981, Lo *et al.* 1985, Jauncey *et al.* 1989) at all wavelengths and have repeated our analysis. We then obtain the estimate of  $2.03 \pm 0.06$  for  $\beta$ . The fit is shown in Figure 2b. It is thus clear that an estimate for  $\beta$  of  $2.0 \pm 0.1$  encompasses every case.

$\theta$ (mas)	$\Delta\theta$	$\log(\theta)$	$\Delta\theta/\theta_0$	$\nu$ (MHz)	$\lambda$ (cm)	$\log(\lambda)$
1.8345	$\pm 0.0936$	0.2635	0.051	22224.99	1.3498	0.13027
16.1368	$\pm 0.3335$	1.2078	0.0206	8409.99	3.5672	0.5523
205.1602	$\pm 4.3744$	2.3120	0.0213	2274.99	13.1869	1.12014

**Table 2: Summary of size determinations**



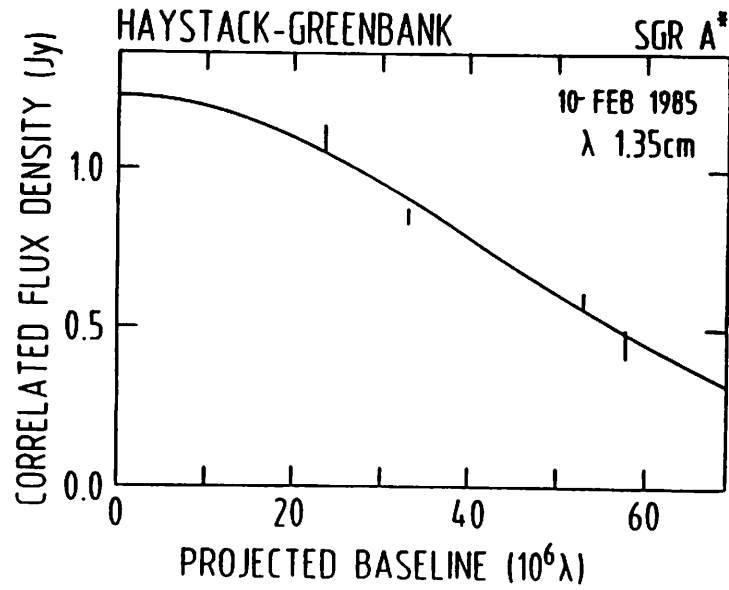


Fig. 1a

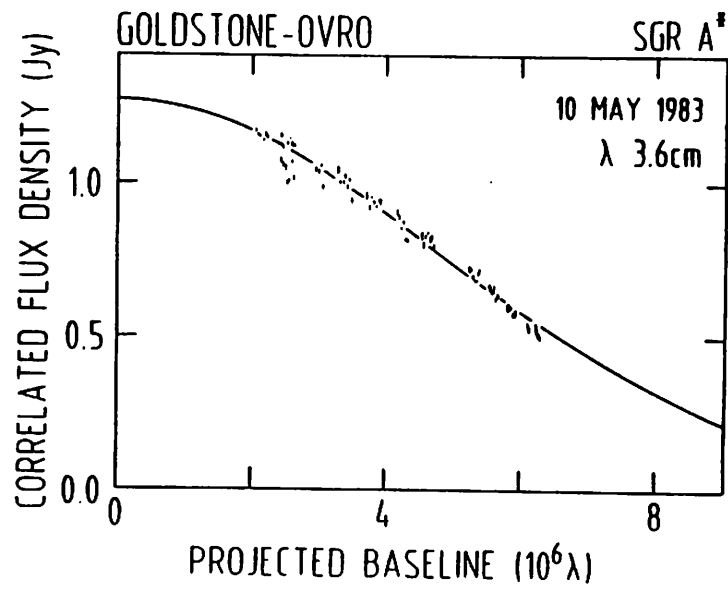


Fig. 1b

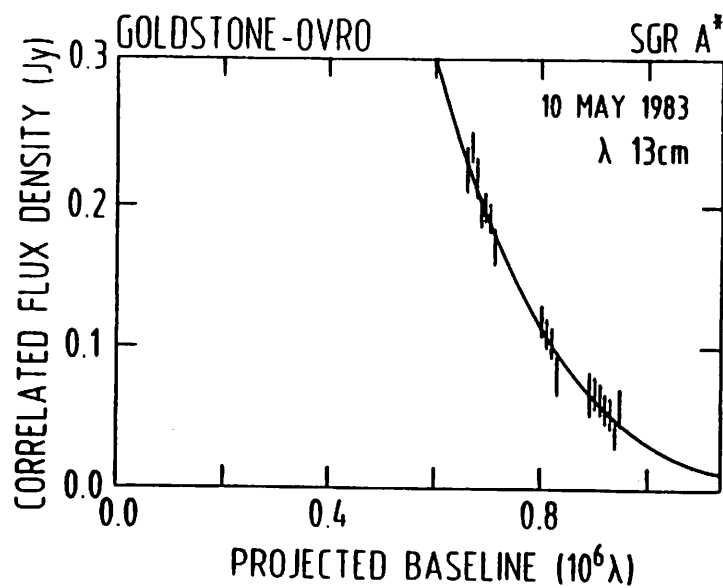


Fig. 1c

**Figure 1:** Correlated flux density versus baseline size at the wavelengths of 1.3 (Figure 1a), 3.6 (Figure 1b), and 13 cm (Figure 1c).

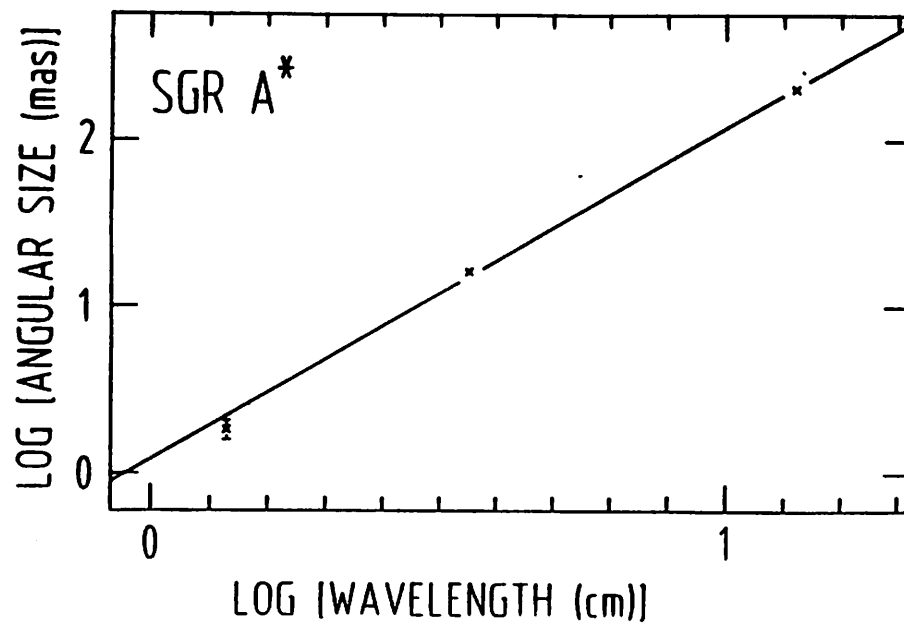


Figure 2a: Size versus wavelength squared at 1.3, 3.6 and 13cm (our observations)

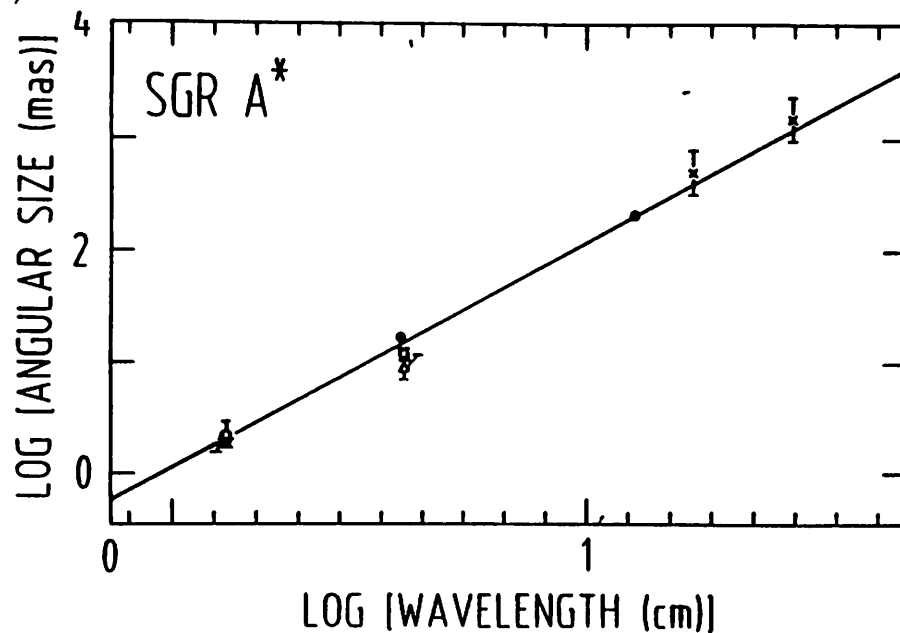


Figure 2b: Size versus wavelength squared (observations from other authors included)

The formal estimates of the total flux densities at the wavelengths of 1.3, 3.6 and 13cm are  $1.20 \pm 0.1$ ,  $1.25 \pm 0.06$  and  $1.05 \pm 0.08$  respectively. The 1.3cm flux density scale must be accurate to 15%. At 3.6 and 13cm the total flux density scales must be better than 5% due to the cross-calibration scheme described in Section II. All in all, we can realistically estimate the total flux densities at 1.3, 3.6 and 13cm as  $1.2 \pm 0.2$ ,  $1.2 \pm 0.1$  and  $1.1 \pm 0.1$  respectively. Hence we can estimate the source spectral index between 3.6 and 13cm as  $+0.12 \pm 0.17$  ( $S \propto \nu^\alpha$ ).

#### IV. Discussion

The source position determination given in Table 1 is the first such a determination ever obtained reliably in the frame of distant extragalactic radio sources, which is a quasi-inertial frame well defined by systematic astrometric and geodetic observations. Admittedly the accuracy of our determination is too low to be useful in any proper motion study. The proper motion study is presently better conducted with differential astrometric VLA observations of SgrA\* and some neighbour extragalactic radio sources (Backer and Sramek, 1987). The situation could be different in the future as more VLBI baselines become available. The VLBI technique should eventually allow to determine not only the absolute position of SgrA\* more accurately than the VLA, but also the differential position with respect to external references. We believe that the determination of the absolute position may be improved by a factor of ten in the future.

The intrinsic structure of SgrA\* is still the big unknown. Our determinations and those of previous authors indicate that observed sizes correspond likely to those due to scattering of interstellar electrons because the observed sizes are proportional to  $\lambda^{2.0 \pm 0.1}$ . This correspondence holds down to wavelengths as short as 1.3cm. No 7mm observations are yet available. Should the source size still be determined at 7mm by interstellar scattering, the size would be of about 0.6mas, which would correspond to a linear size of about 5AU if we use the distance determination to the Galactic Center of Reid et al. (1988). The presently available observations tell us that the intrinsic size is less than 15AU. Since the departure from the  $\lambda^2$  dependence is unlikely to be abrupt one can confidently assume that the size of SgrA\* is unlikely to be larger than 10AU.

#### V. References

- Backer D.C. & Sramek, R. *AIP Proc.* 155: Symposium honoring C. H. Townes edited by D. C. Backer (AIP; New York) 155, 163 (1987)  
 Balick, B. & Brown, R.L. *Astrophys. J.* 194, 265 (1974)  
 Bartel, N. *et al.* *Astrophys. J.* 262, 556 (1982)  
 Clark, T.A. *et al.* *IEEE Trans. of Geoscience and Remote Sensing* GE-23, n. 4, 438 (1985)  
 Davies, R.D. *et al.* *Monthly Notices of the RAS* 177, 319-333 (1976)  
 Jauncey, D. L. *et al.* *Astron. J.* 98(1), 44-48 (1989)  
 Lo, K. Y. *et al.* *Astrophys. J.* 249, 504 (1981)  
 Lo, K. Y. *et al.* *Nature* 315, 124 (1985)  
 Ma, C. *et al.* *Astron. J.* 99, 1284-1298 (1990)  
 Reid, M.J. *et al.* *Astrophys. J.* 330, 809-816 (1988)  
 Robertson, D.S. *Ph.D. Thesis, Massachusetts Institute of Technology* (1975)  
 Serabyn, E. & Lacy, J.H. *Astrophys. J.* 293, 445-448 (1985)

# **Proper Motion of the Quasar 1038+528 A**

**P. ELOSEGUI AND J.M. MARCAIDE**

**Instituto de Astrofísica de Andalucía**

**I.I. SHAPIRO**

**Harvard-Smithsonian Center for Astrophysics**

## **ABSTRACT**

**A proper motion of the core of the quasar 1038+528 A relative to the quasar 1038+528 B of  $26 \pm 8 \mu\text{as/yr}$  has been measured from two VLBI observations, in March 1981 and May 1983. The measured proper motion may correspond either to a real proper motion of the quasar or to a jitter of its core.**

## **1. Introduction**

In VLBI an underlying assumption has been that the compact extragalactic objects (distant quasars and active nuclei of galaxies) are point-like radio sources with fixed sky positions. The constancy of the relative positions of these extragalactic radio sources has been determined with milliarcsecond accuracy (Ma et al. 1990), and thus a primary celestial reference frame which is useful for astrometry, geophysics, and spacecraft navigation has been defined.

Differential VLBI astrometry of radio sources with small relative angular separations can -if interferometric phase-differences free of  $2\pi$  ambiguities can be formed and source structures determined- yield relative positions of radio sources with accuracies well under a milliarcsecond (Shapiro et al. 1979, Gorenstein et al. 1983, Marcaide and Shapiro 1983, 1984, Marcaide et al. 1985, 1990, Bartel et al. 1986, Morabito et al. 1986, Lestrade et al. 1990). This technique is especially

useful if a radio source shows regular morphological changes (e.g., internal proper motion between components): comparing the sky positions of the components of the source to the other (assumed unrelated) radio source permits to distinguish moving components from stationary ones. This determination is fundamental to understand the kinematics of the radio sources and distinguish among theoretical models.

In this contribution we present astrometric results from two sets of observations of the pair of quasars 1038+528 A and B. Both radio sources have typical milliarcsecond "core-jet" morphologies. Their relative angular separation on the sky is only 33 arcseconds, and both quasars fall simultaneously within the main beam of every telescope at  $\lambda=3.6$  cm (the telescopes do not have to beam-switch between the sources during the observations). Hence systematic effects introduced by the propagation medium and the instrumentation will affect very similarly to the observables of both quasars. By forming differenced observables a cancellation of these effects is achieved, and the relative separation of well-defined structural features chosen in each quasar can be determined with microarcsecond precision. For the pair 1038+528 A and B the uncanceled ionospheric contribution at  $\lambda=3.6$  cm should be no more than one microarcsecond (Morabito et al. 1986, Bartel et al. 1986). The tropospheric contribution, more difficult to estimate, should be still smaller.

## 2. Observations

The observations were made with the MarkIII VLBI system (Rogers et al. 1983; Clark et al. 1985) on 17-18 March 1981 and 10-11 May 1983, at  $\lambda=3.6$  and 13 cm wavelengths simultaneously. The pair of radio sources 1038+528 A and B (quasars of magnitudes 17.5 and 18.5 and redshifts 0.678 and 2.296, respectively (Owen et al. 1980)) were observed simultaneously with the following telescopes: Deep Space Network (DSS14, 64-m, California); Deep Space Network (DSS63, 64-m, Spain); Effelsberg (B, 100-m, F.R.G.); Green Bank (G, 43-m, West Virginia); Haystack (K, 37-m, Massachusetts); Onsala (S, 25-m and X, 20-m, Sweden); Owens Valley (O, 40-m, California). Additionally, Fort Davis (F, 26-m, Texas) also participated in the May 1983 experiment. Right-hand circular polarization was recorded at both reception bands at each telescope in each observation. The March 1981 observations were described by Marcaide et al. 1985 and the May 1983 observations will be described in detail elsewhere.

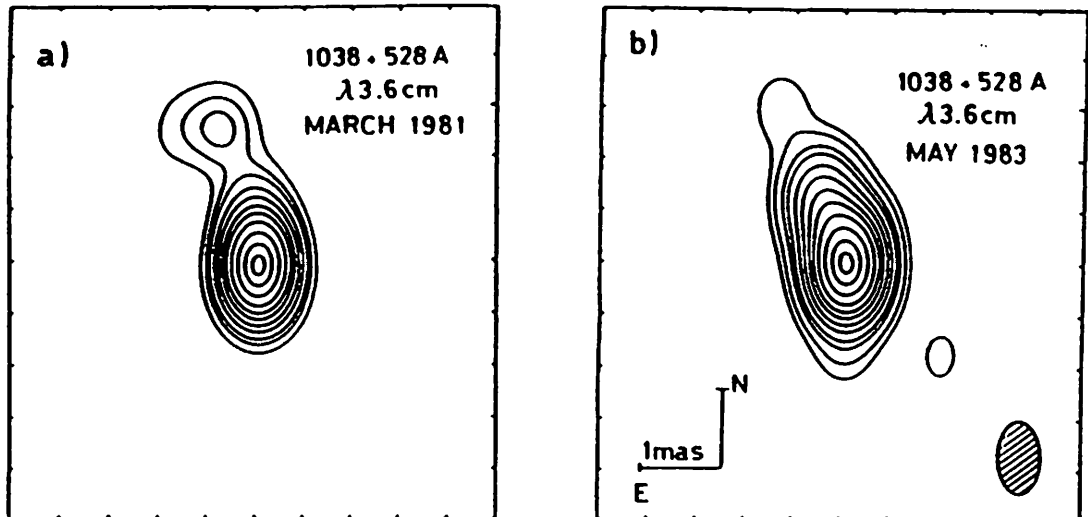


**Figure 1**  $\lambda = 3.6$  cm VLBI maps of the structure of the quasar 1038+528 A for epochs March 1981 and May 1983. The contours correspond to -1,2,4,6,10,15,22,30,42,60,80,95 % and -1,1,2,4,6,10,15,22,30,42,60,80,95 % of the peak of brightness in the March 1981 and May 1983 maps, respectively. Restoring Gaussian beams of  $0.8 \text{ mas} \times 0.6 \text{ mas}$  in P.A.  $-2^\circ$  used for both maps.

The amount of data and the quality of the maps produced were very similar because the participating telescopes, telescope configuration and performance, observing schedule, data reduction, and astrometric analysis were very similar for both epochs. Both data sets were processed with the same software and attempts were made to minimize data-analysis differences between the two epochs.

### 3. Data Analysis and Relative Source Positions

Hybrid maps of the sources were produced with the Caltech VLBI package, using the iterative self-calibration algorithm of Cornwell and Wilkinson (1981). The  $\lambda=3.6$  cm hybrid map obtained for the quasar 1038+528 B from the March 1981 data was equally consistent with the March 1981 and May 1983 data, indicating that this source suffered no significant changes in the interval between these two epochs. This source is therefore an excellent reference source for the study of changes taking place in the quasar 1038+528 A. Figure 1 shows the maps of the quasar 1038+528 A obtained at these two epochs. The emission of the superluminal component ejected from the core at an apparent speed  $3c$  ( $H_0 = 100 \text{ km s}^{-1} \text{ Mpc}^{-1}$ ,  $q_0 = 0.5$ ) dims out while its trajectory bends (by  $20^\circ$  on the map)

TABLE 1 Astrometric Information

Coordinates (J2000.0) for 1038+528 B				
$\alpha = 10^h 41^m 48^s.8960, \delta = 52^\circ 33' 55''.596$				
Station coordinates for epoch 1983.4				
Antennas	Cylindrical Radius (km)	West Longitude (degrees)	Polar Component (km)	Zenith Delay (ns)
DSS63	4862.449121	4.2480157	4115.106810	7.0
DSS14	5203.987730	116.8894585	3677.042425	7.0
T	3444.970820	-11.9263300	5349.830694	7.9
B	4063.238512	-6.8835914	4900.430708	7.9
K	4700.479735	71.4881417	4296.882112	7.0
G	5003.000522	79.8357593	3944.131099	8.0
F	5493.997595	103.9472427	3232.119039	7.0
O	5085.448720	118.2826965	3838.603889	7.0

Estimated position offsets of the core of 1038+528 A  
with respect to the reference position on 1038+528 B.

Epoch	$\Delta\alpha$ ( $\mu$ as)	$\Delta\delta$ ( $\mu$ as)
1981.2	$0.0 \pm 3.0$	$0.0 \pm 4.1$
1983.4	$-19.4 \pm 3.3$	$53.5 \pm 4.0$

towards the NE direction, approaching the position angle (P.A.) of the large scale structure.

For these two epochs, we determined the positions of the peak of brightness in the maps of 1038+528 A (which coincide with the positions of the core) and estimated the separations of these peaks from the reference point (the same point for both epochs) chosen on the 1038+528 B maps. The astrometric solution obtained at  $\lambda = 3.6$  cm for 1038+528 A with respect to 1038+528 B from May 1983 data differs significantly from the solution obtained from March 1981 data. The solution from May 1983 appears  $57 \pm 7 \mu$ as away toward the NW (P.A.  $-20^\circ$ ) from the solution from March 1981, which corresponds to a relative proper motion of the core of 1038+528 A with respect to 1038+528 B of about  $26 \pm 3 \mu$ as/yr. The estimates, along with other relevant astrometric information, are given in Table 1. The error quoted for each estimate is the statistical standard error rescaled to

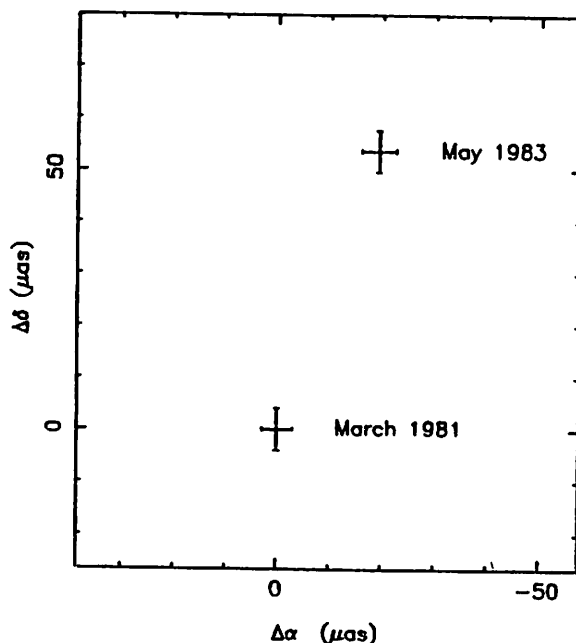


Figure 2 Estimates of the offsets of the position of the core of quasar 1038+528 A, relative to 1038+528 B at epochs 1981.2 and 1983.4 (with 1981.2 offsets subtracted).

normalize to unity the  $\chi^2$  per degree of freedom. Figure 2 shows the two estimates.

This astrometric determination was made in the J2000.0 coordinate system by global weighted-least-squares adjustment techniques, using the program VLBI3 (Robertson D.S., 1975) in its E version (called VLBI3E). The time-dependent Earth-orientation parameters (UT1-UTC and the two components of the position of the Earth's rotation axis), all of them based on a consistent origin, were determined by interpolation from the Goddard Space Flight Center (GSFC) CDP VLBI Global Solution GLB401 Earth Orientation Parameters (EOP) results (Ma and Ryan, private communication).

The coordinates used for the telescopes are those given by the GSFC CDP VLBI Global Solution GLB401 once they have been interpolated to the experiment day. The *a priori* positions used for Goldstone (DSS14) and Madrid (DSS63) were obtained in the GSFC terrestrial reference frame as follows: Jacobs (private communication) provided us the coordinates of the DSS14-DSS15 and the DSS63-DSS61 baseline vectors obtained from DSN local interferometry observations. The coordinates of these DSN baseline vectors were then directly added to the DSS15 and DSS61 station coordinates, respectively, derived in the GSFC CDP VLBI GLB401 solution to obtain those of DSS14 and DSS63. Additionally, using the coordinates thus obtained as *a priori* values we left them as free parameters in the



final global weighted-least-squares adjustment.

#### 4. Error analysis

How significant would be the detected proper motion if systematic effects were taken into account?. A source of systematic error arises in the determination of the source reference point, the peak of brightness of the core. We analyzed the possible errors in the location of the source reference-feature due to errors in the maps caused by: (a) random amplitude-and-phase calibration errors, (b) reduced disjoint data sets used in the map reconstructions, and (c) baseline-based systematic errors (antenna-based errors were corrected by the self-calibration procedure). For each resulting source map, we estimated the position of the peak of brightness of the core with respect to the external reference (assumed stationary) in quasar 1038+528 B.

Additionally, we investigated the effects on the astrometric determination of the relative source positions of introducing antenna-based and baseline-based systematic phase errors into the differential interferometric phase. Antenna-based phase errors can stem from "mispointing" while observing both sources simultaneously. Baseline-based errors are less likely and induce a smaller astrometric error than do antenna-based errors. We estimated that in our experiments the antenna-based systematic interferometric-phase-difference errors were not much larger than  $2^\circ$ .

We have conducted comparable numerical simulations with the May 1983 and March 1981 data. We have obtained similar results for both epochs since data quantity and quality, and source structure are similar. Our numerical simulations indicate that the systematic errors are about three times larger than our initial standard errors. The details of these simulations will be published elsewhere.

#### 5. Conclusions

Taking into account the analysis of systematic errors we find that the solution from May 1983 appears  $57 \pm 17 \mu\text{as}$  away toward the NW (P.A.  $-20^\circ$ ) from the solution from March 1981, corresponding to a relative proper motion of the core of 1038+528 A with respect to 1038+528 B of about  $26 \pm 8 \mu\text{as/yr}$ .

The difference between the March 1981 and May 1983 results may correspond either to a real proper motion of the source 1038+528 A or to a jitter of its core due to several mechanisms. In most accepted theoretical models, for a given frequency, the core corresponds to a jet point where the opacity becomes unity. The sky location of the peak of brightness of the core of the quasar 1038+528 A has a wavelength dependence due to opacity. This dependence was determined by Marcaide and Shapiro (1983, 1984) for the March 1981 epoch. Our present results may indicate a time dependent location of the core due to opacity.

Thus measuring a proper motion we may be measuring the aparent kinematics of the core of quasar 1038+528 A at  $\lambda=3.6$  cm, and not an actual proper motion of the core. The existence of some characteristic length for displacements (at the microarcsecond level) of the apparent core as a function of time or the existence of an actual quasar proper motion should and can be determined with new observations of the pair.

### References

- Bartel, N. *et al.* *Nature* **319**, 733 (1986).  
 Clark, T. A., *et al.* *IEEE Trans. of Geoscience and Remote Sensing* **GE-23**, n.4, 438 (1985).  
 Cornwell, T. and Wilkinson, P. N. *Monthly Notices of the RAS* **142**, 11 (1981).  
 Gorenstein, M.V. *et al.* *Science* **219**, 54 (1983).  
 Lestrade, J.-F. *et al.* *Astron J.* **99**, 1663 (1990).  
 Ma, C. *et al.* *Astron J.* **99**, 1284 (1990).  
 Marcaide, J.M. and Shapiro, I.I. *Astron J.* **88**, 1133 (1983).  
 Marcaide, J.M. and Shapiro, I.I. *Astrophys. J.* **276**, 56 (1984).  
 Marcaide, J.M. *et al.* *Astron. Astrophys.* **142**, 71 (1985).  
 Marcaide, J.M., Elósegui, P., and Shapiro, I.I. in *Parsec Scale Radio Jets*, ed. J.A. Zensus and T.J. Pearson, Cambridge University Press (1990), p. 43.  
 Morabito, D.D. *et al.* *Astron. J.* **91**, 1038 (1986).  
 Owen, F. N., Wills, B. J., and Wills, D. *Astrophys. J. Lett.*, **235**, L57 (1980).  
 Robertson, D. S. *Ph.D. thesis, Massachusetts Institute of Technology* (1975).  
 Rogers, A. E. E *et al.* *Science* **219**, 51 (1983).  
 Shapiro, I.I. *et al.* *Astron J.* **84**, 1459 (1979).

# **VLBI Monitoring of the milliarcsecond structure of 4C39.25 at 2.8 and 3.6cm**

**A. Alberdi, J.M. Marcaide, P. Elósegui**  
*Instituto de Astrofísica de Andalucía, C.S.I.C.*

**C.J. Schalinski, A. Witzel**  
*Maz Planck Institut für Radioastronomie*

## **Abstract**

**We present the most recent VLBI maps of 4C39.25 at 2.8 and 3.6cm, and discuss all the available experimental evidence on the source in light of a specific model. We show that physical parameters like component separation and component flux densities can be reliably obtained from the IRIS geodetic experiments.**

## **I. Introduction**

The quasar 4C39.25 ( $z=0.699$ ,  $m_v=18$ ) is an interesting subject of study. Studied with milliarcsecond (*mas*) resolution since the early days of VLBI, it was once considered the paradigm of a non-superluminal source (Cohen et al. 1982) since its compact structure over the decade of the seventies consisted of two stationary -with respect to each other- components separated by about 2 *mas* (1 *mas*=3.99  $h^{-1}$ pc for  $H_0=100$   $h$  km s $^{-1}$  Mpc $^{-1}$ ,  $q_0=0.5$ ). At closer look, even in those days the flux density of the westernmost component was systematically increasing by about the same amount that the flux density of the easternmost component was decreasing, in a remarkably balanced way (Shaffer et al., 1987).

Marcaide et al. (1985) reported the detection of a new component in the middle of the old structure and named the components as a, b, and c from east to west, a nomenclature we will follow. Subsequently Shaffer et al. (1987) and Schalinski et al. (1988) reported superluminal motion of component b relative to the other two components which remained stationary relative to each other. With observations at 1.3cm, Marscher et al. (1987) showed that none of the three components had the characteristics usually associated to the cores of compact radiosources. Browne et al. (1982) and Marcaide et al. (1989) have shown that it exists elongated arc-second emission at both sides of the compact mas-source with a certain degree of symmetry.

In order to try to understand the nature of this radio quasar and especially in order to understand its kinematics a concerted multiwavelength approach has been undertaken. Here we report on those results recently gathered from VLBI observations at 2.8 and 3.6cm. The 3.6cm data come from the IRIS (International Radio Interferometric Surveying) runs. During each IRIS run, 14 extragalactic radio sources distributed in the Northern hemisphere, between them 4C39.25, are observed.

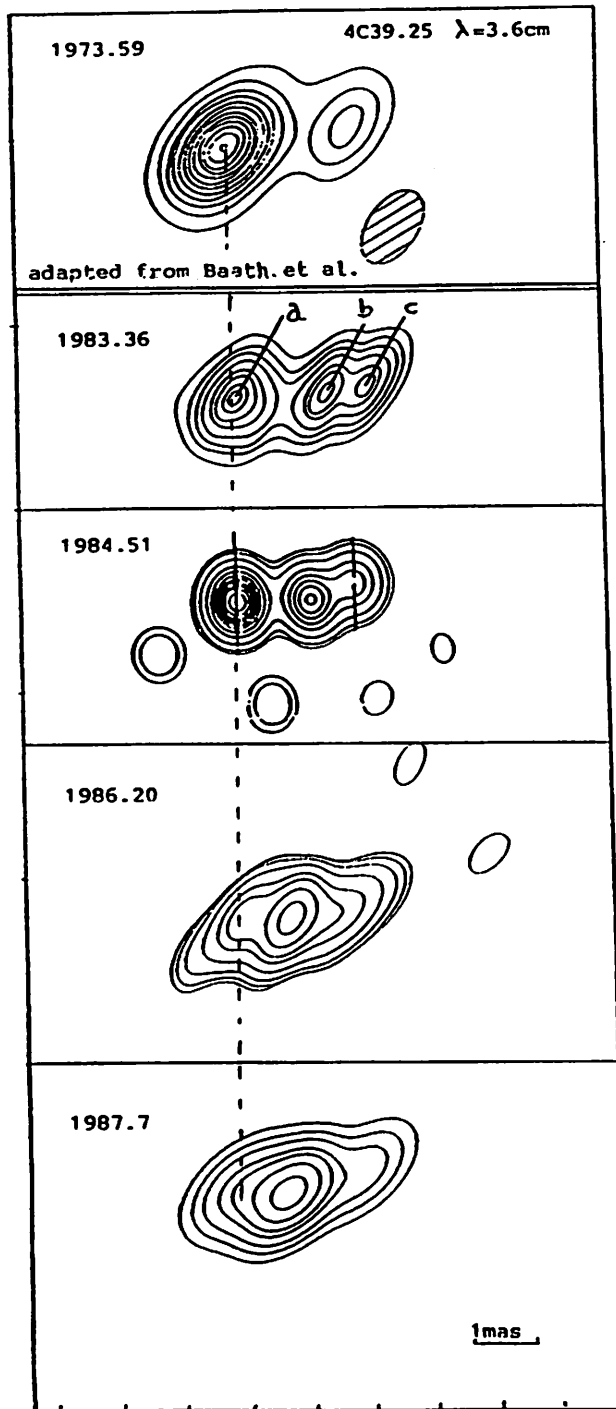


Figure 1: VLBI hybrid maps of 4C39.25 at 3.6cm. The contours correspond to 2, 5, 10, 20, 30, 50, 70 and 90 % of the peak brightness. They are arbitrarily aligned at the position of component a (See text).

## II. Observations

The VLBI observations at 2.8 were made on March 1986, September 1987 and September 1988, and at 3.6cm in March 1986 and September 1987. The resulting maps are shown in Marcaide et al. (1990) for 2.8cm and in Figure 1 for 3.6cm. They have been added to a sequence of maps already published by Marscher et al. (1987) and Marcaide et al. (1989).

The 3.6cm maps were obtained from the IRIS data. We have selected two sources for our investigations: 4C39.25 and 1803+784 (calibrator). Both sources have a regular uv-coverages in the experiments. Their structures are well defined and well known from VLBI experiments at other different frequencies and epochs. The amplitude calibration of geodetic-VLBI data is a major problem due to insufficient radiometry and a very sparse uv-coverage. A new calibration-approach was then required, using 1803+784 as a calibrator (See Schalinski et al., these proceedings, for more details).

For a later discussion we have collected in Figure 2 the flux density measurements we have made during our VLBI observations over the last years complemented with data taken from antenna calibration purposes at the Effelsberg radiotelescope.

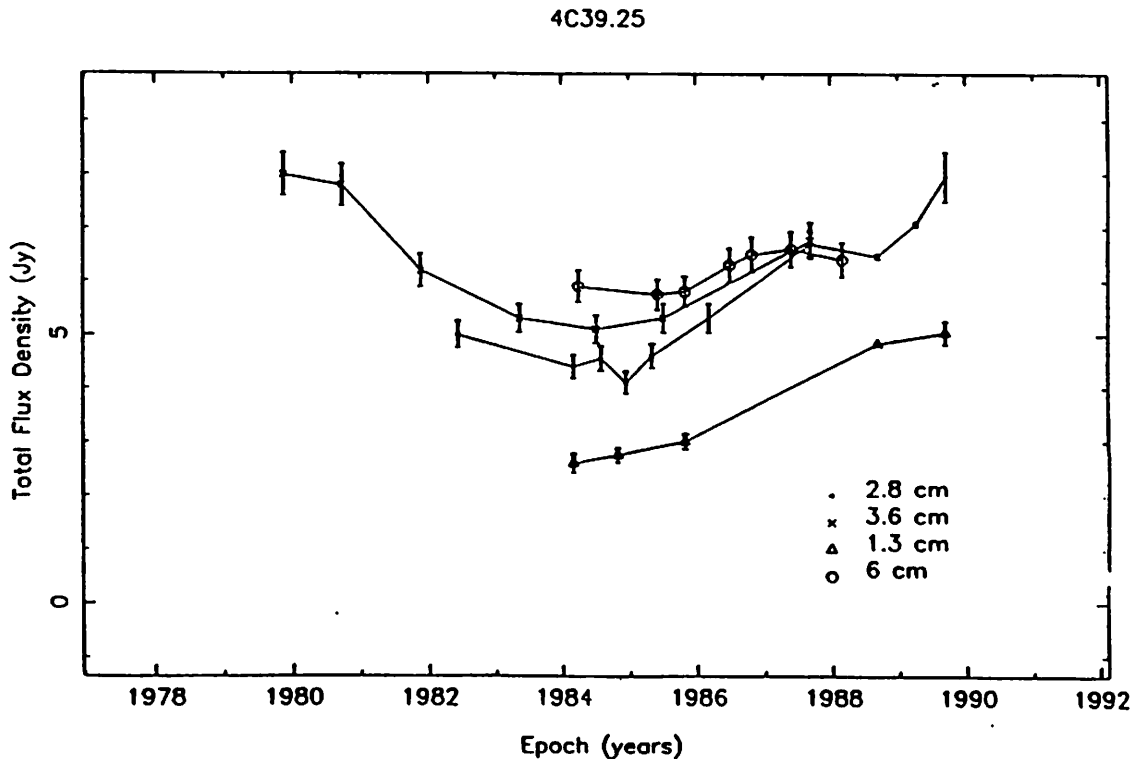


Figure 2: Total flux density evolution of 4C39.25 at 6.0, 3.6, 2.8 and 1.3cm.

### III. Discussion

From Figure 1 and maps already published elsewhere, systematic changes in the structure are evident:

- The components a and c remain stationary with respect to each other while component b is moving away from component c towards component a. We have plotted in Figure 3 the angular separations a-c and a-b against time. Clearly a-c remains constant in time while a-b decreases more or less uniformly.
- The flux density emissions from the three components are changing systematically. In Figure 4 we plot the 2.8 and 3.6cm total and component flux densities of 4C39.25 versus time. It can be seen that the evolution of the total flux density mimics the evolution of that of component b.

Marcaide et al. (1989) have proposed a model in which 4C39.25 consists of a doubly bent nozzle that contains and directs the relativistic plasma. Bright radio emission occurs at the bends owing to standing shocks that bend the flow in response to external pressure. Thus, our observed components a and c would be associated to these bends. The moving component b would then correspond to a shock travelling down the jet. From Figure 2 we can deduce a time delay at the beginning of a rise for different wavelengths as it would be expected in the case of shocks propagating through confined jets, lending thus some support to the interpretation given above for component b.

In this model, the source core, that is the jet position where the opacity becomes unity, should be close to the location of the central engine feeding the jet, that is to the west of component c. We may not see the core in the 2.8 and 3.6cm maps because its spectral index may be very inverted, the geometry unfavorable and the map dynamic ranges low. In a 1.3cm experiment performed in September 1987 a new component (we will label it "d") was detected 2.6mas west of component a. Perhaps, the new found fourth component can be the source's core, but it can also be a new b-type component travelling downstream, away from the unseen core, towards component c in a process of recurrent events like those found in many other superluminal sources. It should be noted that the total spectrum of the source is consistent with component d turning over at about 1.3cm.

Figure 3 shows that the proper motion of component b relative to components a and c is uniform at a  $0.16 \pm 0.02 \text{ mas/yr}$  rate, but a closer look shows that if we take only the last three epochs (better calibrated than previous ones and also with 2.8 and 3.6cm quasi-simultaneous at each epoch) then the rate is  $0.10 \pm 0.01 \text{ mas/yr}$ . Thus, our model demands a slowing down of component b as it approaches component a and an apparent uniform change of position angle of component b with respect to component a. From the results from epochs March 1986 and September 1987 it appeared that indeed the slowing down and rotation were happening.

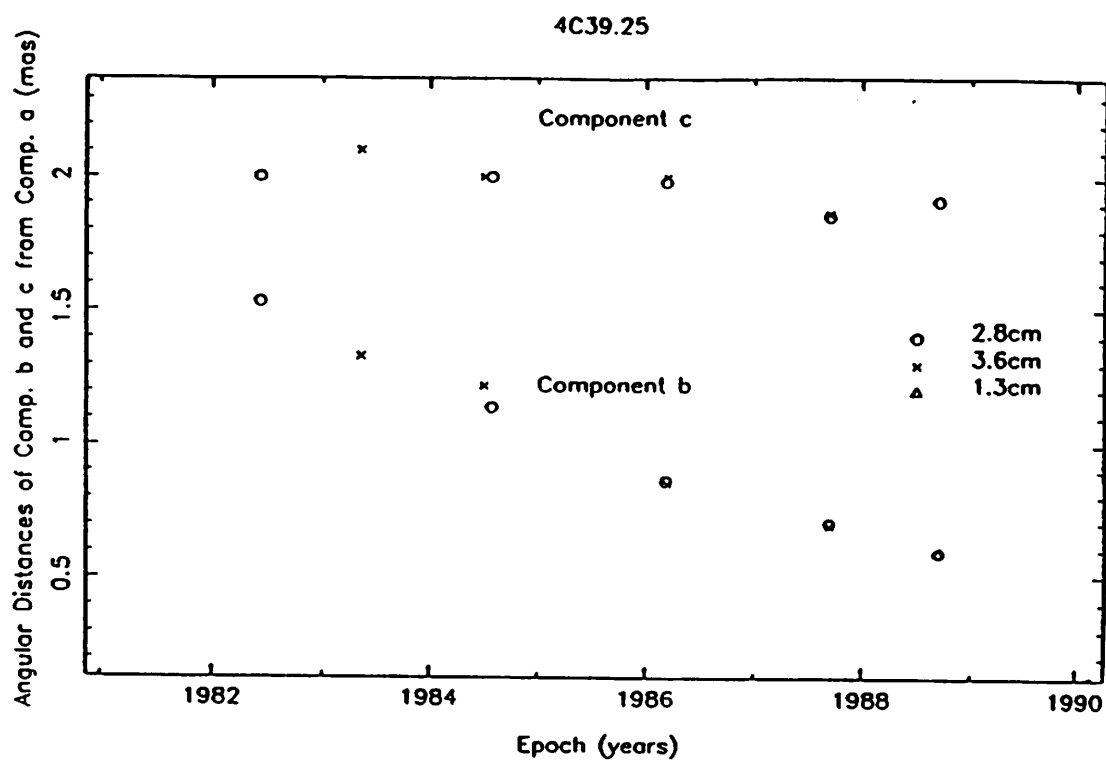


**Figure 3:** Angular distances of components b and c from component a at 3.6, 2.8 and 1.3cm.

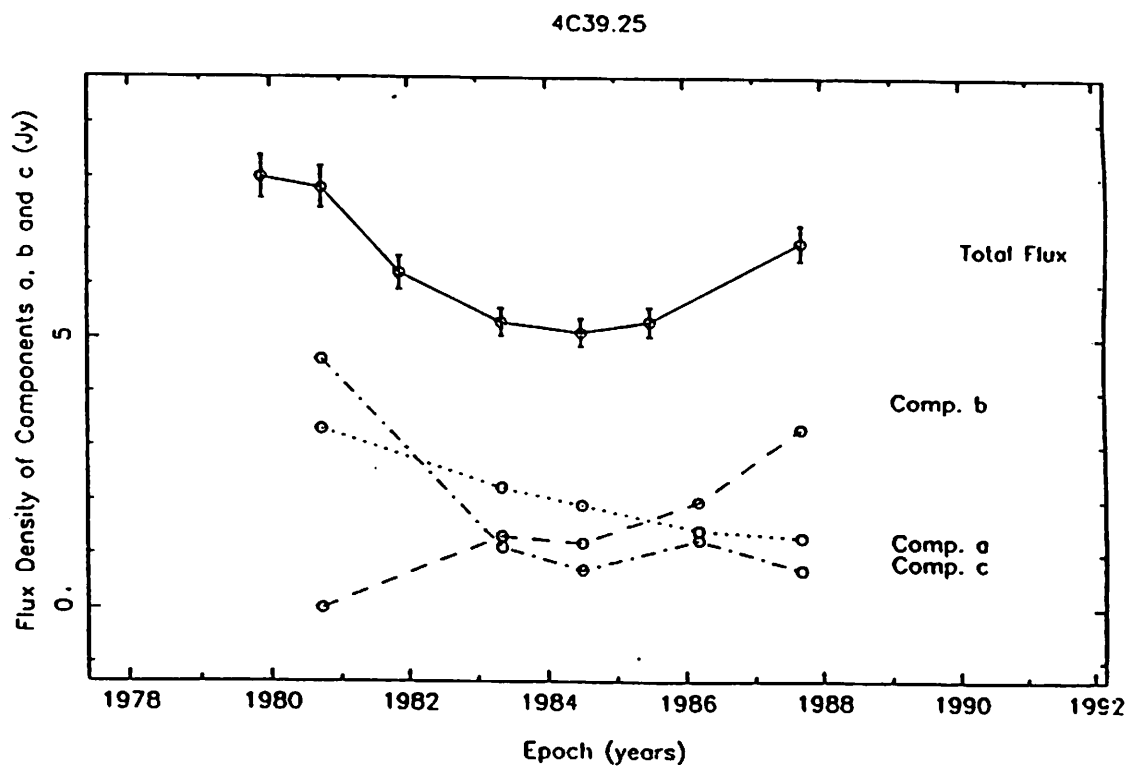


**Figure 4:** Time evolution of total flux density and component flux density at 3.6cm (IRIS data).

The interpretation of component **b** as a shock propagating along the jet could explain the increase in the polarized flux density, apparent in the data of Aller et al. (1985). Being the jet favorably oriented towards the observer, the magnetic field component perpendicular to the axis of the shock compression is enhanced. This enhancement of the magnetic field aligned with the observer against the other components of an originally random and turbulent field, produces the increase of the polarized flux density.

#### IV Conclusions

The mapping-scheme we have applied to the IRIS data provides results consistent with the 2.8cm ones. Further improvements of calibration and dynamic range of the maps will improve the results. We can relate the structure at 3.6cm to that at 2.8cm. This is important since an insufficient number of antennas will be available at 2.8cm beyond 1990, to make VLBI worthwhile at this frequency.

#### References

- Aller, H.D. et al. *Astrophys. J. Suppl.* **59**, 513 (1985)  
 Blandford, R.D. & Königl, A. *Astrophys. J.* **232**, 34 (1979)  
 Browne, I.W.A. et al. *Nature* **299**, 788 (1982)  
 Cohen, M.H. & Unwin S.C. *Proc. IAU Symp. No. 97*, 345 (1982)  
 Marcaide, J.M. et al. *Nature* **314**, 424 (1985)  
 Marcaide, J.M. et al. *Astr. Astrophys. Lett.*, **211**, L23 (1989)  
 Marcaide, J.M. et al. in *Parsec Scale Radio Jets*, ed. J.A. Zensus and T.J. Pearson, Cambridge University Press (1990)  
 Marscher, A.P. et al. *Astrophys. J. Letters* **319**, L69 (1987)  
 Schalinski, C.J. et al. *Proc. IAU Symp. No. 129*, 39 (1988)  
 Shaffer, D.B. et al. *Astrophys. J.* **218**, 353 (1977)  
 Shaffer, D.B. et al. 1987, *Astrophys. J. Letters* **314**, L1



## Phase-refencing using DEGRIAS

Anton A.W. Jongeneelen  
Leiden Observatory  
the Netherlands

**ABSTRACT.** A method is presented for preparing phase-referenced observations to get accurate relative positions of sources on degree-scale distances from each other. An experiment on M81 and two reference sources show an positional accuracy of .5 arcseconds using delay-rate data and a 1 mas accuracy when using delay data.

### 1. INTRODUCTION

In order to be able to measure proper motion of M81 with respect to some background sources, a first epoch observation has been done in june 1988. Because the chosen reference sources were not observable in the same beam as M81 we had to choose phase-refencing with source switching. 10 MkIII VLBI stations participated in this 6cm Global Mode B experiment.

### 2. DEGRIAS

Delft Geodetic Radio-Interferometry Adjustment System is a multi-baseline multi-parameter least-square software package. Using delay and delay-rate as input data , this package is able to model basic parameters like position of station, source position, clock-offset and -drift, atmosphere and polar motion. In addition to this all sorts of corrections can be applied to the data, like retarded baseline, antenna motion, tropospheric refraction, earth tides etc.

### 3. OBSERVATION

In switching between sources the limiting factor was the ionosphere, so we had to switch quickly (within 10 minutes back on the same source). Of the 10 telescopes 3 where lost due to bad clocks , but we were able to use this data to make hybrid maps of the observed sources. One telescope had recording problems , that left 6 telescopes : Westerbork, Medicina, Onsala, Haystack, Greenbank and VLA. 11 of these 15 baselines proved to have enough detections to try the phase-refencing technique.

### 4. REDUCTION

Since we first had to create a correct set of basic model parameters in DEGRIAS , we started with the delay-rate data; eliminating bad data. The result was that we were now able to determine the relative source positions within .5 arcsecond. then we took the delay data and after adjusting with DEGRIAS the result was an accuracy of 1 mas. Because we think the accuracy is 20 as, we now have to continue with the phase data, which are not direct usable in DEGRIAS.

## 5. PHASE-CONNECTION

In principle delay and phase are the same except that *in phase* a lot of cycles ( wavelength ambiguities ) are missing. That is why DEGRAS can't handle these data.

In order to connect the phases, we now interpolate the phase separately for every source, we use the phase plus the delay-rate made from the basic geometric model of the best fit using Degrias. Now we can take the phase difference of the different source by interpolating the phase of the reference source to the time of observation of the main source.  
see Alef, Thesis 1986.

## 6. CONCLUSION

If an second epoch observation is done we are able to determine the proper motion of M81. The usability of DEGRAS has been proven to be the first step towards phase-referencing using source switching. If an relative position accuracy of not better than 1 mas is needed, a source switching experiment can be reduced with DEGRAS alone.